

DISSERTATION

INVESTIGATING NITRATE UPTAKE AND TRANSIENT STORAGE IN
HEADWATER STREAMS AMONG GRADIENTS OF GEOMORPHIC
COMPLEXITY, LAND USE, AND RESTORATION TECHNIQUES

Submitted by

Jennifer Suzanne Mueller Price

Department of Civil and Environmental Engineering

In partial fulfillment of the requirements

For the Degree of Doctor of Philosophy

Colorado State University

Fort Collins, Colorado

Summer 2010

COLORADO STATE UNIVERSITY

July 6, 2010

WE HEREBY RECOMMEND THAT THE DISSERTATION PREPARED UNDER OUR SUPERVISION BY JENNIFER SUZANNE MUELLER PRICE ENTITLED INVESTIGATING NITRATE UPTAKE AND TRANSIENT STORAGE IN HEADWATER STREAMS AMONG GRADIENTS OF GEOMORPHIC COMPLEXITY, LAND USE, AND RESTORATION TECHNIQUES BE ACCEPTED AS FULFILLING IN PART REQUIREMENTS FOR THE DEGREE OF DOCTOR OF PHILOSOPHY.

Committee on Graduate Work

Michael N. Gooseff

Jim C. Loftis

Ellen E. Wohl

Advisor: Brian P. Bledsoe

Department Head: Luis A. Garcia

ABSTRACT OF DISSERTATION

INVESTIGATING NITRATE UPTAKE AND TRANSIENT STORAGE IN
HEADWATER STREAMS AMONG GRADIENTS OF GEOMORPHIC
COMPLEXITY, LAND USE, AND RESTORATION TECHNIQUES

Headwater streams are a crucial component of nutrient processing in watersheds, owing to high surface-to-volume ratios that favor nitrate uptake and to the large percentage of headwater stream length in the total length of a river system. In this study, I explore how geomorphic characteristics may influence transient storage and nitrate uptake of streams across a gradient of land use and restoration practices. To examine linkages among geomorphic complexity, transient storage, and nitrate uptake in streams, I investigated an urban stream and two agricultural streams. Study reaches representing distinct geomorphic settings with varying substrate size, sinuosity, bed slope, and styles of restoration and management were chosen within each stream. I performed detailed physical characterizations and multiple nutrient injections of bromide and nitrate to estimate transient storage and nitrate uptake in each reach. Comprehensive data sets, including pebble counts, longitudinal profiles, cross-section surveys, hydraulic measurements, and benthic organic matter (fine and coarse), were collected to characterize physical complexity along each reach. To estimate parameters of transient storage and nitrate uptake, the OTIS model was run through UCODE for optimization of parameter estimates.

Regression models were developed to relate attributes of flow and geomorphic complexity with transient storage and nitrate uptake parameters. The models showed associations among nitrate uptake velocity and length (v_f , S_w) and transient storage parameters (F_{med}^{200}), which were influenced by key factors of geomorphic complexity (longitudinal roughness), flow (Reynolds number), and substrate condition (median grain size and fine benthic organic matter). There were no conclusive patterns showing that in-channel structures and natural revegetation of riparian areas promoted nitrate uptake in the study streams. For example, a reach with instream wood but without restoration structures exhibited more transient storage and comparable nitrate uptake when compared to a paired reach with extensive J-hook vane structures. Finally, an investigation of the urban stream before and after a high flow event indicated that transient storage and nitrate uptake are highly context-specific and mediated by interactions between geomorphic setting and flow variability.

Jennifer Suzanne Mueller Price
Department of Civil and Environmental Engineering
Colorado State University
Fort Collins, CO 80523
Summer 2010

ACKNOWLEDGMENTS

I would like to thank the National Science Foundation's Faculty Early Career Development (CAREER) Program for funding my doctoral research. I would also like to thank my advisor, Brian Bledsoe, for his help and encouragement throughout this project. Thank you to my graduate committee, Brian Bledsoe, Jim Loftis, Ellen Wohl, and Mike Gooseff; to the Department of Civil and Environmental Engineering at Colorado State University; and to Gloria Garza for her help in formatting my dissertation. A huge thank you goes to everyone that helped with field data collection and to Dan Baker for his partnership in this project. Finally, thank you to my husband, my family, and my friends for their encouragement.

TABLE OF CONTENTS

ABSTRACT OF DISSERTATION	iii
ACKNOWLEDGMENTS	v
LIST OF FIGURES	viii
LIST OF TABLES	x
LIST OF SYMBOLS AND ABBREVIATIONS	xi
1 INTRODUCTION	1
2 BACKGROUND	5
2.1 Nitrate Uptake	5
2.2 Hyporheic Exchange	6
2.3 Previous Nitrate Uptake Studies.....	8
2.4 Modeling Approaches in Transient Storage and Nitrate Uptake.....	9
2.5 Restoration Goals to Promote Nitrate Uptake	11
2.6 Land Use Effects on Nitrate Uptake.....	12
3 METHODOLOGY	14
3.1 Site Selection	14
3.1.1 Spring Creek – urban stream.....	15
3.1.2 Sheep Creek – agricultural stream	19
3.1.3 Nunn Creek – agricultural stream	22
3.2 Data Collection	24
3.2.1 Nutrient Injections	24
3.2.2 Physical Habitat Units.....	28
3.2.3 Benthic Organic Matter.....	31
3.2.4 Hydraulic Measurements	33
3.2.5 Dissolved Oxygen Measurements.....	33
3.2.6 Substrate Distribution	34
3.2.7 Channel Geometry Survey	35
3.3 Data Analysis and Modeling	36
3.3.1 Lab Analysis of Water Samples.....	36
3.3.2 Lab Analysis of BOM Samples	37
3.3.3 Post-processing of Physical Variables	39
3.3.4 Modeling Whole-stream Metabolism	42
3.3.5 Modeling Transient Storage and Nitrate Uptake	43
3.3.6 Statistical Analyses	48

4	INTERSITE COMPARISON OF CHARACTERISTICS AMONG ALL THREE STREAMS	51
4.1	Overview	51
4.2	Results	53
4.3	Discussion.....	77
5	RESTORATION INTRASITE COMPARISON	81
5.1	Overview	81
5.2	Results	85
5.3	Discussion.....	101
6	FLASH FLOOD EFFECTS ON SPRING CREEK.....	110
6.1	Overview	110
6.2	Results	113
6.3	Discussion.....	131
7	CONCLUSION	137
8	REFERENCES.....	140
	APPENDIX A: SUMMARY OF UNCERTAINTY AND SENSITIVITY IN PARAMETER ESTIMATES FROM OTIS/UCODE MODELING	153

LIST OF FIGURES

Figure 1.1: Diagram of nitrogen spiraling in stream ecosystems (Mulholland 2004)	2
Figure 3.1: Location of study reaches.....	15
Figure 3.2: Location of Spring Creek in Fort Collins, Colorado (image courtesy of U. S. Geological Survey (USGS)); study reaches highlighted in yellow	17
Figure 3.3: Study reaches along Spring Creek.....	18
Figure 3.4: Location of Sheep Creek in Northern Colorado (image courtesy of USGS); yellow-shading denotes study reaches	20
Figure 3.5: Sheep Creek study reaches	21
Figure 3.6: Location of Nunn Creek in Northern Colorado (image courtesy of USGS); yellow-shading denotes study reaches	23
Figure 3.7: Nunn Creek study reaches	23
Figure 3.8: Downstream view of baffle placement.....	25
Figure 3.9: Nutrient Release Planning Sheet used for injections.....	26
Figure 3.10: Example of Physical Habitat Field Sheet used in visual characterization and classification of areal sub-reaches into habitat units.....	29
Figure 3.11: Channel Geomorphic Unit classification (Hawkins <i>et al.</i> 1993).....	30
Figure 3.12: Side-view of Multi-parameter Probe Deployment	34
Figure 3.13: Sampling frame (Bunte and Abt 2001a).....	35
Figure 3.14: Concept basis of OTIS model (Runkel 1998)	43
Figure 3.15: OTIS/UCODE modeling flowchart (Baker 2009).....	48
Figure 4.1: Spring Creek Bromide BTC simulations.....	62
Figure 4.2: Spring Creek Nitrate BTC simulations	63
Figure 4.3: Sheep Creek Bromide BTC simulations	64
Figure 4.4: Sheep Creek Nitrate BTC simulations	65
Figure 4.5: Nunn Creek Bromide BTC simulations	66
Figure 4.6: Nunn Creek Nitrate BTC simulations	67

Figure 4.7: Comparison of characteristics describing geomorphic complexity	68
Figure 4.8: Comparison of measures describing flow	69
Figure 4.9: Comparison of physical parameters influenced by geomorphic setting and flow area.....	70
Figure 4.10: Comparison of transient storage and uptake parameters.....	71
Figure 4.11: Compiled Dataset of Nitrate Uptake Studies (Tank <i>et al.</i> 2008).....	73
Figure 4.12: Relative submergence relationship (Julien 2002)	77
Figure 5.1: Results of Monte Carlo simulations of transient storage parameters for Sheep Creek study reaches.....	92
Figure 5.2: Results of Monte Carlo simulations of transient storage parameters for Nunn Creek study reaches.....	93
Figure 5.3: Results of Monte Carlo simulations of nitrate uptake parameters for Sheep Creek and Nunn Creek study reaches	94
Figure 5.4: Results of Monte Carlo simulations of F_{med}^{200} and A_s/A for Sheep Creek.....	95
Figure 5.5: Results of Monte Carlo simulations of S_w and v_f for Sheep Creek.....	96
Figure 5.6: Results of Monte Carlo simulations of F_{med}^{200} and A_s/A for Nunn Creek.....	97
Figure 5.7: Results of Monte Carlo simulations of S_w and v_f for Nunn Creek.....	98
Figure 5.8: Percentage of storage zone area composed of instream and hyporheic storage.....	105
Figure 6.1: Post-flood conditions include bank failure at Edora Park and deposition below grade-control structure at Stuart.....	115
Figure 6.2: Results of Monte Carlo simulations of transient storage parameters for Spring Creek study reaches.....	118
Figure 6.3: Results of Monte Carlo simulations of nitrate uptake parameters for Spring Creek study reaches	119
Figure 6.4: Results of Monte Carlo simulations of F_{med}^{200} and A_s/A for Spring Creek.....	120
Figure 6.5: Results of Monte Carlo simulations of S_w and v_f for Spring Creek.....	121
Figure 6.6: Percent change of post-flood parameters from pre-flood parameters	126
Figure 6.7: Percent change of 1-yr parameters from pre-flood parameters.....	127
Figure 6.8: Percent change of 1-yr parameters from post-flood parameters	128
Figure 6.9: Thalweg elevation along the study reaches at pre-flood, post-flood, and conditions 1 yr after flash flood.....	130

LIST OF TABLES

Table 4.1: Summary of physical and ecological parameters for Spring Creek	58
Table 4.2: Summary of physical and ecological parameters for Sheep Creek and Nunn Creek	59
Table 4.3: Summary of transient storage and nitrate uptake parameters for Spring Creek	60
Table 4.4: Summary of transient storage and nitrate uptake parameters for Sheep Creek and Nunn Creek	61
Table 4.5: Best-fit regression models of transient storage and nitrate uptake	74
Table 5.1: Description of paired study reaches	82
Table 5.2: Summary of Sheep Creek physical and ecological characteristics Table 5.3: Summary of Nunn Creek physical and ecological characteristics	88
Table 5.3: Summary of Nunn Creek physical and ecological characteristics	89
Table 5.4: Summary of Sheep Creek transient storage and nitrate uptake parameter estimates	90
Table 5.5: Summary of Nunn Creek transient storage and nitrate uptake parameter estimates	91
Table 6.1: Characteristics of August 2, 2007 storm in Fort Collins, Colorado	112
Table 6.2: Summary of Spring Creek physical and ecological parameters	116
Table 6.3: Summary of Spring Creek transient storage and nitrate uptake parameters	117
Table A.1: Uncertainty and sensitivity summary of parameter estimates from OTIS/UCODE modeling on Spring Creek	154
Table A.2: Uncertainty and sensitivity summary of parameter estimates from OTIS/UCODE modeling on Sheep Creek	156
Table A.3: Uncertainty and sensitivity summary of parameter estimates from OTIS/UCODE modeling on Nunn Creek	158

LIST OF SYMBOLS AND ABBREVIATIONS

Symbols

A	cross-sectional area of main channel (m^2)
A_{avg}	average cross-sectional area of the reach (m^2)
A_i	measured cross-sectional area (m^2)
A_s	cross-sectional area of the storage zone (m^2)
C	solute concentration in main channel (mg/L)
C_b	background concentration of solute (mg/L)
C_{inj}	solute concentration of injection solution (mg/L)
C_s	solute concentration in storage zone (mg/L)
d_{16}	grain size for which 16% of the clasts are finer (mm)
d_{50}	median grain size (mm)
d_{84}	grain size for which 84% of the clasts are finer (mm)
d_{max}	maximum grain size (mm)
D	dispersion coefficient (m^2/s)
DaI	Damkohler number
F_{med}^{200}	fraction of median travel time due to transient storage
g	acceleration due to gravity (9.81 m/s^2)
h	flow depth (m)
i	individual measurement number

L	reach length (m)
L_V	valley length (m)
LR	longitudinal roughness (m)
n	sample size
P	sinuosity
q	unit discharge (m^2/s)
Q	discharge (m^3/s)
Q_{inj}	flow rate of pump injecting solution into stream (m^3/s)
r	Pearson correlation coefficient
R	hydraulic radius (m)
R/d_{84}	relative submergence
Re	Reynolds number
S_o	bedslope
S_w	uptake length (m)
t	time (s)
T_{str}	stream residence time
T_{sto}	storage residence time
u	velocity (m/s)
u^*	shear velocity (m/s)
ν	kinematic viscosity ($10^{-6} \text{ m}^2/\text{s}$)
v_f	uptake velocity (m/s)
w	channel width (m)
w_{avg}	average wetted width of the reach (m)

x	distance (m)
$z_{obs,i}$	measured thalweg elevation at each point
$z_{pred,i}$	predicted thalweg elevation based on bed slope
α	storage zone exchange coefficient (s^{-1})
χ	metric of complexity
ε_A	variability in cross-sectional area
ε_w	width variability
λ	first-order decay coefficient in main channel (s^{-1})
λ_s	first-order decay coefficient in storage zone (s^{-1})
ρ	water density (1000 kg/m^3)
ω	unit stream power (W/m^2)

Abbreviations

AFDM	ash-free dry mass
ANOVA	analyses of variance
APHA	American Public Health Association
BOM	benthic organic matter
Br^-	bromide
BTCs	break-through curves
CBOM	coarse benthic organic matter
DI	deionized
DO	dissolved oxygen
DS	downstream

EPA	U. S. Environmental Protection Agency
FBOM	fine benthic organic matter
GPP	gross primary production
HCl	hydrochloric acid
KNO ₃	potassium nitrate
LINX	Lotic Intersite Nitrogen eXperiment
MDL	method detection limit
NaBr	sodium bromide
NE	not estimated
NO ₃ ⁻	nitrate
NO ₃ ⁻ -N	nitrate measured as nitrogen
NRCS	Natural Resources Conservation Service
OTIS	One-dimensional Transport with Inflow and Storage
RSTM	reactive solute transport model
SA:V	ratios of surface area to volume
SMP	Stream Metabolism Program
STIR	Solute Transport in Rivers
T1	transect at upstream end of the reach
T11	transect at middle of the reach
T21	transect at downstream end of the reach
TSMs	transient storage models
UCODE	universal inverse modeling code
US	upstream

USGS U. S. Geological Survey

XS cross-section

1 INTRODUCTION

Anthropogenic alteration of landscapes continues to grow through urban development and agricultural practices. Changing land use and land cover within watersheds can increase runoff volumes and nutrient loads that drain into streams and rivers (Brooks *et al.* 2003). Due to the mass production of nitrogen fertilizers through the Haber-Bosch process, as well as nitrogen emissions from burning fossil fuels, the nitrogen cycle has become extremely unbalanced (Gijzen and Mulder 2001). When fertilizers are applied to lawns and cropland, excess nitrogen is transported in runoff and groundwater to surface waters. Increased levels of inorganic nitrogen in surface waters have caused degraded water quality and impacts on aquatic ecosystem structure and function throughout the world (Camargo and Alonso 2006) and can lead to eutrophication and fish kills in coastal areas (Fisher and Fisher 2001).

Headwater streams, which encompass a large portion of stream length in watersheds, have high surface-to-volume ratios that favor nitrate uptake and removal of nitrogen loads (Peterson *et al.* 2001). Therefore, understanding nitrogen dynamics in small, headwater streams is important for ascertaining how these streams can influence downstream nitrogen loads, as well as identifying potential strategies for reduction of downstream nitrogen loading through watershed and stream restoration.

characterization of study reaches, including such attributes as width variation, cross-sectional variation, and substrate characteristics. Prior studies have also shown linkages between transient storage and uptake (Hall *et al.* 2009; Mulholland *et al.* 2009), but these studies did not include a detailed geomorphic component. Additionally, I examine temporal variability in nitrate uptake by exploring the effects of geomorphic changes due to a single high flow event, as well as flow variability. Although relationships between stream restoration approaches and nitrate uptake have gained attention (Craig *et al.* 2008; O'Connor *et al.* 2009), few studies have documented effects of restoration implementation on nitrate uptake. In this study, I investigate how different restoration techniques in agricultural streams can affect transient storage and nitrate uptake. Furthermore, I explicitly examine uncertainty in transient storage and nitrate uptake parameters and develop models to describe how physical characteristics relate to transient storage and nitrate uptake parameters.

The objectives in this study are (1) to examine how characteristics of geomorphic complexity and flow relate to transient storage and nitrate uptake, (2) to investigate the potential of two stream restoration approaches in promoting transient storage and nitrate uptake in two agricultural streams, and (3) to explore temporal variation in an urban stream by comparing data collected from physical measurements and nutrient injections performed immediately before and after a flash flood. Specific hypotheses are presented in Chapters 4 through 6. This dissertation is organized into seven chapters. Chapter 2 provides a summary of relevant background literature to describe the context of this research. A detailed methodology of this study is presented in Chapter 3. In Chapter 4, I address the first objective and develop regression models to describe associations among

geomorphic and flow characteristics, transient storage, and nitrate uptake. Chapter 5 focuses on the second objective, where I investigate transient storage and nitrate uptake, as influenced by two restoration approaches. In Chapter 6, I address the third objective and quantify changes in geomorphic characteristics, transient storage, and nitrate uptake due to a single high flow event. Lastly, I present a brief statement of general conclusions in Chapter 7.

2 BACKGROUND

2.1 NITRATE UPTAKE

Agricultural and urban land uses influence watershed processes and the ecological integrity of streams. Nutrient enrichment, sedimentation, clearing of riparian vegetation, nonpoint input of pollutants, and hydrologic alterations are among the adverse effects of anthropogenic land uses on lotic systems (Allan 2004). Anthropogenic land use changes associated with urbanization and agriculture can decrease the geomorphic complexity of streams (Jacobson *et al.* 2001), thereby potentially reducing transient storage and biogeochemical cycling (Gooseff *et al.* 2007). Elevated nitrogen inputs can markedly affect patterns of seasonal and storm-related nitrate loading from the landscape into streams (Poor and McDonnell 2007).

Many studies have been performed to explore nitrate dynamics in streams. One method used to estimate nitrate uptake over a stream reach involves determining the spiraling length from a linear regression of the nutrient concentration at incremental distances downstream from a constant-rate nutrient injection (Hall *et al.* 2002; Payn *et al.* 2005; Ensign and Doyle 2006). Spiraling, or uptake, length is a measure of the efficiency of nutrient use in a stream (Mulholland *et al.* 2002) and is defined as the mean distance that a nutrient atom travels in a stream before uptake by biota (Newbold *et al.* 1981). Nutrient uptake in streams is the net difference between solute transfer from the water

column into the streambed and solute release from the streambed back into the water column (Stream Solute Workshop 1990). Water and solutes are exchanged between surface water and groundwater through the hyporheic zone, where important biogeochemical processes (e.g., denitrification) occur (Boulton *et al.* 1998). Hyporheic exchange is promoted through variations in physical characteristics of the streambed along channels (Tonina and Buffington 2009). As solutes move from the landscape into streams and downstream receiving waters, the composition of reactive solutes can change through processes occurring in the hyporheic zone (Findlay 1995). Quantifying nitrate uptake rates in natural systems is complex due to coupled processes of biogeochemical reactions, which are influenced by microbial communities, organic carbon content, and hyporheic exchange as affected by flow and substrate characteristics (O'Connor and Harvey 2008). Additionally, denitrification is a major biogeochemical process occurring in the hyporheic zone that removes nitrate from stream systems.

2.2 HYPORHEIC EXCHANGE

The potential for nutrient uptake increases with longer residence times of stream water mixing with subsurface water and biota within the hyporheic zone (Valett *et al.* 1996). Physical drivers of hyporheic exchange include bed material size and mobility, extent of alluvial volume, and variation in hydraulic conductivity and pressure head (Tonina and Buffington 2009). Hyporheic exchange can be directly related to substrate permeability and the square of average stream velocity (Packman and Salehin 2003). Another scaling relationship based on effective diffusion in sediments links hyporheic

exchange with bed roughness, shear velocity (in the form of shear Reynolds number), and sediment permeability and porosity (O'Connor and Harvey 2008).

The potential for hyporheic exchange is also related to longitudinal variability in the geomorphic characteristics of streams. Variation in streambed topography (i.e., riffle-pool sequences) promotes exchange between surface water and hyporheic zone, thereby affecting solute retention and transport (Harvey and Bencala 1993). In a study of streams with varying levels of geomorphic complexity, increased longitudinal roughness was associated with increases in both nitrate uptake and transient storage, supporting the linkage among geomorphic characteristics, transient storage, and biogeochemical processing of nitrate (Baker 2009). Hyporheic exchange has been shown to increase with increasing water surface concavity (Anderson *et al.* 2005), and abrupt steps in the thalweg profile have been shown to enhance hyporheic exchange (Wondzell 2006). In-stream structures can drive hyporheic exchange by producing local increases in slope and backwater areas upstream of structures (Hester and Doyle 2008). Although riffle-pool sequences can promote hyporheic exchange, fine sediment can clog the interstices of cobbles and boulders in riffles and reduce exchange through the streambed (Kasahara and Hill 2006). As channel morphology changes with stream size and order through river networks, the physical characteristics that affect hyporheic exchange also change and lead to varying magnitudes and rates of hyporheic exchange (Buffington and Tonina 2009). The dominant characteristics driving hyporheic flow vary from pool-step sequences in second-order streams to secondary channels and high sinuosity in fifth-order streams (Kasahara and Wondzell 2003). Headwater streams may have more extensive

hyporheic exchange zones than third- through fifth-order streams (D'Angelo *et al.* 1993). These studies underscore the importance of headwater streams in hyporheic exchange.

2.3 PREVIOUS NITRATE UPTAKE STUDIES

The Lotic Intersite Nitrogen eXperiment (LINX), an inter-biome comparison study of nutrient uptake, is a significant contribution to the study of nitrogen dynamics in streams. A key aspect of LINX is a large number of study sites throughout the US, where a highly refined and consistent protocol is used for data collection at all sites. The first phase of LINX showed that smaller streams were more efficient in the uptake of ammonium than larger streams (Peterson *et al.* 2001). The second phase, LINX II, addressed the fate of nitrate in streams across eight sites in various regions. Each site included nine streams spanning a gradient of land use, including urban, agricultural, and reference (Mulholland *et al.* 2004). By investigating a large sample of streams across diverse regions, the LINX studies addressed limitations of previous studies that investigated a relatively small number of sites in one region.

Although LINX II studies may not have involved robust geomorphic characterizations, physical influences including F_{med}^{200} (fraction of median travel time due to transient storage) and slope were still found to influence total nitrate uptake lengths (Hall *et al.* 2009). Mulholland *et al.* (2009) focused on denitrification rates in small streams and found that although denitrification rates were higher in streams with higher nitrate concentrations, the removal efficiency by denitrification decreases as streams become saturated with nitrate and a smaller percentage of stream nitrate load is removed. Denitrification rates were higher, as represented by shorter denitrification

uptake lengths, in streams with higher F_{med}^{200} values, indicating longer residence times in transient storage zones (Mulholland *et al.* 2009). Furthermore, larger transient storage zones may be associated with higher rates of nutrient uptake when compared to streams with smaller transient storage zones (Mulholland *et al.* 1997). Further biological associations were found through structural modeling performed in LINX II studies where denitrification was linked with ecosystem respiration, and total nitrate uptake was linked with ecosystem photosynthesis (Mulholland *et al.* 2008). Nitrate removal efficiency generally increased with increases in gross primary production (GPP), which implies that autotrophic assimilation was a key mechanism of nitrate removal in these study reaches, whereas reaches with higher nitrate concentrations tended to have reduced total nitrate removal efficiency (higher uptake lengths) when compared to reaches with lower nitrate concentrations (Hall *et al.* 2009).

2.4 MODELING APPROACHES IN TRANSIENT STORAGE AND NITRATE UPTAKE

Because it is important to distinguish between hydrologic and non-hydrologic processes affecting nitrate uptake (Stream Solute Workshop 1990), models that explicitly include transient storage have also been used as an alternative to the spiraling length method. Transient storage includes both in-stream backwater areas and hyporheic exchange, and is described as temporary retention of water and solutes that are moving slower than water in the main channel (Webster and Valett 2007). The use of transient storage models (TSMs) characterizes transport processes and residence times in storage zones, which can be associated with estimates of nutrient uptake (O'Connor *et al.* 2009).

TSMs simulate the transport processes of advection, dispersion, and transient storage of a conservative solute (D'Angelo *et al.* 1993; Ensign and Doyle 2005).

Solute transport models, such as the One-dimensional Transport with Inflow and Storage (OTIS) model, provide a means of differentiating between uptake in the main channel versus uptake in storage zones by estimating uptake rates separately for both areas independently (Runkel 2007). Adding a reactive solute to the model yields a reactive solute transport model (RSTM), which accounts for first-order uptake and sorption to sediments (Scott *et al.* 2003; Gooseff *et al.* 2005). Improved understanding of biogeochemical cycling processes is acquired by simulating reactive solute dynamics in streams using RSTMs (Bencala 2005). Because transient storage consists of in-channel storage and hyporheic storage, models have been developed to differentiate these storage zones. The Solute Transport in Rivers (STIR) model is an extension of a TSM that includes an advective pumping model to simulate hyporheic retention and distinguish among multiple storage zones (Marion *et al.* 2008). Additionally, Briggs *et al.* (2009; 2010) utilized the OTIS model to develop a two-zone model, separating in-stream surface transient storage from hyporheic transient storage, as biogeochemical processes operate differently in each zone.

Output data from the OTIS model include the cross-sectional area in the main channel (A) and a representative cross-sectional area of the storage zone (A_s). The ratio A_s/A normalizes the size of the storage zone to allow for comparisons of water and solute retention in streams (Morrice *et al.* 1997). Retention of water and solutes through hyporheic exchange is a primary control on nutrient dynamics and biogeochemical processes in streams, which further impacts solute dynamics (Bencala 2005). In a study

examining the influence of hyporheic exchange on nitrate uptake across three streams, the ratio A_s/A accounted for most of the variability in nitrate uptake lengths among streams (Valett *et al.* 1997).

2.5 RESTORATION GOALS TO PROMOTE NITRATE UPTAKE

With a goal of enhancing nitrate uptake in streams, restoration projects can be designed to implement approaches that can also promote nitrogen removal, such as increasing connectivity with adjacent floodplains and improving contact of stream water and substrate (Craig *et al.* 2008). From a holistic standpoint, restoring ecosystem function in streams includes “hyporheic restoration” through implementation of channel features or restoration of processes to build such features that promote hyporheic exchange and lead to more complexity by creating backwater areas and local changes in bedslope (Hester and Gooseff 2010). By enhancing hydrologic connectivity with the hyporheic zone, stream restoration could promote reach-scale denitrification (Klockner *et al.* 2009).

In a study comparing maintained (removal of fine sediments and vegetation) and unmaintained agricultural ditches, Powell and Bouchard (2010) found that unmaintained ditches developed vegetated benches that accrued organic material and increased denitrification. Although the potential efficacy of stream restoration as tool for enhancing nitrate uptake can be inferred to some extent from previous studies, few studies have directly documented effects of restoration implementation on nitrate uptake. The growing empirical evidence of linkages between geomorphic characteristics, hydraulics, transient storage, and nutrient uptake underscores the importance of

developing empirical relationships or scaling techniques so that these associations can be applied in stream restoration design (O'Connor *et al.* 2009). Because restoration projects are often implemented without verification in the field, it is important to evaluate methods and outcomes of restoration projects, including ecological responses (Palmer 2009).

2.6 LAND USE EFFECTS ON NITRATE UPTAKE

Changes in land use alter hydrologic and geomorphic characteristics of streams, which, in turn, can markedly influence ecological responses including nutrient dynamics (Poff *et al.* 1997; Allan 2004). Urbanization alters flow regimes and typically leads to increased magnitude and frequency of moderate to high flows and increased flashiness, or how quickly flow magnitudes change (Poff *et al.* 2006). In relating flashy flow regimes to nutrient transport, Konrad and Booth (2005) showed that the movement of organic matter and nutrients in flashy flow regimes with high storm flows mainly occurs in quick periods of swift movement with limited retention. Urban streams often have elevated levels of nutrients and flashier hydrographs, as well as reduced efficiency of nutrient retention (Walsh *et al.* 2005). Additionally, fine benthic organic matter (FBOM) is flushed from streambeds during high flows and that FBOM was associated with nutrient uptake, both of which declined with increasing urbanization (Meyer *et al.* 2005). Because high flows can reconfigure substrate material and flush streambeds of algal biomass, hyporheic exchange is a prominent source of nutrient uptake shortly after high flow events (Orr *et al.* 2009). As time passes after major flow events and algal biomass accumulates on streambeds, bed porosity decreases and nutrient uptake shifts from being

limited by physical controls (hyporheic exchange) to biological controls (benthic interactions) (Orr *et al.* 2009). By studying coupled effects of physical and biogeochemical drivers of nitrate uptake, nitrate removal efficiency was found to decrease with independent increases in nitrate concentrations and discharge (Alexander *et al.* 2009).

Although many nutrient uptake studies are performed when discharges are near base flow, Doyle (2005) included hydrologic variability in nutrient uptake modeling to determine an effective discharge that accounts for the largest quantity of nutrient retention, but did not incorporate transient storage and variation in geomorphic and biotic influences on nutrient uptake. Furthermore, variability in geomorphic setting and temporal variability may not yield a monotonic relationship between discharge and nitrate uptake. Nitrate uptake is a complex process that is mediated by physical characteristics of stream type, geomorphic setting, and restoration techniques, as well as biogeochemical conditions that vary among streams. Accordingly, nitrate uptake in streams is likely to exhibit a complex response to flow variation.

3 METHODOLOGY

3.1 SITE SELECTION

To examine linkages between geomorphic complexity, transient storage, and nitrate uptake in streams affected by different land use influences, I chose a total of nine study reaches along an urban stream and two agricultural streams for investigation. Study reaches were chosen across a gradient of restoration techniques and modifications within each stream such that the study reaches represent distinct geomorphic settings. After designating study reaches of varying geomorphic characteristics including substrate size, sinuosity, and bed slope, and with various styles of restoration and management, I performed detailed physical characterizations and multiple nutrient injections in each reach. The following sections provide an overview of the locations (Figure 3.1), geomorphic setting, and intrasite variability of the three streams.

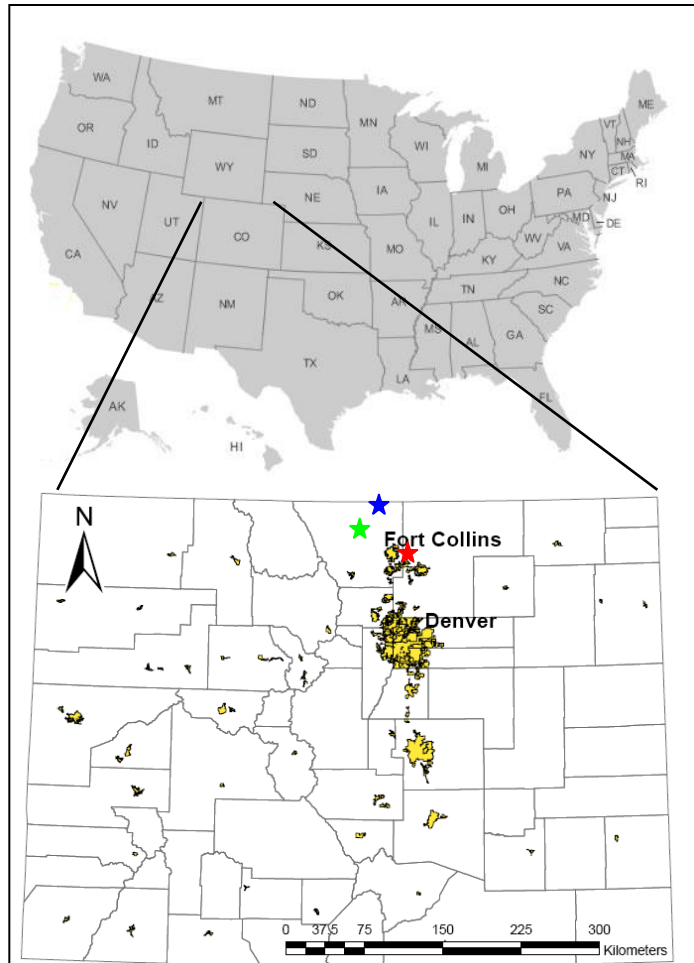


Figure 3.1: Location of study reaches

3.1.1 Spring Creek – urban stream

- Location: Fort Collins, Colorado
- Geographic Coordinates: N 40°30'50", W 105° 4' 7"
- Elevation: approximately 1525 m

Spring Creek is represented by the red star in Figure 3.1. Spring Creek runs through the city of Fort Collins (Figure 3.2) and acts as a primary conduit for storm water drainage within the city. The flow in Spring Creek is highly regulated by storm water retention facilities yet retains a flashy flow regime. Due to flooding history, several sections of the stream have undergone channelization, bank and bed stabilization, and loss of riparian

vegetation. Other reaches are more “naturalized” and have connected floodplains with patches of riparian forest, and lack conspicuous channel armoring features. I selected three reaches along Spring Creek to investigate (Figure 3.3). The chosen reaches vary substantially in their overall physical characteristics and provide a range of geomorphic complexity and potential influences on nitrate uptake. Each reach is about 180 m in channel length and free of tributary inputs, dams, irrigation offtakes, and major land use changes. The study reaches are characterized as a pool-riffle reach (Edora Park), a stabilized reach (Stuart), and a plane bed reach (Railroad). Edora Park, the least modified reach, is located in a city park and has lost some riparian vegetation due to lawn maintenance and mowing close to the stream banks. Edora Park is the most sinuous of the three reaches and has the median gradient and grain size of the three chosen reaches. Stuart has been greatly modified with grouted bank stabilization and grade-control structures. Stuart has the highest gradient and grain size and has the median sinuosity of the three reaches. Railroad has banks covered with dense, tall grasses and has also been modified through channelization. Railroad is the straightest reach and has the lowest gradient and smallest grain size of the three reaches on Spring Creek.



Figure 3.2: Location of Spring Creek in Fort Collins, Colorado (image courtesy of U. S. Geological Survey (USGS)); yellow shading denotes study reaches



(a) Edora Park



(b) Stuart



(c) Railroad

Figure 3.3: Study reaches along Spring Creek

3.1.2 Sheep Creek – agricultural stream

- Location: 88 km northwest of Fort Collins, Colorado, and 16 km north of Red Feather Lakes
- Geographic Coordinates: N 40° 55' 48", W 105° 38' 16"
- Elevation: approximately 2550 m

Sheep Creek is represented by the blue star in Figure 3.1. Sheep Creek is located in north central Colorado in the Roosevelt National Forest along Larimer County Road 80C and drains Eaton Reservoir (Figure 3.4). Despite the reservoir, Sheep Creek typically has high flow volumes and duration in the spring and summer from snowmelt runoff, as well as drainage from emptying the reservoir. Much of the open rangeland surrounding Sheep Creek has been grazed by cattle for at least a century. In the 1950s, sections of Sheep Creek were fenced off and exclosed from cattle grazing. The riparian corridors of these sections naturally revegetated and are now dense with willows. Other sections of Sheep Creek are currently being grazed. Continual cattle-grazing can lead to bank failure and nutrient loading in streams (Waters 1995). I located four reaches along Sheep Creek to investigate (Figure 3.5). Each reach is about 180 to 200 m in channel length and free of tributary inputs, dams, irrigation offtakes, and major land use changes. Two reaches have been exclosed from grazing since the 1950s, and two reaches are currently grazed. Reaches A and B are located within the cattle grazing exclosures, and Reaches C and D are currently grazed. Reach A is straighter, has a higher gradient, and has a larger grain size than Reach B. Similarly, Reach C is straighter, has a higher gradient, and has a larger grain size than Reach D. I chose these reaches so that I could compare two similar

stream types that have been naturally rehabilitated from grazing pressure and two similar stream types that are currently grazed.

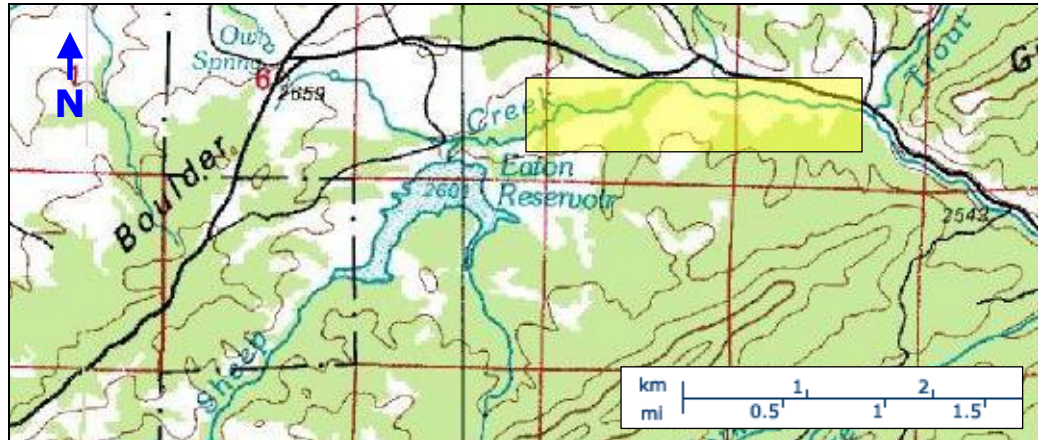


Figure 3.4: Location of Sheep Creek in Northern Colorado (image courtesy of USGS); yellow shading denotes study reaches



(a) Sheep A



(b) Sheep C



(c) Sheep B



(d) Sheep D

Figure 3.5: Sheep Creek study reaches

3.1.3 Nunn Creek – agricultural stream

- Location: 55 km northwest of Fort Collins, Colorado, and 25 km west of Red Feather Lakes, Colorado
- Geographic Coordinates: N 40° 47' 56", W 105° 52' 21"
- Elevation: approximately 2800 m

Nunn Creek is represented by the green star in Figure 3.1. Nunn Creek is located on Rose Valley Ranch in the Laramie River Basin in North Central Colorado near the Rawah Wilderness area of the Roosevelt National Forest (Figure 3.6). Nunn Creek is a tributary of the Laramie River, and the area surrounding Nunn Creek is grazed by horses and cattle that belong to the owners of Rose Valley Ranch. Dave Rosgen of Wildland Hydrology utilized a combination of boulders and rootwads to design J-hook and log vane structures (Natural Resources Conservation Service (NRCS) 2007) for bank stabilization and trout habitat enhancement along portions of Nunn Creek within the property of Rose Valley Ranch. These restoration structures were constructed in 2003. I located two reaches along Nunn Creek – one where structures have been implemented and one with no restoration structures present (Figure 3.7). The study reach with restoration structures contains one combination J-hook/log vane structure and four J-hook vane structures near meander bends, as well as some riprap bank stabilization. The study reach without restoration structures is located downstream of the restored reach and upstream of the confluence with the Laramie River. Both reaches have relatively similar sinuosity and gradient. For consistency, each reach is about 180 m in channel length and free of tributary inputs, dams, irrigation offtakes, and major land use changes. This is the longest reach length that could be attained without structures present for Nunn A,

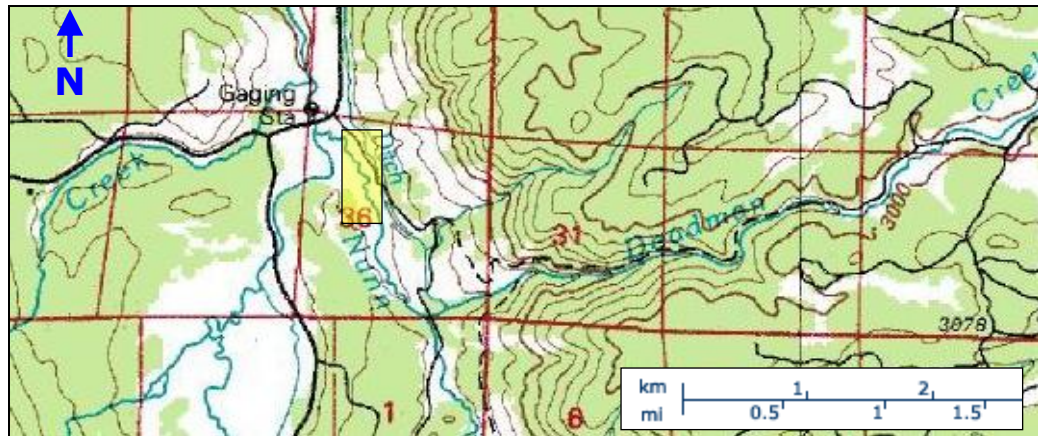


Figure 3.6: Location of Nunn Creek in Northern Colorado (image courtesy of USGS); yellow-shading denotes study reaches



(a) Nunn A



(b) Nunn B

Figure 3.7: Nunn Creek study reaches

3.2 DATA COLLECTION

For consistency, the typical reach length used in this study is 180 to 200 m, due to constraints of reach lengths free of visible tributary or pipe inflows and outflows. For the purpose of physical characterization, including hydraulic measurements and channel geometry survey, each reach was divided by twenty-one equally-spaced transects with T1 representing the most upstream transect and T21 representing the most downstream transect. Each transect was positioned perpendicular to the flow at that point along the reach.

3.2.1 Nutrient Injections

The protocol for nutrient injection and sample collection was developed to provide the data needed for modeling transient storage and nitrate uptake. Nutrient injections were performed before any of the physical characterization to avoid disturbance in the streams that would influence nitrate uptake and transient storage. Because nitrate concentrations were very low in the collected samples, special care was taken to thoroughly sanitize sample bottles and sampling equipment and to avoid cross-contamination between the equipment and the injection solution. All sample bottles, filter heads, and syringes were cleaned using a four-step process of 10% HCl acid bath,alconox solution, and two tubs of nanopure water. Nitrile gloves were worn during this process, as well as during the capping and labeling of the bottles. All bottles were air dried before capping. Pre-printed waterproof adhesive labels were applied to the sample bottles prior to sample collection for ease in the field. Labels noted the sample date, stream and reach location, time of sample collection, and individual sample

identification. The labeled bottles were arranged in trays in chronological order of sampling times.

Samples were collected on a time-series basis at the downstream end (last transect; T21) of the reach. The injection point was located in a turbulent mixing zone approximately 180 to 200 m upstream of the last transect of the reach. When a well-mixed turbulent zone was not adequate for good mixing, baffles (Figure 3.8) were made from acrylic panels and rebar and placed at strategic locations immediately downstream of the injection point to promote mixing.

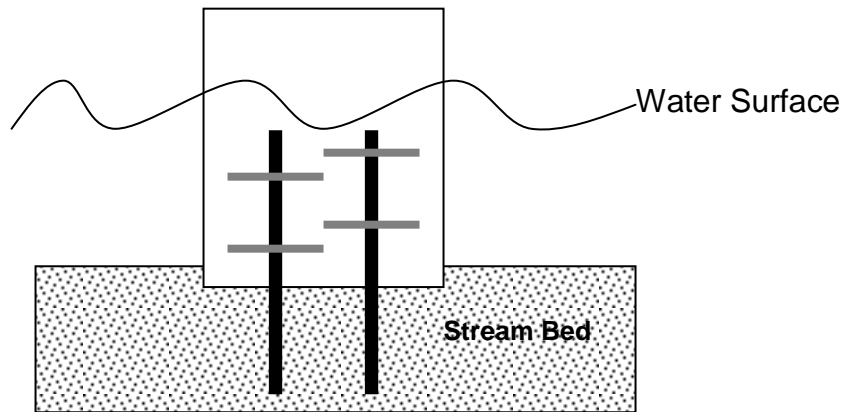


Figure 3.8: Downstream view of baffle placement

The injection solution of potassium nitrate (KNO_3) and sodium bromide (NaBr) was prepared with nanopure water on the day prior to the injection. The conservative tracer of NaBr was used, and $[\text{Br}^-]$ was measured because Br^- does not naturally occur in these streams. The mass of KNO_3 and NaBr in the injection solution was based upon a typical flow rate of 70 L/s, which was within the range of previous flows measured in the study reaches. The background $[\text{NO}_3^-\text{-N}]$ was measured at approximately 0.4 mg/L in Spring Creek. This was the background $[\text{NO}_3^-\text{-N}]$ used when mixing the injection solution. The background $[\text{NO}_3^-\text{-N}]$ was elevated by a factor of four, and the $[\text{Br}^-]$,

assumed to be negligible in the study reaches, was elevated to 2 or 3 mg/L. Based upon these desired in-stream concentrations and a typical flow rate, the injection solution was mixed with known concentrations of KNO₃ and NaBr. The mass of the solutes in the volume of solution was compared with a solubility chart to ensure that the mixture would not be super-saturated. This standard injection solution was prepared for all reaches, and the rate at which the solution was injected into the stream depending upon the flow rate on the day of the injection. A nutrient release planning sheet (Figure 3.9) was created in Microsoft Excel[®] and used to determine the injection solution mixture and the injection rate on the day of injection.

Nutrient Release Planning Sheet								
LAB CALCULATION			FIELD CALCULATION					
	Discharge ==>	70	L/s		Discharge ==>	40	L/s	
	Level 2 Pump Rate ==>	250	mL/min		Level 2 Pump Rate ==>	143	mL/min	
	Release Duration ==>	60	min		Release Duration ==>	60	min	
	L of Sol Needed ==>	15.00	Liters		L of Sol Required ==>	8.57	Liters	
0	KNO ₃	Bkgrnd [NO ₃ -N] ==>	0.400	mg/L strm H2O	KNO ₃	Bkgrnd [NO ₃ -N] ==>	0.400	mg/L strm H2O
1	4	Desired Add'n [NO ₃ -N] ==>	1.600	mg/L strm H2O	4	Desired Add'n [NO ₃ -N] ==>	1.600	mg/L strm H2O
2	Add'n x	molecular weight KNO ₃ ==>	101.11	g/mol	Add'n x	molecular weight KNO ₃ ==>	101.1	g/mol
3		molecular weight N ==>	14.01	g/mol		C of [NO ₃ -N] inj ==>	26.88	g/L release sol
4		C of [NO ₃ -N] inj ==>	26.88	g/L release sol		C of KNO ₃ inj ==>	193.993	g/L release sol
5		C of KNO ₃ inj ==>	193.993	g/L release sol				
6								
7	NaBr	Bkgrnd [Br] ==>	0	mg/L strm H2O	KBr	Bkgrnd [Br] ==>	0	mg/L strm H2O
8		Desired Add'n [Br] ==>	3.00	mg/L strm H2O		Desired Add'n [Br] ==>	2.00	mg/L strm H2O
9		molecular weight NaBr ==>	102.89	g/mol		C of [Br] inj ==>	50.40	g/L release sol
0		molecular weight Br ==>	79.9	g/mol		C of NaBr inj ==>	64.90	g/L release sol
1		C of [Br] inj ==>	50.40	g/L release sol				
2		C of NaBr inj ==>	64.90	g/L release sol				
3								

Figure 3.9: Nutrient Release Planning Sheet used for injections

On the day of injection, the flow rate was measured using a Marsh-McBirney flow meter to measure velocity and a metric wading rod to measure depth. The wading rod was used to adjust each velocity reading to 0.4*depth from the streambed at each station for the depth-averaged velocity at that point. A measuring tape was stretched across the stream perpendicular to the predominant flow direction at each transect. The

station of the edge of water was noted at the left and right banks. Approximately 10 to 15 points were measured in between the wetted edges of the stream, noting station, depth, and velocity. This was performed at two cross-sections to calculate two separate discharge measurements using the velocity-area method (Harrelson *et al.* 1994). If the flow calculations fell within 10% of each other, the average flow rate was used to determine the rate of injection. If not, flow rates were measured at additional cross-sections until two flow rate calculations were within 10% of each other.

Additionally, prior to injection, background water samples were collected at the upstream end (T1), middle (T11), and downstream end (T21) of the reach. Samples were collected using a 60 mL syringe and a 0.7 μm filter placed in a filter head at the end of the syringe. The water samples were filtered through the syringe into 20 mL plastic bottles. After collection, the water samples were stored in a plastic resealable bag on ice in a cooler until placed in a freezer at the end of day of data collection. The background water samples were collected to verify the background concentrations of NO_3^- -N and Br^- . One sample bottle was collected at each of the three background locations along the reach, with a duplicate background sample at the upstream end at T1.

The aqueous KNO_3 and NaBr solution was injected into the stream as a steady-rate pulse for 60 min using a Watson Marlow (Model 323S/D) peristaltic pump. Samples were collected at 3-min intervals at T21 for downstream break-through curves (BTCs) of NO_3^- and Br^- . Sample collection began 10 min before the injection started to obtain a background level of NO_3^- and Br^- , and it continued for 1 hr and 50 min after the injection stopped, totaling 3 hrs of sample collection, to obtain a plateau and tail of the BTCs. As with the background samples, samples were collected using a 60 mL syringe and a 0.7

μm filter placed in a filter head at the end of the syringe. The filter and syringe were rinsed three times between each 3-min sampling interval. The water samples were filtered through the syringe into 20-mL plastic bottles. Duplicate samples were collected at time steps of 0:15, 1:00, 1:45, and 2:30. After collection, the water samples were stored in a plastic resealable bag on ice in a cooler until placed in a freezer at the end of day of data collection.

3.2.2 Physical Habitat Units

On the day of injection, each reach was classified into physical habitat units. The layout of transects divided the reach into twenty equally-spaced sub-reaches. A visual characterization was performed to describe the physical condition of the reach, including channel type and channel modifier. Channel types were assigned following Montgomery and Buffington (1997). Each reach was further described as having any channel modifications, such as drop structures, toe protection, and bank stabilization. An example of the field sheet used for the physical habitat unit classification is shown in Figure 3.10.

Sub-reaches were classified by specific habitat units, including distinct combinations of geomorphic unit, sediment classification, substrate condition, and flow obstruction. This type of classification can be referred to as describing patchiness or spatial heterogeneity (Pringle *et al.* 1988; Cooper *et al.* 1997). Each areal sub-reach was designated by the percent of each distinct habitat unit falling within that area. Each transect was assigned by the habitat unit that it intersected. If the transect was the

dividing line between two different habitat units, it was not assigned a distinct habitat unit. Each specific habitat unit was identified by a different letter (i.e., A, B, C, etc.).

Physical Habitat Field Sheet												
STREAM NAME:						DATE:						Page 1
CHANNEL TYPE:			CHANNEL MODIFIER:									
Pool Riffle	Bedrock		Drop Structures									
Step Pool	Toe Protection											
Plane Bed	Colluvial		Cascade									
	Bank Stabilization		Grassy Banks									
	Cascade		Riffle									
Dune Ripple			Bedrock									
			Run									
			Cobble									
			Fines Draped									
			Armored									
			Vegetated									
			None									
			A %0 to %25									
			B %25 to %50									
			C %50 to %75									
			D %75 to %100									
Habitat Unit Identification			Components of Habitat Unit Classification						Composition of Flow Obstruction			
UNIT	US Station (m)	% of Area	Transect Assigned	Left Bank Riparian Veg	Right Bank Riparian Veg	Geomorphic Unit	Sediment Size Class.	Substrate Condition	Extent of Flow Obstruction	% Inorganic	% Woody/Leaf	% Vegetation

Figure 3.10: Example of Physical Habitat Field Sheet used in visual characterization and classification of areal sub-reaches into habitat units

The riparian vegetation was characterized separately for the left and right banks along each unit based upon the Hey and Thorne (1986) classification of grassy banks (Type I), 1 to 5% tree/shrub cover (Type II), 5 to 50% tree/shrub cover (Type III), and greater than 50% tree/shrub cover (Type IV). The main distinguishing classification between the habitat units was the geomorphic unit, which was adapted from Level II Channel Geomorphic Unit classification of Hawkins *et al.* (1993) (Figure 3.11). The turbulent fast water is termed as riffle, and the non-turbulent fast water is termed as run. Turbulent riffles are more likely to induce flow into the hyporheic zone, whereas slow-moving pools may have areas of in-stream transient storage, as well as providing longitudinal breaks in slope that can induce hyporheic exchange (Harvey and Bencala 1993). This is an important distinction to make when characterizing geomorphic complexity as it relates to transient storage and hyporheic exchange.

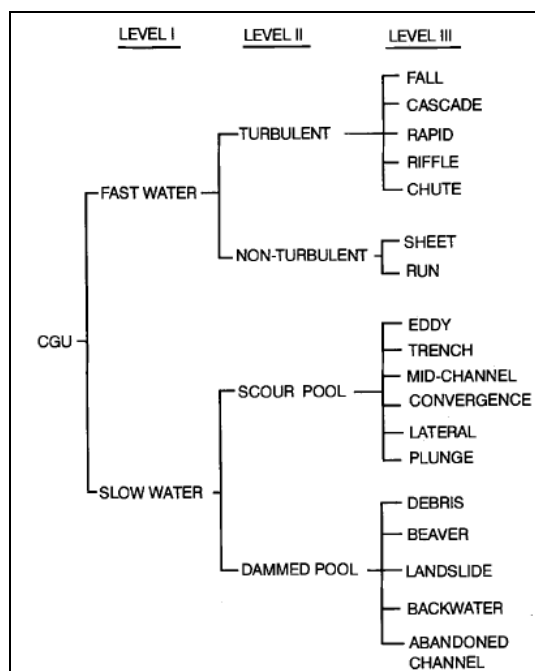


Figure 3.11: Channel Geomorphic Unit classification (Hawkins *et al.* 1993)

Another component of the physical habitat unit classification was the sediment size class. A detailed pebble count, as described in Section 3.2.6, was performed to further characterize the sediment size distribution, but a visual estimate of general sediment size class was noted when determining physical habitat units. The following classes of sediment size were used to characterize habitat units: bedrock, boulder (4,096 to 256 mm), cobble (64 to 256 mm), gravel (2 to 64 mm), sand/silt/clay (<2 mm) (Julien 1998). Because sediment size class can vary across geomorphic units, different habitat units would be assigned to the same geomorphic unit if there were multiple sediment size classes within one geomorphic unit.

To further characterize the stream bed, the condition of the substrate was also noted for each habitat unit. Observing the substrate condition can provide insight into

local hyporheic processes. The substrate was described by one of the following six categories.

- Fines particle drape over all particles
- Armored surface with more fines in subsurface than on surface (surface $d_{50} >$ subsurface $2d_{50}$)
- Vegetated channel bottom (not including algae/periphyton)
- Algal mat covering substrate
- Fine sediment (<2 mm) matrix around gravel and/or cobbles
- No difference between surface and subsurface

Because flow obstructions in streams can lead to slower velocities, greater contact time with substrate, and retention of organic matter (Craig *et al.* 2008), the final element observed in describing physical habitat units was flow obstruction. Both the extent of flow obstruction and the composition of the obstruction were noted for each habitat unit. A new habitat unit was not designated based upon flow obstruction extent or composition, but flow obstruction was used as a modifier of each habitat unit to further depict the stream character. Each habitat unit was categorized as having an extent of flow obstruction within the areal unit of none, 0 to 25%, 25 to 50%, 50 to 75%, or 75 to 100%. The composition of flow obstruction was classified as inorganic materials (e.g., boulders), instream wood and leaf litter, and vegetation.

3.2.3 Benthic Organic Matter

On the day of injection, samples of benthic organic matter (BOM) were collected to study any relationships between BOM and nutrient uptake along the stream ecosystem,

as organic matter can be a source of carbon and energy for nitrogen-processing microbial communities. BOM samples were collected at particular transects based upon the distribution of habitat units. The number of samples collected along each reach ranged from six to ten samples, depending on the number and proportion of habitat units for that reach. Samples were divided between fine BOM (FBOM; <0.5 mm) and coarse BOM (CBOM; >0.5 mm).

A cylinder of known circular area, such as a 5-gal bucket with the bottom removed, was driven several centimeters into the stream bed to form a seal that would hinder water from the water column entering into or leaving the cylinder. Any large pieces of organic matter within the cylinder, such as leaves, sticks, grasses, or algae, were removed and placed into an aluminum foil pouch. The substrate was then stirred up to a depth of approximately 10 cm, where possible. The resulting slurry consisted of suspended BOM and fine sediments in the water column in the cylinder. A plastic container approximately 1 L in volume was used to scoop the slurry mix from the cylinder and through a 0.5-mm sieve attached to the top of a 5-gal bucket. The FBOM passed through the sieve and collected in the bottom of the bucket. The CBOM was retained in the sieve. After filling the bucket to a same depth as the water depth at that point in the stream, the CBOM was removed from the sieve and placed in the aluminum foil pouch. The FBOM sample was collected by stirring the slurry water in the bucket to ensure suspension of any settled particles and filling a 4-oz plastic bottle with the water. This procedure was adapted from Golladay *et al.* (1989).

3.2.4 Hydraulic Measurements

On the day of injection, depth, width, and depth-averaged velocity were measured at each transect to further describe the variation in physical attributes along each reach. Hydraulic measurements were collected in the same manner as described for measuring flow rate in Section 3.2.1. At least five points were measured across the wetted width of the stream. The station, depth, and velocity were measured at each point, and the point representing the thalweg was noted as such. The hydraulic measurements at each transect were used to characterize the flow attributes of the habitat unit assigned to that transect.

3.2.5 Dissolved Oxygen Measurements

After physical measurements were complete on the day of injection, dissolved oxygen (DO), temperature, and barometric pressure were recorded with an In-Situ Troll 9000 Multi-parameter Probe, using the optical DO, temperature, and barometric sensors. The probe was deployed near the middle of the reach length and recorded DO and temperature at 10-min intervals for a period of 48 hrs. The 48-hr deployment period was used for calculating whole-stream metabolism and should be representative of weather conditions on the day of the injection. The probe was secured to the stream bed by enclosing it in 4-in. drainage pipe and staking the drainage pipe to the bed with 24-in. sections of #4 rebar (Figure 3.12). For correct DO measurements that did not require adjustments for changes in barometric pressure, a vented cable was attached to the probe, and a desiccant cap was placed in the end of the cable. The end of the cable was secured to the rebar above the water surface so that it would not be submerged, and the vented cable was open to the atmosphere.

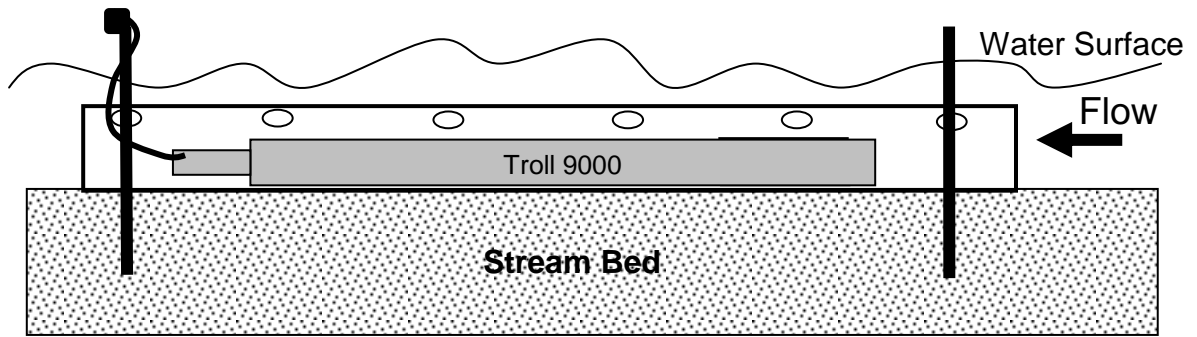


Figure 3.12: Side-view of Multi-parameter Probe Deployment

3.2.6 Substrate Distribution

Data were collected on the size distribution of the surface bed sediments to further describe the patchiness of the areal habitat units. Pebble counts were performed based on Bunte and Abt (2001b), using a sampling frame (Figure 3.13) and gravelometer. The sampling frame helps to prevent bias towards larger clasts or clasts protruding higher into the water column (Bunte and Abt 2001a). The stone that falls at each intersection on the grid is measured using gravelometer. Instead of using a ruler to measure the intermediate diameter of the stone, the gravelometer is a template that has square holes of 0.5-incremental Φ sizes, and the stone is identified by the largest Φ size that retains the stone. The Φ size relates to intermediate diameter of the stone by the equation $2^\Phi = \text{mm length of intermediate diameter}$. The Φ sizes on the gravelometer distinguish each sediment class from silt and clay ($<2 \text{ mm} = \Phi \text{ size } <1.0$) to small cobbles ($128 \text{ mm} = \Phi \text{ size } 7$). Stones larger than this are measured along their intermediate diameter and are assigned to an Φ size class accordingly. In an attempt to avoid double-counting of the same stone, the frame was assembled so that the grid was between d_{max} (the intermediate diameter of

the largest surface stone in the reach) and $2*d_{max}$. If a stone happened to cross two intersections in the grid, the stone was only counted once.

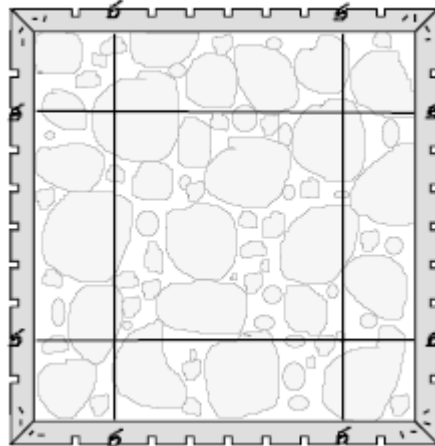


Figure 3.13: Sampling frame (Bunte and Abt 2001a)

Clasts were counted at each transect by placing the frame along the cross-section. The number of stones measured at each transect depended on which habitat unit was assigned to that transect. Each habitat unit had a count of at least 100 stones, with a minimum of 300 stones for the entire reach. The number of stones measured at each transect was distributed proportionally among the habitat units.

3.2.7 Channel Geometry Survey

Longitudinal and cross-section surveys were performed using a Leica Total Station and prism rod. A cross-section survey was performed at each of twenty-one transects along each reach. A string was stretched across the stream perpendicular to the predominant flow direction at each transect to represent the line to follow during the cross-section surveys. Each cross-section survey noted the left and right bankfull levels, the left and right edges of water, and the thalweg. To measure cross-sectional area,

survey points were taken at least every 0.5 m across each transect. In addition to a thorough survey of each transect geometry, intermediate points of the thalweg and the left and right edges of water were surveyed between each transect at least at 3-m intervals, making sure to characterize any breaks in slope, meanders, contractions, or expansions. By collecting a high density of points within each reach, the geometry can be characterized by the longitudinal profile, variation in cross-sectional area, width variability, and water surface profile.

3.3 DATA ANALYSIS AND MODELING

Water samples collected during the nutrient injection were analyzed for NO_3^- and Br^- , and BOM samples were analyzed as ash-free dry mass (AFDM). Post-processing of physical data collected was performed to obtain the necessary parameters used to further investigate geomorphic complexity.

3.3.1 Lab Analysis of Water Samples

All water samples collected, both background and BTC samples, were frozen when sampling was complete for the day. The samples remained frozen until they were taken to an analytical lab. Samples were analyzed by Stewart Environmental Consultants, Inc. in Fort Collins, Colorado, where the lab would thaw the samples just prior to analysis. Each sample was analyzed for concentration in mg/L of nitrate as nitrogen (NO_3^- -N) and Br^- using U. S. Environmental Protection Agency (EPA) Method 300.0 on an ion chromatograph. The method detection limit (MDL) is 0.1 mg/L. Any samples with concentrations less than the MDL were reported as “Not Detected.”

Duplicates were analyzed on a frequency of approximately one duplicate in every thirteen samples to check for quality assurance.

3.3.2 Lab Analysis of BOM Samples

All BOM samples were analyzed using the drying oven and muffle furnace in the Civil and Environmental Engineering Water Quality Laboratory in the Engineering Building at CSU. Each sample was thawed in a lukewarm water bath just prior to analysis. The lab techniques in accordance with the *Standard Methods for the Examination of Water and Wastewater* (American Public Health Association (APHA) 1998).

For measuring FBOM quantity in each sample, a glass-fiber filter (Whatman GF/A, 1.6- μm particle retention) was placed into a Buchner funnel attached to a vacuum pump. Each FBOM sample was thoroughly shaken to ensure that all particles were in suspension. A subsample of 50 mL was measured out into beaker, and the subsample was poured onto the filter paper in funnel. The beaker was rinsed out several times with deionized (DI) water to ensure that no particles were left in the beaker. The edges of the funnel were also rinsed with DI water to make sure that all particles were on filter. After all water was pulled through funnel, the filter paper was removed and placed in a crucible. The crucible number was cross-referenced with the sample number and recorded on the BOM analysis data sheet. The crucible was placed in the drying oven at 105°C overnight or for 24 hrs. The crucible was then removed from the drying oven and placed on a ceramic tray to cool.

Each crucible was weighed, and the mass of the crucible with dried sample and filter was recorded. Next the crucible was placed in the muffle furnace at 500°C to oxidize. The amount of time that each sample spent in the muffle furnace depended on the amount of organic matter in the sample. CBOM would spend more time in the muffle furnace than FBOM to ensure that the organic matter was completely ashed. The crucible was removed from muffle furnace with tongs and mitts, and the crucible was allowed to cool. The crucible was reweighed, and the mass of the crucible with remaining sample and filter was recorded. The oxidized mass was subtracted from the dried mass, and the difference in mass was divided by the subsample volume to get a concentration. The volume of stream water in the bucket cylinder used to collect the sample was calculated by multiplying the average depth at the transect on the day the sample was collected by the area of the bucket cylinder. The subsample concentration was multiplied by the volume of stream water in the bucket cylinder to obtain the total mass in the bucket cylinder. This total mass was divided by the area of the bucket cylinder to result in the AFDM in units of mg/cm^2 .

To measure the quantity of CBOM in the samples, each aluminum foil sample pouch was placed in an aluminum pie/loaf pan. Each sample number was cross-referenced with the pan number. The foil sample pouch was unfolded to lay flat in the pan, and small holes were ripped open in the top of the pouch to promote drying, making sure that none of the sample was lost. Each pan was placed in the drying oven at 105°C overnight or for 24 hrs. The pan was then removed from the drying oven and let cool. Next, the pan was weighed, and the mass of the pan with dried sample and foil pouch was recorded. Each pan was placed in the muffle furnace at 500°C to oxidize. The amount of

time that each sample spent in the muffle furnace depended on the amount of organic matter in the sample to ensure that the organic matter was completely ashed. The pan was removed from the muffle furnace with tongs and mitts and allowed to cool. Each pan was reweighed, and the mass of the pan with remaining sample and foil pouch was recorded. The oxidized mass was subtracted from the dried mass, and the difference in mass was divided by the area of the bucket cylinder used to collect the sample. The result is the AFDM in units of mg/cm².

3.3.3 Post-processing of Physical Variables

Collected physical data were processed using formulas in Microsoft Excel[®] spreadsheets for the following equations. These variables were chosen based upon *a priori* knowledge, including mechanistic understanding and previous research on physical characteristics that may influence transient storage and nitrate uptake.

- Longitudinal roughness (Gooseff *et al.* 2007) = average residual between measured thalweg elevation at each point ($z_{obs,i}$) and predicted thalweg elevation based on bed slope ($z_{pred,i}$):

$$LR = \frac{\left(\sum_{i=1}^n |z_{obs,i} - z_{pred,i}| \right)}{n} \quad (3.1)$$

where n = number of measurements; sample size; and

i = individual measurement number.

- Width variability = average residual between each measured wetted width and average wetted width of the reach (w_{avg}):

$$\varepsilon_w = \frac{\left(\sum_{i=1}^n |w_{avg} - w_i| \right)}{n} \quad (3.2)$$

- Variability in cross-sectional area = average residual between each measured cross-sectional area (A_i) and average cross-sectional area of the reach (A_{avg}):

$$\varepsilon_A = \frac{\left(\sum_{i=1}^n |A_{avg} - A_i| \right)}{n} \quad (3.3)$$

- Bed substrate distribution (percent fines, d_{16} , d_{50} , d_{84}) and gradation coefficient:

$$\text{Gradation coefficient} = \frac{1}{2} \left(\frac{d_{84}}{d_{50}} + \frac{d_{50}}{d_{16}} \right) \quad (3.4)$$

- Relative submergence = ratio of hydraulic radius (R) to d_{84} :

$$\text{Relative submergence} = \frac{R}{d_{84}} \quad (3.5)$$

- Sinuosity = ratio of channel length along centerline (L) to the straight line valley length (L_v):

$$P = \frac{L}{L_v} \quad (3.6)$$

- Metric of complexity (Gooseff *et al.* 2007) = measure of potential variability in pressure head represented by bed slope (S_o) and potential variability in

lateral hydraulic complexity represented by sinuosity (P), including longitudinal roughness (LR):

$$\chi = S_o PLR \quad (3.7)$$

- Unit discharge = channel discharge (Q) divided by channel width (w):

$$q = \frac{Q}{w} \quad (3.8)$$

- Unit stream power = the product of water density ($\rho = 1000 \text{ kg/m}^3$), acceleration due to gravity ($g = 9.81 \text{ m/s}^2$), channel discharge (Q), and bed slope (S_o) divided by channel width (w):

$$\omega = \frac{\rho g Q S_o}{w} \quad (3.9)$$

- Reynolds number = ratio of inertial forces (uR) to viscous forces (ν):

$$\text{Re} = \frac{uR}{\nu} \quad (3.10)$$

where u = downstream velocity (m/s); and

ν = kinematic viscosity ($10^{-6} \text{ m}^2/\text{s}$).

- Shear velocity = kinematic surrogate for bed shear stress

$$u_* = \sqrt{gRS_o} \quad (3.11)$$

3.3.4 Modeling Whole-stream Metabolism

The Stream Metabolism Program (SMP) was used to model whole-stream metabolism for each reach, corresponding to the same time as the nutrient injection (Bales and Nardi 2007). The following measured data were used as input data in the modeling procedure.

- Reach length
- Reach-averaged wetted width
- Stream discharge
- Barometric pressure
- DO concentration measured continuously for at least 24 hrs, capturing at least one complete sunrise to sunset cycle
- Water temperature measured with DO concentration
- Specific conductivity measured with DO concentration

Because the reaeration rate coefficient was not determined directly from a propane injection, as described in Marzolf *et al.* (1994), the reaeration rate coefficient was assumed to be 0.09/min based upon model assumptions from empirical relationships. The stream metrics of length, wetted width, and stream discharge were calculated from the channel survey data and hydraulic measurements for each reach. The DO, temperature, specific conductivity, and barometric pressure were recorded with an In-Situ Troll 9000 Multi-parameter Probe.

The overall equation used in the SMP is that the sum of net ecosystem production and community respiration is equal to gross primary production (Bales and Nardi 2007). The single-station application of SMP was used due to limitations with only one available

DO probe per reach. Output data from the model include GPP rates in $\text{gO}_2/\text{m}^2/\text{day}$. These measures of whole-stream metabolism help to explain ecosystem function and may relate to nutrient uptake.

3.3.5 Modeling Transient Storage and Nitrate Uptake

The OTIS model was used to model the shape of the BTC input to estimate parameters describing transient storage and nitrate uptake (Runkel 1998). OTIS was operated through a universal inverse modeling code (UCODE), using nonlinear regression for optimizing parameter estimates (Poeter and Hill 1999). The theoretical basis for OTIS is shown in the conceptual model in Figure 3.14.

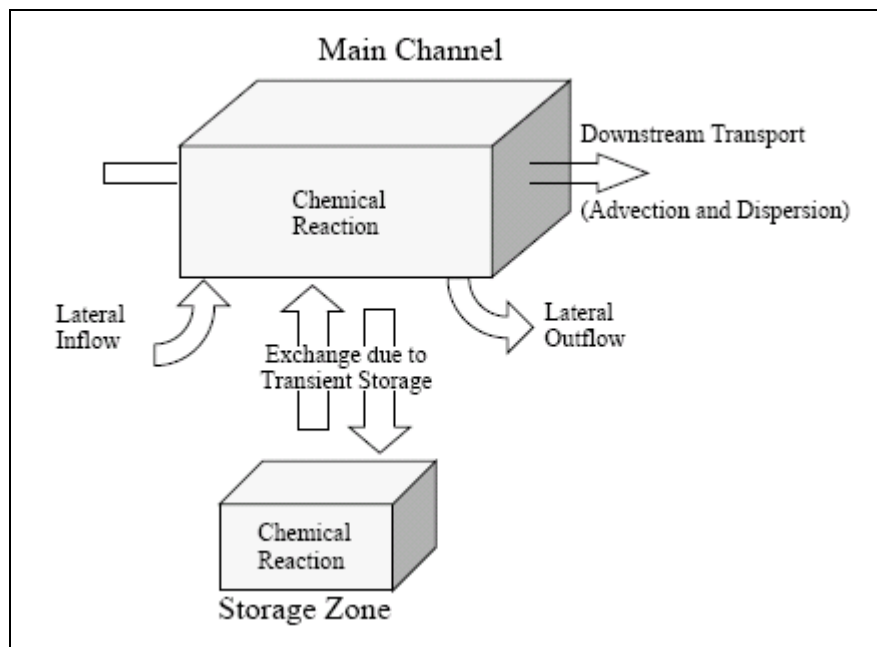


Figure 3.14: Concept basis of OTIS model (Runkel 1998)

The OTIS model is based upon the hydrologic processes of advection, dispersion, and transient storage, as well as chemical transformation through first-order decay and

sorption (Runkel 1998). For this project, the lateral inflow and outflow were assumed to be negligible, and sorption was not accounted for because nitrate does not typically adsorb to sediment particles. The resulting equations OTIS uses for this modeling, without lateral flux and sorption, are shown as Equations 3.12 and 3.13:

$$\frac{\partial C}{\partial t} = \underbrace{-\frac{Q}{A} \frac{\partial C}{\partial x}}_{\text{Advection}} + \underbrace{\frac{1}{A} \frac{\partial}{\partial x} \left(AD \frac{\partial C}{\partial x} \right)}_{\text{Dispersion}} + \underbrace{\alpha (C_s - C)}_{\text{Transient Storage}} - \underbrace{\lambda C}_{\text{1st-Order Decay}} \quad (3.12)$$

$$\frac{\partial C_s}{\partial t} = \alpha \frac{A}{A_s} (C - C_s) - \lambda_s C_s \quad (3.13)$$

where C = solute concentration in main channel (mg/L);
 t = time (s);
 x = distance (m);
 Q = discharge (m³/s);
 A = cross-sectional area of main channel (m²);
 D = dispersion coefficient (m²/s);
 α = storage zone exchange coefficient (s⁻¹);
 C_s = solute concentration in storage zone (mg/L);
 A_s = cross-sectional area of storage zone (m²);
 λ = first-order decay coefficient in main channel (s⁻¹); and
 λ_s = first-order decay coefficient in storage zone (s⁻¹).

First, transient storage was modeled using the BTCs of the conservative tracer, Br⁻. The following input data were need to model transient storage:

- Upstream boundary condition at injection point

- Downstream BTC
- Simulation start and end times
- Time interval between samples
- Reach length
- Flow rate

The background [Br⁻] was subtracted from all points along the downstream Br⁻ BTC for each reach. A moving three-point median approach was applied to the entire BTC to remove outliers. The upstream boundary condition at the injection point was entered into the model as a three-point step curve of concentration versus time, similar to the downstream boundary condition of the continuous field data BTC. The upstream boundary condition was based upon the pre- and post-injection (background) concentrations, the injection start and end times, and the concentration during the injection (Runkel 1998). The following simple mass balance equation was used to calculate the concentration during the injection:

$$C = C_b + \frac{Q_{inj} C_{inj}}{Q} \quad (3.14)$$

where C_b = background concentration of solute (mg/L);

Q_{inj} = flow rate of pump injecting solution into stream (m³/s); and

C_{inj} = solute concentration of injection solution (mg/L).

Output from this simulation yielded A , A_s , D , and α . These parameters were used with downstream velocity, u , and reach length, L , to calculate the fraction of median travel time along the reach due to exchange with storage, F_{med} (Runkel 2002):

$$F_{med} = \left(1 - e^{-\frac{L\alpha}{u}}\right) \frac{A_s}{A + A_s} \quad (3.15)$$

By using a reach length of 200 m, F_{med}^{200} can be calculated as a way to compare reaches of various lengths. The Damkohler number, DaI , was also calculated from the transient storage parameters resulting from simulations for each reach (Wagner and Harvey 1997) to determine if the reach length is appropriate for measuring transient storage. If $DaI \ll 1.0$, too small of an amount of solute has been exchanged with the storage zone, and the reach length is too short to accurately estimate transient storage parameters. If $DaI \gg 1.0$, the solute has been completely exchanged with the storage zone, and so the reach length may be too long. Parameter estimates have the least uncertainty when DaI is on the order of 1.0 (Wagner and Harvey 1997).

$$DaI = \alpha \frac{(1 + A/A_s)L}{u} \quad (3.16)$$

The ratio of A_s/A was also calculated as a measure of the amount of storage along the reach. Stream residence time was calculated as $T_{str} = 1/\alpha$, and storage zone residence time was related to the area ratio and exchange coefficient (Valett *et al.* 1997):

$$T_{sto} = (A/A_s) \times \alpha \quad (3.17)$$

Next, nitrate uptake was modeled using the BTCs of the reactive solute, NO_3^- . Similar to the Br^- BTC, the background $[\text{NO}_3^-]$ was subtracted from all points along the downstream NO_3^- BTC for each reach. A moving three-point median approach for smoothing (Tukey 1977) also was applied to the entire BTC to remove outliers. The upstream and downstream boundary conditions, as well as all other input data, for

modeling nitrate uptake using NO_3^- were similar to that for modeling transient storage using Br^- . The estimated values of the modeled transient storage parameters were held constant to model nitrate uptake. Output from this simulation yielded λ and λ_s . Figure 3.15 displays a flowchart of the modeling approach to optimize parameter estimates by running OTIS through UCODE (Baker 2009). The following equation was used to calculate uptake velocity along each reach, v_f , by using the average flow depth, h (Runkel 2007; Webster and Valett 2007):

$$v_f = \lambda h \quad (3.18)$$

A measure of uptake, or spiraling, length, S_w , was calculated based upon the mean distance that a nutrient atom travels in a stream before uptake by biota (Newbold *et al.* 1981). The following equation was used to calculate S_w (Webster and Valett 2007):

$$S_w = \frac{u}{\lambda} \quad (3.19)$$

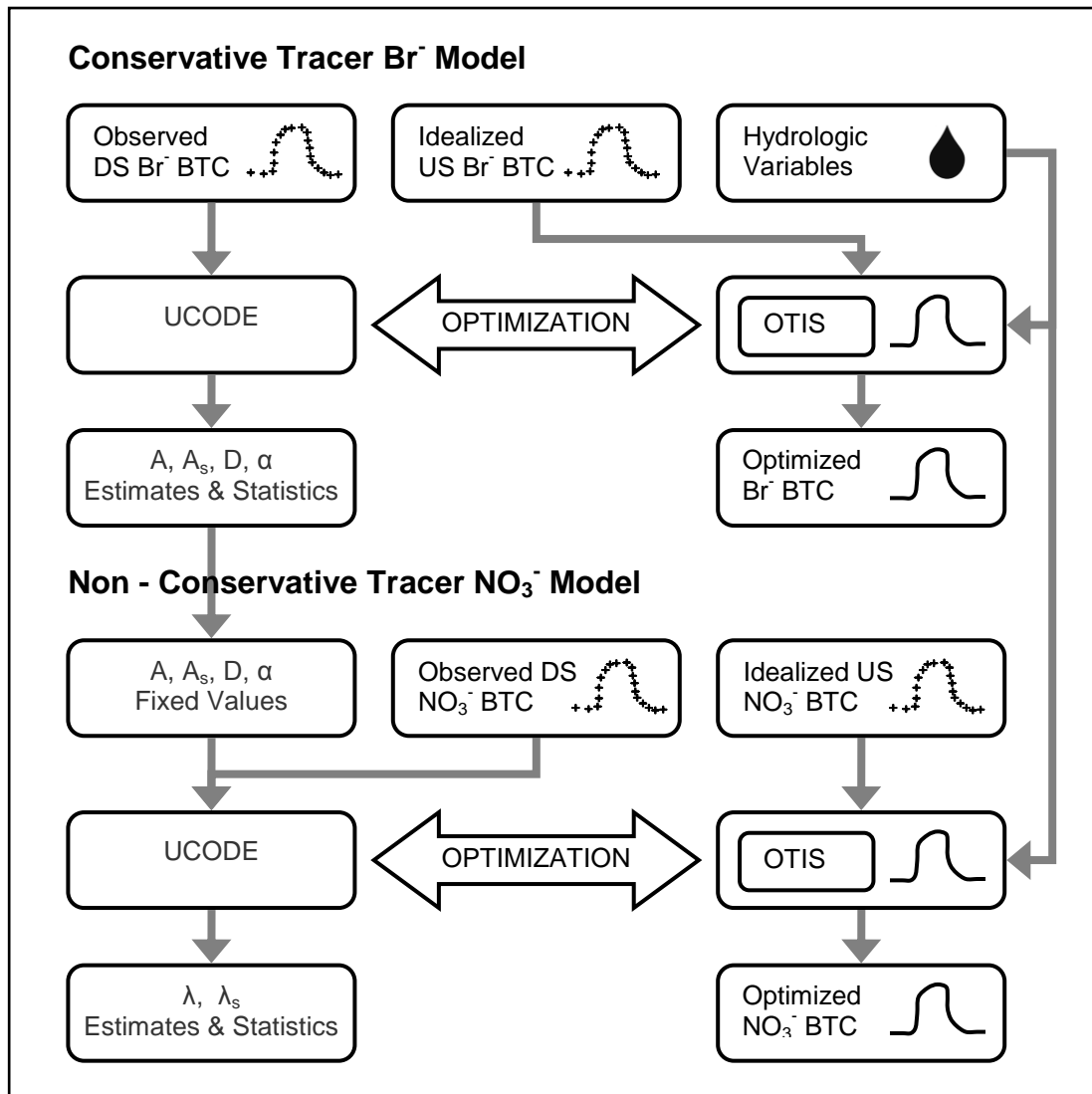


Figure 3.15: OTIS/UCODE modeling flowchart (Baker 2009)

3.3.6 Statistical Analyses

Utilizing SAS[®] 9.2 (SAS Institute, Inc. 2008), correlation matrices of log-transformed data were developed to explore relationships among transient storage, nitrate uptake, and physical descriptors from a total of twenty-three site visits along nine different study reaches of three different streams. Multiple regression analyses were performed to develop relationships that describe F_{med}^{200} in terms of physical variables and

v_f and S_w in terms of physical and transient storage variables. Based upon *a priori* knowledge of possible linkages and significant relationships ($p < 0.1$) in the correlation matrices, the descriptors were reduced to a set of variables that were used as candidates in the best subsets multiple regression analysis. Inter-correlation was also reduced by removing variables that held similar information, as noted by correlation coefficients of 0.7 or higher. To incorporate variables that describe important processes and potential drivers of transient storage and nitrate uptake, each set of final candidate variables contained surrogates representing flow, roughness, and bed characteristics. This reduced candidates describing F_{med}^{200} to a final set of variables, including longitudinal roughness, median grain size, fine benthic organic matter, relative submergence, and flow. Candidate variables describing v_f were reduced to a final set of variables, including F_{med}^{200} , dispersion coefficient, Reynolds number, depth, and median grain size. The final set of variables used to describe S_w included F_{med}^{200} , dispersion coefficient, flow, median grain size, and longitudinal roughness. Model selection was performed based upon 10 best subsets, which were modeled through analyses of variance (ANOVA). Regression models for v_f , S_w , and F_{med}^{200} were chosen based upon significance of the relationship (p -value) and how well the independent variables describe the dependent variable (adjusted R^2 value).

Monte Carlo simulations were also performed to investigate the model uncertainty in the parameter estimates of A , A_s , D , α , λ , and λ_s . Each set of parameter estimates from a single BTC was optimized in UCODE (Poeter *et al.* 2005). Parameter estimates were given in the model output as mean values with coefficients of variation and confidence limits. The coefficients of variation (standard deviation/mean) and mean values were

used to calculate standard deviations for each parameter estimate. Assuming a normal distribution based upon the mean value and standard deviation for each parameter estimate, 1,000 random numbers were generated from the given distribution for each parameter estimate of each BTC. Ranges of values for calculated parameters of A_s/A , F_{med}^{200} , S_w , and v_f were then obtained through 1,000 calculated iterations of the values generated for the modeled parameters. The Monte Carlo simulations were used to estimate mean values, standard deviations, quartiles, and 10th and 90th percentiles describing the range of values for each modeled and calculated parameter.

4 INTERSITE COMPARISON OF CHARACTERISTICS AMONG ALL THREE STREAMS

4.1 OVERVIEW

Geomorphic attributes and varying flow rates interact to influence stream processes and characteristics. In this study, I perform physical measurements and nutrient injections on contrasting study reaches of an urban stream and two agricultural streams in the Front Range of Colorado to examine how geomorphic characteristics relate to transient storage and nitrate uptake. Previous research has shown relationships between thalweg variation and hyporheic exchange (Anderson *et al.* 2005; Wondzell 2006; Gooseff *et al.* 2007), and I extend the description of geomorphic complexity through detailed physical characterization of study reaches, including such attributes as width variation, cross-sectional variation, and substrate sizes.

I selected three reaches of varying geomorphic and hydraulic characteristics in Spring Creek, an urban stream in Fort Collins, Colorado. Each reach along Spring Creek (Figure 3.3 in Chapter 3) was visited on three different occasions for a total of nine nutrient injections and physical datasets. The two agricultural streams, Sheep Creek (Figure 3.5 in Chapter 3) and Nunn Creek (Figure 3.7 in Chapter 3), are located in northern Colorado and have been influenced by livestock grazing and varied restoration techniques. Descriptions and analyses of the effects of these restoration techniques on

transient storage and nitrate uptake were discussed in the previous chapter. I chose four reaches along Sheep Creek and two reaches along Nunn Creek. Each reach along Sheep Creek was visited on two separate occasions for a total on eight nutrient injections and physical datasets, and each reach along Nunn Creek was visited on three different occasions for a total of six nutrient injections and physical datasets. This completes my overall dataset with a total of twenty-three site visits along nine different study reaches of three different streams.

Although many studies have been performed to explore nitrate uptake in streams, few studies have involved repeat injections along the same study reach to capture various flow rates. I hypothesize that physical differences in geomorphic setting and flow rate among the nine study reaches of three different streams will affect the amount of transient storage and nitrate uptake occurring in each reach. Specifically, increased geomorphic complexity, as described by coupling effects of bed characteristics, flow, and longitudinal roughness, will be associated with increased amounts of transient storage and nitrate uptake. Increases in substrate size can lead to greater porosity and permeability in the streambed, and increases in longitudinal roughness, or variation in thalweg elevation, can help drive flow into the bed, which both promote hyporheic exchange, a component of transient storage.

To investigate this hypothesis, I collected comprehensive datasets to characterize physical complexity along each reach, including pebble counts, longitudinal profiles, cross-section surveys, hydraulic measurements, benthic organic matter (fine and coarse), and spatial distributions of physical habitat units. Field injections of bromide and nitrate were used to estimate transient storage and nitrate uptake in each reach. The measured

physical data and modeled transient storage and nitrate uptake data were examined for patterns and relationships among physical measurements, transient storage values, and nitrate uptake values. I provide a detailed description of physical characteristics across all study reaches and develop models to describe how these physical characteristics relate to transient storage and nitrate uptake parameters. A detailed description of methods used is provided in Chapter 3.

4.2 RESULTS

By performing repeat nutrient injections and physical characterizations on separate occasions along the same study reach, I explored the influence of flow on transient storage and nitrate uptake, as well as the relationships among geomorphic complexity, transient storage, and nitrate uptake. To collect data needed to develop these regression models, each of the study reaches along Spring Creek was visited twice in Summer 2007 and once in Summer 2008. For Sheep Creek, Sheep A and C were visited in July 2007 and early September 2008. Sheep B and D were visited in early September 2008 and again in early September 2009. For Nunn Creek, there were three nutrient injections performed on each reach within the month of August 2009 to capture a variety of stream flows.

As described in detail below, regression models based on all twenty-three field experiments show positive associations between transient storage and nitrate uptake, as well as the influence of various stream physical characteristics. Nitrate uptake is positively correlated with dispersion, Reynolds number, median grain size, and

longitudinal roughness, while transient storage (F_{med}^{200}) is negatively associated with fine benthic organic matter that can clog pore space in the bed.

Quantified measures of geomorphic complexity, including longitudinal roughness, width variability, cross-sectional area variability, sinuosity, and bed substrate distribution; and ecological characteristics, including FBOM, CBOM, and GPP; vary substantially among all twenty-three study reaches (Tables 4.1 and 4.2). In addition to differences in physical characteristics, modeled transient storage and nitrate uptake parameters are also quite variable and span up to three orders of magnitude among all twenty-three site visits (Tables 4.3 and 4.4). The OTIS/UCODE models converged on BTCs that were used to estimate transient storage parameters from bromide BTCs (Figures 4.1, 4.3, and 4.5) and nitrate uptake parameters from nitrate BTCs (Figures 4.2, 4.4, and 4.6).

Descriptors of flow (e.g., q , ω , u_* , and Re) and geomorphic complexity (e.g., S_o , P , LR , and d_{50}) vary appreciably across the study reaches (Tables 4.1 and 4.2), as do modeled and calculated parameters describing transient storage and nitrate uptake (Tables 4.3 and 4.4). Some of these data are also presented graphically for visual comparison of parameters across all study reaches and site visits (Figures 4.7 through 4.10). Figures 4.7 through 4.9 cover several aspects of geomorphic complexity (S_o , LR , % fines, d_{50} , P , and number of different habitat units), flow variation (Q , q , ω , and u_*), and coupled effects of geomorphic setting and flow area (XS area variability, width variability, h , and R/d_{84}) to fully describe physical characteristics of each study reach and site visit. Figure 4.10 displays comparisons among transient storage and nitrate uptake parameters (F_{med}^{200} , A_s/A , v_f , and S_w) across all study reaches and site visits.

Sheep A has the steepest bedslope, while Railroad has the mildest bedslope. Nunn B also shows the greatest longitudinal roughness due to implementation of restoration structures along the reach that create pool-riffle sequences, while the channelized Railroad has the least longitudinal roughness. Railroad also has the smallest substrate size, as shown in the highest values of percent fines and lowest median grain size. In contrast, Nunn B, with one of the steepest gradients and highest values of longitudinal roughness of the reaches in this study, has one of the coarsest substrate sizes. Nunn A and B show minimal values of percent fines and the highest median grain sizes. The second site visits along Spring Creek (Edora, Stuart, and Railroad) show lower values of percent fines compared to the first site visits due to the effect of the flash flood as described in Chapter 6. Of the reaches in this study, Sheep B is the most sinuous, and Railroad is the straightest reach. According to grain size and longitudinal roughness, Nunn B could be characterized as being one of the most geomorphically complex reaches, and Railroad could be characterized as one of the least geomorphically complex reaches (Figure 4.6).

Because nutrient injections were performed at varying flows along the same study reaches, hydraulic parameters, which are a function of flow, were investigated to explore how flow may affect transient storage and nitrate uptake. The highest flow rates were captured along Edora Park at 152 L/s and along Nunn Creek A and B at 209 L/s and 191 L/s, respectively (Figure 4.8). The lowest flow rate captured was on Railroad at a flow of 17 L/s. The other parameters shown (q , w , and u_*) demonstrate a pattern similar to that of Q among the study reaches (Figure 4.8). Nunn B shows the highest mean values of u_* over all visits, and Railroad shows the lowest mean values of u_* over all visits. Some

parameters are influenced by the geomorphic setting of the individual reach and by the flow area at the time of data collection (Figure 4.9). Stuart shows the highest variability in cross-sectional area, and Railroad showed the lowest cross-sectional area variability. The grade-control structure in the Stuart Reach creates large pooled areas, while other areas are wider and shallower, which leads to high variability in cross-sectional area. Width variability is highest in Edora Park and Sheep C and lowest in Railroad and Nunn B. Due to channelization of Railroad Reach and bank stabilization in Nunn B, these reaches have fairly consistent wetted widths along the length of the channel. Flow depth was highest in Stuart and Nunn B due to in-stream structures creating deep pooled areas, while Railroad has the lowest flow depth. Flows, and flow depths, measured at Railroad Reach were the lowest observed in the study. This is likely due to retention ponds upstream of the reach along Spring Creek, where flow is highly regulated. Railroad Reach also has the smallest substrate size, which results in the largest relative submergence ratio of around 22. Relative submergence values of all other reaches at various flows are low in comparison to that of Railroad Reach and are on the order of 1.

Comparisons of transient storage and nitrate uptake parameters among all reaches and site visits (Figure 4.10) indicate that Nunn A and Sheep D exhibited the highest values of F_{med}^{200} and A_s/A , showing greater fractions of median travel time due to exchange with storage and larger ratios of transient storage area to main-channel area. Sheep C exhibited the lowest values of F_{med}^{200} and A_s/A , showing less time in transient storage and smaller ratios of transient storage area to main-channel area. Just as Nunn A showed some of the highest values of F_{med}^{200} and A_s/A among the reaches in this study, it also showed some of the greatest nitrate uptake values (highest v_f and low S_w). Nunn B

also exhibited one of the highest values of v_f , showing greater nitrate uptake than other reaches in this study. Just as Nunn B (one of the most geomorphically complex reaches in the study) showed one of the highest values of nitrate uptake velocity, Railroad Reach (one of the least geomorphically complex reaches in the study) showed one of the lowest values of nitrate uptake velocity. The results from these sites support my hypothesis that the most physically complex reaches, as described by combined effects of bed characteristics (median grain size and percent fines) and longitudinal roughness, will have the highest amounts of transient storage and nitrate uptake.

Table 4.1: Summary of physical and ecological parameters for Spring Creek

	Spring Creek								
	Edora Park 2007a	Edora Park 2007b	Edora Park 2008	Stuart 2007a	Stuart 2007b	Stuart 2008	Railroad 2007a	Railroad 2007b	Railroad 2008
Reach length (m)	178	180	176	180	181	181	181	181	186
Flow, Q (L/s)	72	152	66	46	107	57	17	21	21
Unit discharge, q (m ² /s)	0.017	0.037	0.015	0.011	0.026	0.014	0.007	0.010	0.008
Ambient [NO ₃ ⁻ -N] (mg/L)	0.74	0.71	0.64	0.72	0.66	0.64	1.07	1.60	0.93
Sinuosity	1.16	1.18	1.15	1.05	1.05	1.05	1.01	1.02	1.04
Bedslope, S_o	0.0046	0.0044	0.0050	0.0108	0.0108	0.0109	0.0025	0.0024	0.0024
Unit stream power, ω (W/m ²)	0.78	1.58	0.73	1.18	2.75	1.47	0.18	0.23	0.19
Shear velocity, u_* (m/s)	6.5E-03	9.0E-03	9.2E-03	1.9E-02	2.6E-02	2.9E-02	2.9E-03	2.4E-03	4.6E-03
Reynolds number, Re	16,500	45,090	26,800	12,530	34,520	24,920	6,100	7,930	12,710
Longitudinal roughness, LR (m)	0.13	0.13	0.14	0.11	0.10	0.12	0.05	0.04	0.05
Width variability (m)	1.00	1.13	1.20	0.96	0.83	0.86	0.45	0.48	0.62
XS area variability (m)	0.22	0.40	0.37	0.24	0.49	0.46	0.04	0.05	0.10
Percent fines (<2 mm)	34%	1%	9%	25%	0.4%	7%	75%	33%	75%
d_{16} (mm)	4	13	8	9	17	13	< 2	< 2	< 2
d_{50} (mm)	14	28	21	26	41	28	< 2	5	< 2
d_{84} (mm)	40	65	63	84	129	72	4	14	7
Gradation coefficient	3.1	2.3	2.8	3.1	2.8	2.4	1.7	2.9	2.6
Relative submergence, R/d_{84}	3.1	2.8	2.7	1.7	1.6	3.2	22.9	6.2	22.2
Metric of complexity	7.1E-04	6.8E-04	8.1E-04	1.3E-03	1.2E-03	1.4E-03	1.1E-04	8.9E-05	1.3E-04
FBOM AFDM (g/m ²)	320	98	207	389	79	316	120	101	209
CBOM AFDM (g/m ²)	26	10	63	107	7	171	48	24	97
GPP (gO ₂ /m ² /day)	0.35	0.19	0.32	0.13	0.22	0.12	0.14	0.27	0.11

Table 4.2: Summary of physical and ecological parameters for Sheep Creek and Nunn Creek

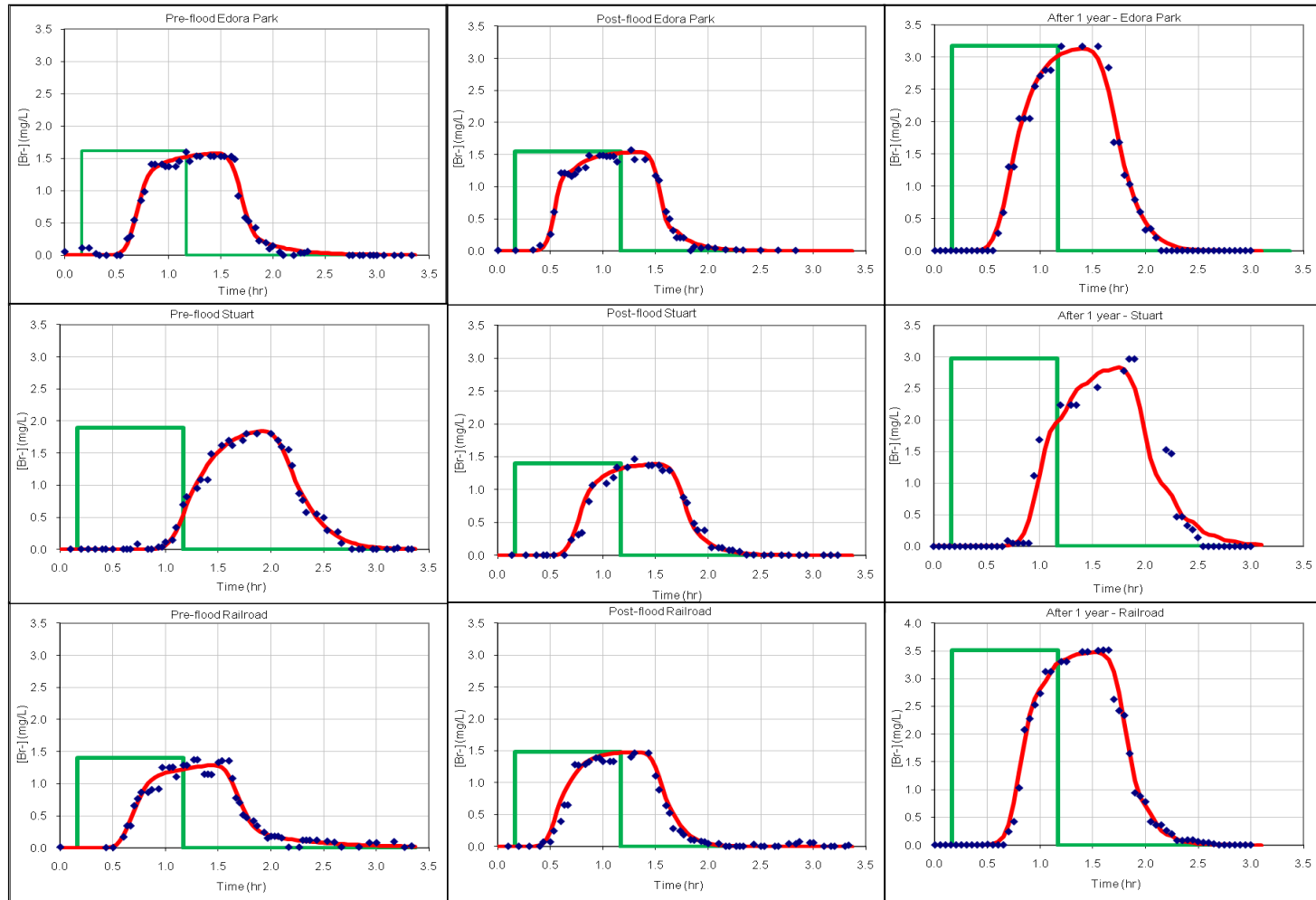
	Sheep Creek								Nunn Creek					
	Sheep A 2007	Sheep C 2007	Sheep A 2008	Sheep B 2008	Sheep C 2008	Sheep D 2008	Sheep B 2009	Sheep D 2009	Nunn A 2009a	Nunn A 2009b	Nunn A 2009c	Nunn B 2009a	Nunn B 2009b	Nunn B 2009c
Reach length (m)	189	191	189	184	189	185	176	194	174	174	174	163	163	163
Flow, Q (L/s)	104	102	72	72	34	32	52	35	209	98	87	191	125	101
Unit discharge, q (m ² /s)	0.029	0.022	0.022	0.022	0.009	0.011	0.016	0.012	0.043	0.023	0.020	0.038	0.027	0.022
Ambient [NO ₃ ⁻ -N] (mg/L)	0.10	0.13	0.10	0.10	0.10	0.10	0.10	0.10	0.10	0.10	0.10	0.10	0.10	0.10
Sinuosity	1.11	1.24	1.11	1.63	1.24	1.49	1.63	1.49	1.44	1.44	1.44	1.61	1.61	1.61
Bedslope, S_o	0.0146	0.0115	0.0146	0.0074	0.0115	0.0029	0.0074	0.0029	0.0133	0.0133	0.0133	0.0134	0.0134	0.0134
Unit stream power, ω (W/m ²)	4.20	2.51	3.15	1.67	1.00	0.30	1.12	0.34	5.64	2.96	2.65	4.97	3.56	2.88
Shear velocity, u_* (m/s)	2.3E-02	1.6E-02	2.0E-02	1.3E-02	1.3E-02	6.4E-03	9.5E-03	4.7E-03	2.5E-02	1.8E-02	2.0E-02	3.6E-02	3.5E-02	3.5E-02
Reynolds number, Re	29,310	13,540	10,710	22,120	9,100	10,790	15,830	11,790	43,250	22,690	20,330	37,800	27,070	21,880
Longitudinal roughness, LR (m)	0.07	0.08	0.07	0.11	0.09	0.14	0.11	0.14	0.12	0.12	0.12	0.16	0.16	0.16
Width variability (m)	0.65	1.23	0.58	0.56	1.06	0.60	0.63	0.69	0.94	0.88	0.81	0.66	0.48	0.52
XS area variability (m)	0.10	0.18	0.12	0.20	0.15	0.29	0.21	0.27	0.19	0.17	0.16	0.29	0.40	0.42
Percent fines (<2 mm)	13%	10%	6%	1%	9%	9%	0.2%	8%	0%	0%	0%	0.4%	0.4%	0.4%
d_{16} (mm)	4	5	10	13	7	8	12	6	28	28	28	30	30	30
d_{50} (mm)	37	34	38	39	27	21	29	18	63	63	63	74	74	74
d_{84} (mm)	142	117	105	76	74	48	56	40	112	112	112	197	197	197
Gradation coefficient	6.3	5.0	3.2	2.5	3.3	2.5	2.2	2.7	2	2	2	2.6	2.6	2.6
Relative submergence, R/d_{84}	0.9	1.0	1.0	1.8	1.3	4.1	2.0	3.7	1.3	1.1	1.1	1.1	1.2	1.1
Metric of complexity	1.1E-03	1.2E-03	1.1E-03	1.3E-03	1.2E-03	5.8E-04	1.3E-03	6.2E-04	2.3E-03	2.3E-03	2.3E-03	3.5E-03	3.5E-03	3.5E-03
FBOM AFDM (g/m ²)	8	58	10	22	16	85	21	27	16	21	11	33	27	33
CBOM AFDM (g/m ²)	16	4	1	7	7	11	3	3	72	8	24	10	4	5
GPP (gO ₂ /m ² /day)	0.64	0.07	0.01	0.04	0.01	0.04	0.03	0.05	0.07	0.04	0.04	0.07	0.04	0.03

Table 4.3: Summary of transient storage and nitrate uptake parameters for Spring Creek

	Spring Creek								
	Edora Park 2007a	Edora Park 2007b	Edora Park 2008	Stuart 2007a	Stuart 2007b	Stuart 2008	Railroad 2007a	Railroad 2007b	Railroad 2008
A (m ²)	0.54	0.74	0.49	0.62	0.91	0.62	0.15	0.11	0.20
A_s (m ²)	0.08	0.20	0.12	0.17	0.14	0.21	0.04	0.06	0.05
D (m ² /s)	0.44	0.45	0.67	0.05	0.27	0.03	0.49	0.30	0.08
α (s ⁻¹)	1.6E-04	5.9E-04	8.3E-04	7.1E-04	3.3E-04	6.1E-04	1.6E-04	2.1E-03	8.1E-04
λ (s ⁻¹)	3.2E-05	6.5E-05	9.1E-05	4.4E-05	4.3E-05	2.6E-05	1.1E-04	1.3E-04	6.3E-06
λ_s (s ⁻¹)	2.3E-10	7.0E-05	6.8E-05	6.0E-09	7.7E-05	-1.6E-04	7.4E-05	2.6E-09	-3.8E-05
A_s/A	0.15	0.27	0.25	0.27	0.16	0.33	0.29	0.52	0.27
F_{med}^{200}	0.03	0.09	0.17	0.18	0.06	0.22	0.07	0.33	0.20
S_w (m)	4,350	3,120	980	1,740	2,950	2,300	700	920	8,190
v_f (m/s)	4.7E-06	1.4E-05	1.7E-05	7.9E-06	1.1E-05	7.1E-06	1.3E-05	1.3E-05	1.2E-06

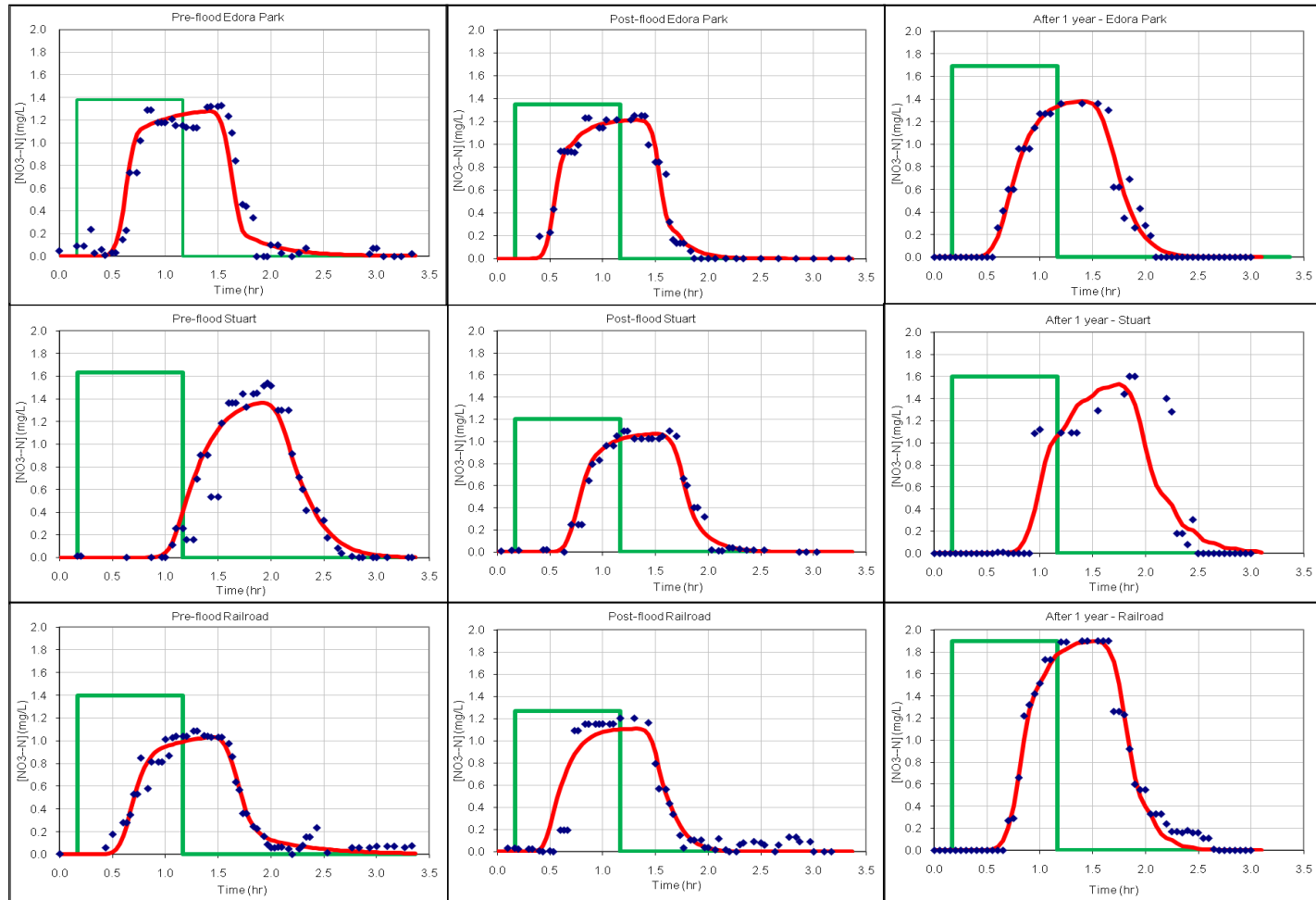
Table 4.4: Summary of transient storage and nitrate uptake parameters for Sheep Creek and Nunn Creek

	Sheep Creek								Nunn Creek					
	Sheep A 2007	Sheep C 2007	Sheep A 2008	Sheep B 2008	Sheep C 2008	Sheep D 2008	Sheep B 2009	Sheep D 2009	Nunn A 2009a	Nunn A 2009b	Nunn A 2009c	Nunn B 2009a	Nunn B 2009b	Nunn B 2009c
A (m ²)	0.28	0.60	0.33	0.49	0.30	0.54	0.35	0.42	0.43	0.40	0.37	1.09	0.98	1.00
A_s (m ²)	0.10	0.26	0.11	0.13	0.07	0.09	0.16	0.25	0.25	0.12	0.22	0.22	0.21	0.13
D (m ² /s)	0.16	0.79	0.15	0.19	0.14	0.11	0.24	0.23	0.56	0.27	0.81	0.19	0.27	0.13
α (s ⁻¹)	3.3E-03	3.4E-05	4.2E-03	1.7E-03	1.0E-03	5.5E-04	2.1E-03	1.0E-02	6.7E-03	2.5E-03	2.0E-02	1.5E-03	1.1E-03	7.5E-04
λ (s ⁻¹)	2.1E-04	2.6E-05	3.2E-05	1.2E-05	2.8E-05	4.8E-05	4.9E-05	8.3E-05	3.0E-04	3.4E-04	3.4E-04	1.4E-04	2.3E-04	5.8E-05
λ_s (s ⁻¹)	4.2E-10	3.4E-04	4.2E-04	4.0E-04	4.8E-04	9.6E-06	7.9E-05	8.6E-08	2.1E-04	5.2E-05	1.3E-04	7.6E-05	5.5E-10	1.8E-03
A_v/A	0.36	0.43	0.34	0.28	0.24	0.17	0.46	0.60	0.57	0.30	0.60	0.20	0.21	0.13
F_{med}^{200}	0.25	0.01	0.25	0.19	0.17	0.12	0.30	0.37	0.36	0.22	0.38	0.14	0.15	0.09
S_w (m)	1,090	7,380	6,230	13,770	3,350	1,130	2,850	960	1,000	560	510	1,250	510	1,690
v_f (m/s)	3.3E-05	3.6E-06	4.3E-06	2.0E-06	3.4E-06	1.1E-05	6.6E-06	1.4E-05	5.8E-05	4.7E-05	5.1E-05	3.9E-05	6.2E-05	1.4E-05



Legend: — US Boundary Condition; ◆ DS Boundary Condition; — Modeled Results

Figure 4.1: Spring Creek Bromide BTC simulations



Legend: — US Boundary Condition; ◆ DS Boundary Condition; — Modeled Results

Figure 4.2: Spring Creek Nitrate BTC simulations

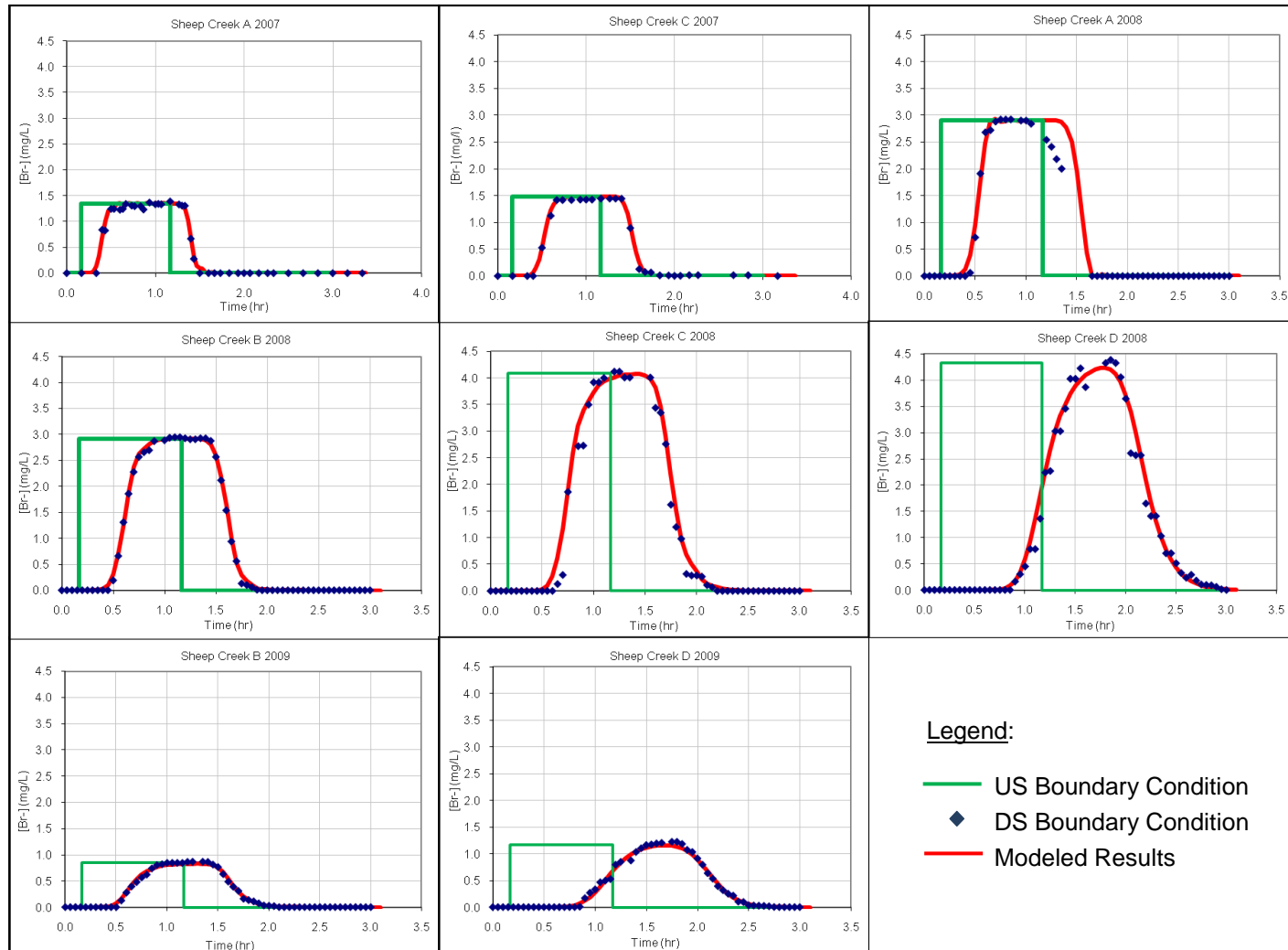


Figure 4.3: Sheep Creek Bromide BTC simulations

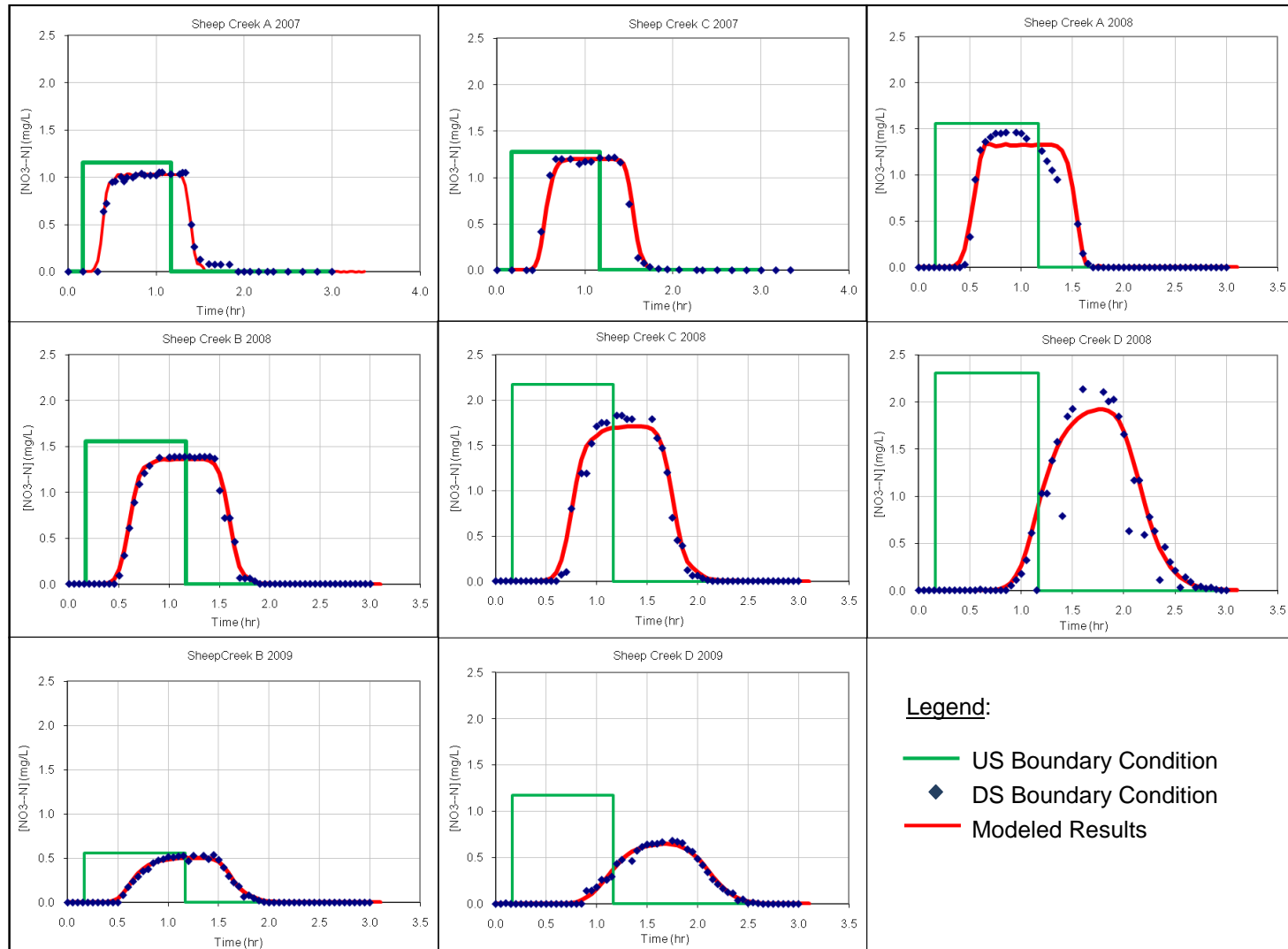
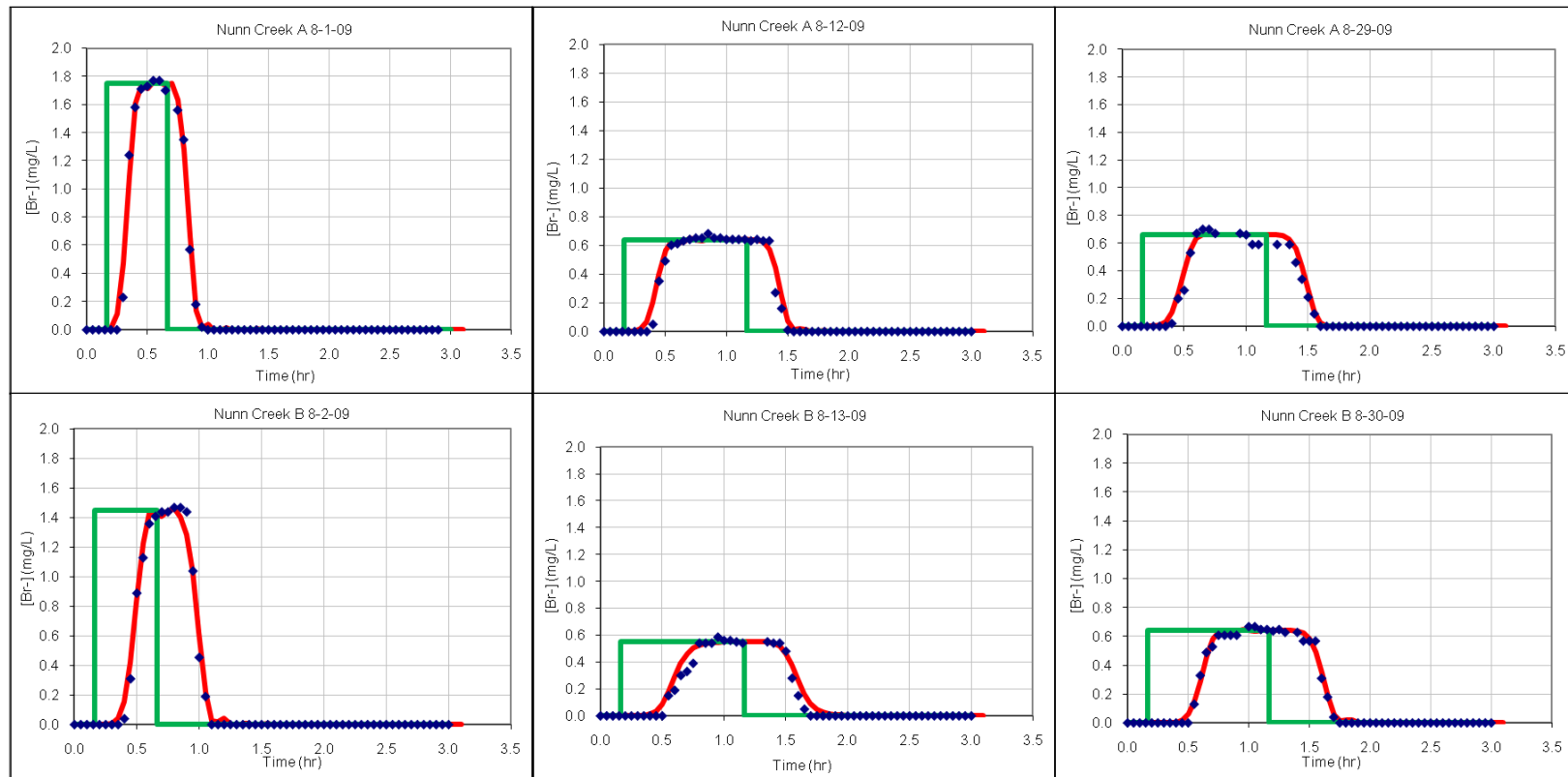


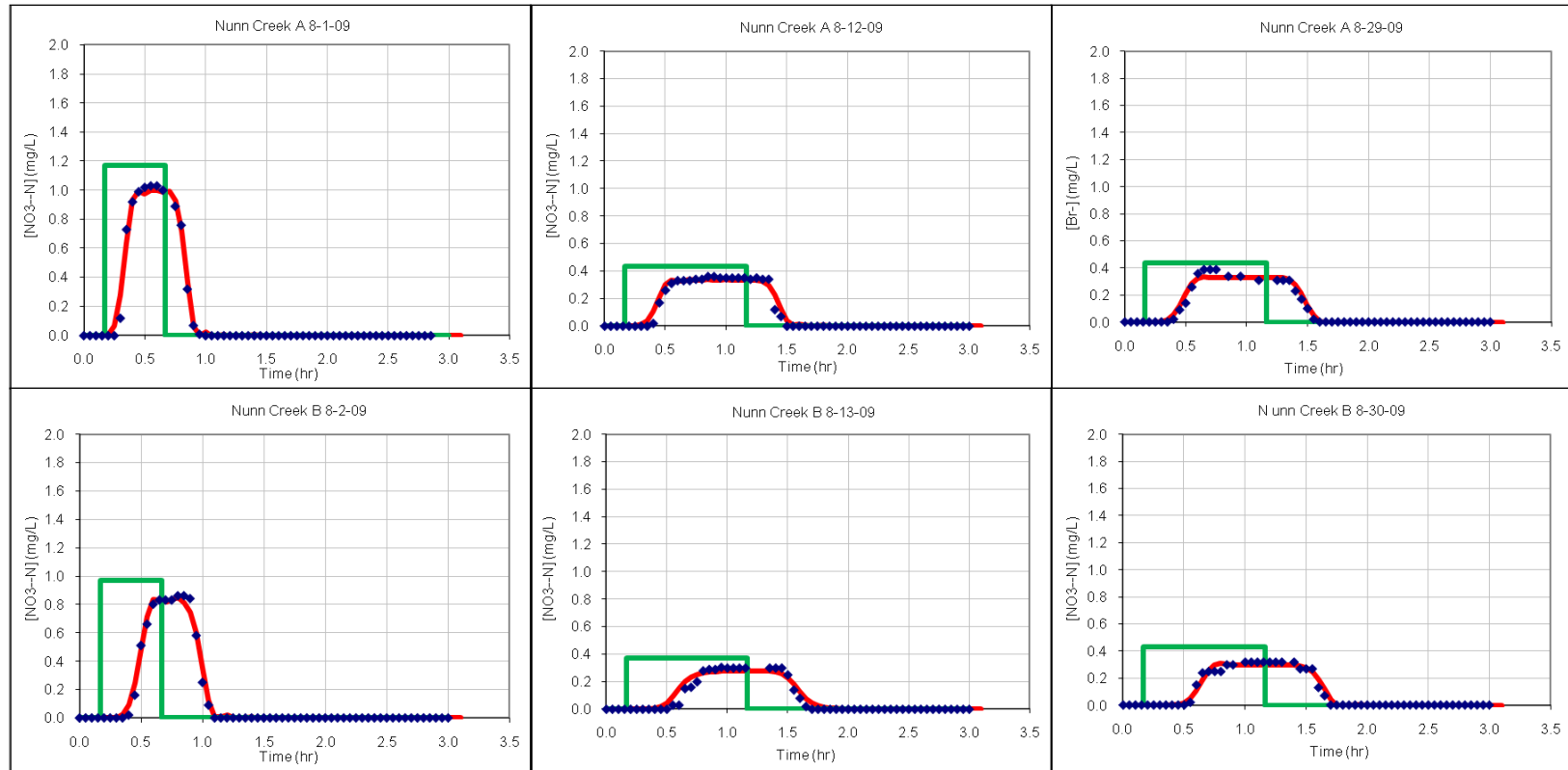
Figure 4.4: Sheep Creek Nitrate BTC simulations



Legend:

- US Boundary Condition
- ◆ DS Boundary Condition
- Modeled Results

Figure 4.5: Nunn Creek Bromide BTC simulations



Legend:

- US Boundary Condition
- ◆ DS Boundary Condition
- Modeled Results

Figure 4.6: Nunn Creek Nitrate BTC simulations



Figure 4.7: Comparison of characteristics describing geomorphic complexity

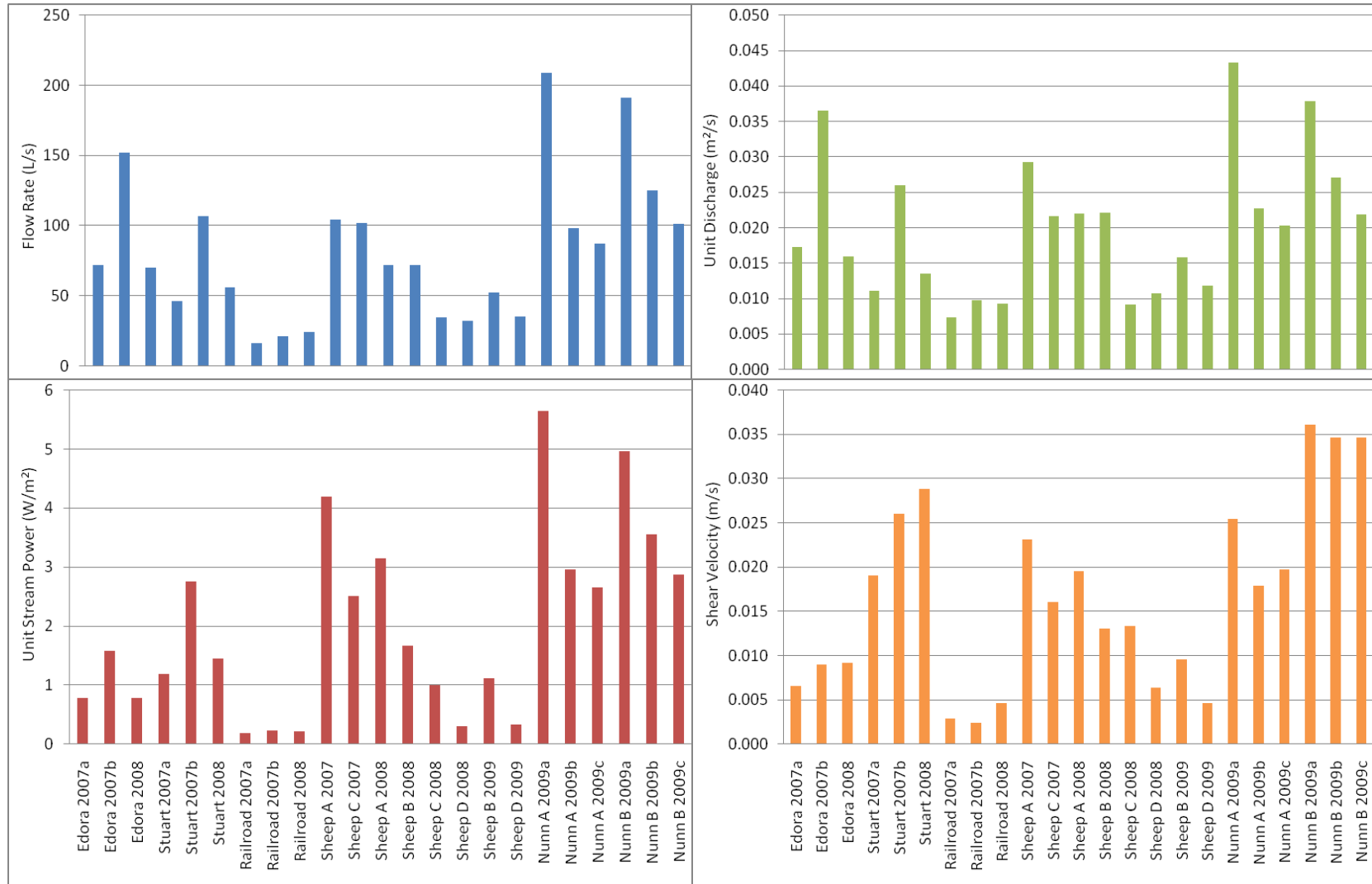


Figure 4.8: Comparison of measures describing flow

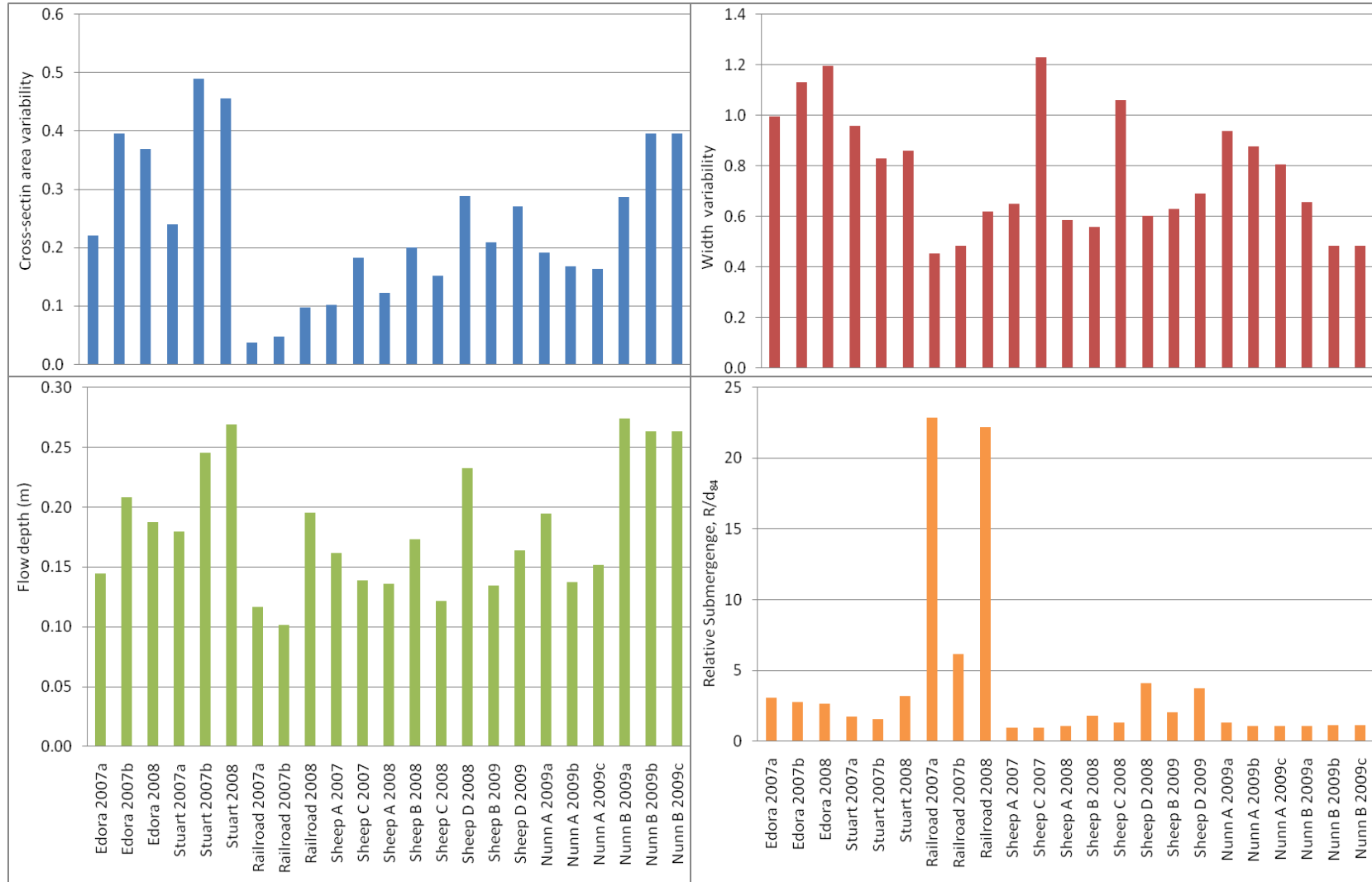


Figure 4.9: Comparison of physical parameters influenced by geomorphic setting and flow area

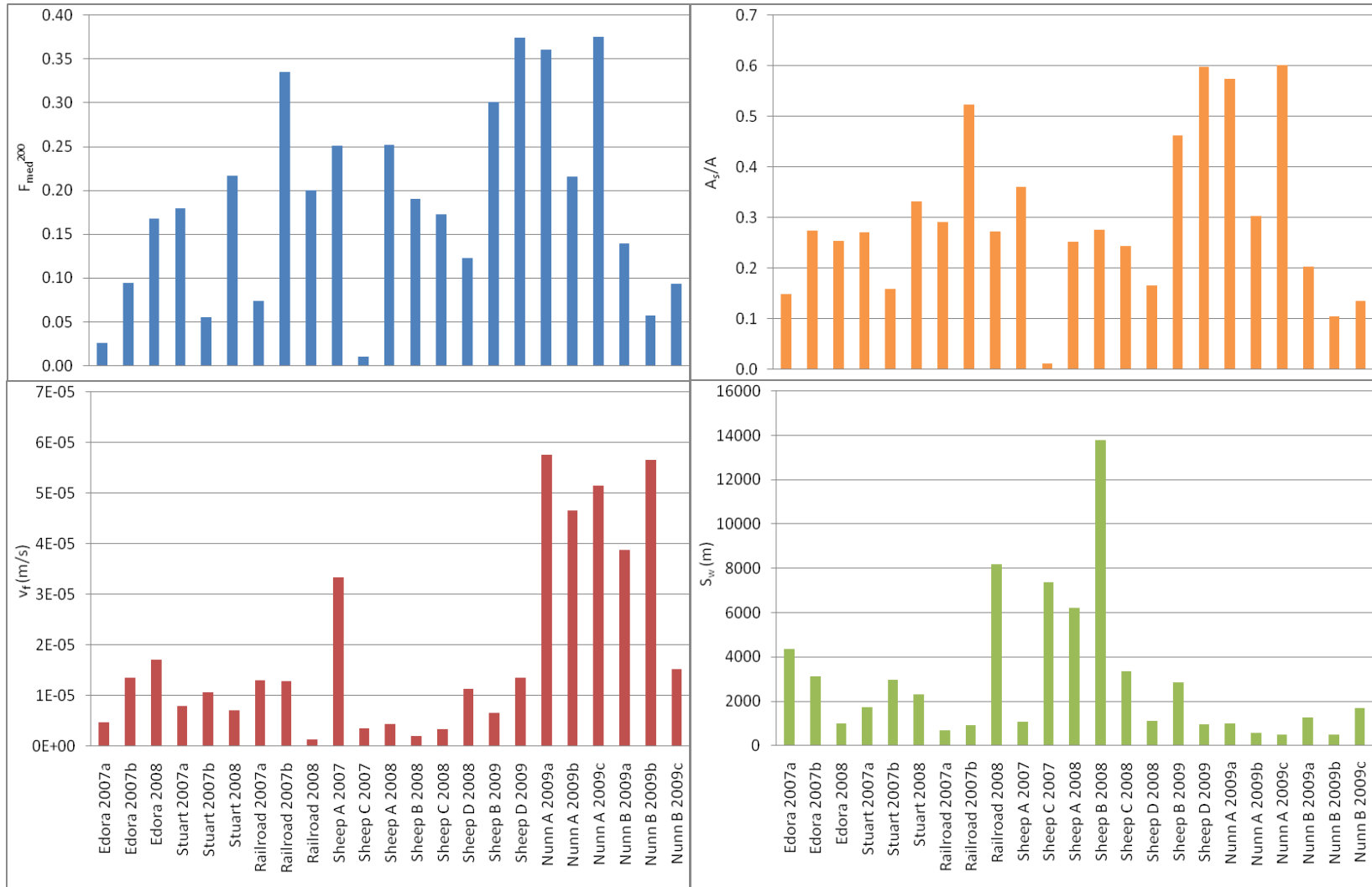


Figure 4.10: Comparison of transient storage and uptake parameters

Many studies have been performed to investigate nitrate uptake in streams. Figure 4.11 displays the nitrate uptake velocity data collected in this study with nitrate uptake velocity values from a compilation of previously published data, including LINX II data (Tank *et al.* 2008). Comparing nitrate uptake velocity to ambient nitrate concentrations, as well as nitrate uptake velocity to flow rate, the data from this study fall within the range of previous data collected. In both cases, most of the data from this study lie with the quadrant of higher ambient nitrate concentrations and lower uptake velocities, as well as higher flow rates and lower uptake velocities, when compared to data in previous studies. In the case of ambient nitrate concentrations, it should be noted that the MDL for the analytical process used to measure $[\text{NO}_3^-\text{-N}]$ was 0.1 mg/L. For the purpose of this study, any concentrations noted below the MDL were assumed to be 0.1 mg/L.

To describe relationships among physical, transient storage, and nitrate uptake variables, regression models for v_f , S_w , and F_{med}^{200} (Table 4.5) were chosen based upon significance of the relationship (p-value) and how well the independent variables describe the dependent variable (adjusted R^2 value).

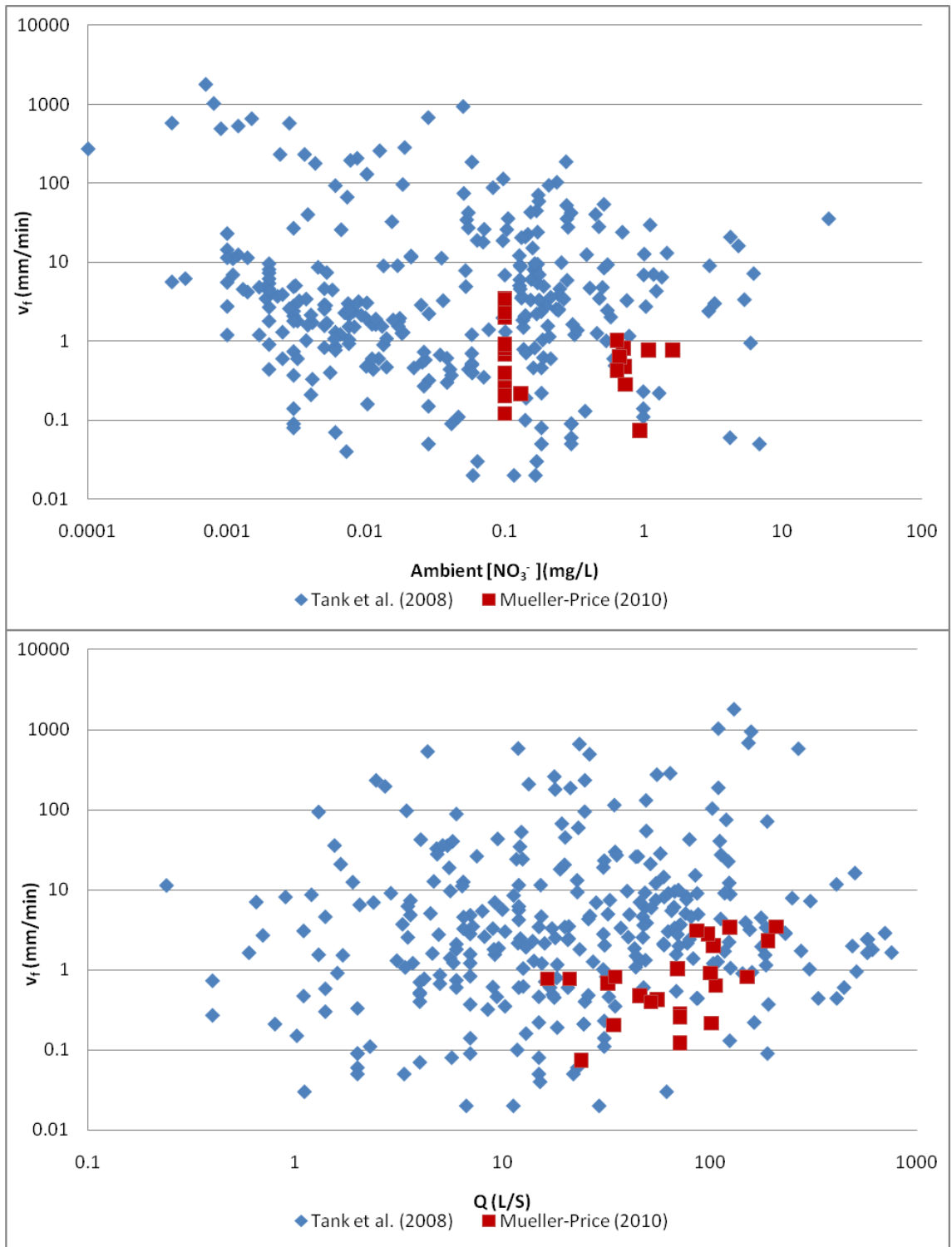


Figure 4.11: Compiled Dataset of Nitrate Uptake Studies (Tank *et al.* 2008)

Table 4.5: Best-fit regression models of transient storage and nitrate uptake

Equation	Regression Model	Adjusted R ²	p-value
(4.1)	$v_f = 10^{-2.52} D^{0.84} (F_{med}^{200})^{0.62} h^{1.81}$	0.401	0.005
(4.2)	$v_f = 10^{-9.90} (F_{med}^{200})^{0.35} Re^{1.24}$	0.365	0.004
(4.3)	$v_f = 10^{-5.34} (F_{med}^{200})^{0.33} d_{50}^{0.48}$	0.231	0.028
(4.4)	$S_w = 10^{2.11} D^{-0.40} (F_{med}^{200})^{-0.52} LR^{-0.47}$	0.184	0.078
(4.5)	$S_w = 10^{2.49} (F_{med}^{200})^{-0.41} LR^{-0.44}$	0.092	0.147
(4.6)	$F_{med}^{200} = 10^{-1.29} d_{50}^{0.61} FBOM^{-0.44} (R/d_{84})^{1.02}$	0.171	0.090
(4.7)	$F_{med}^{200} = 10^{-0.99} (d_{50}/FBOM)^{0.46} (R/d_{84})^{0.86}$	0.207	0.038
(4.8)	$F_{med}^{200} = 10^{-0.22} FBOM^{-0.43} (R/d_{84})^{0.34}$	0.147	0.078

All three models describing uptake velocity are significant ($p < 0.05$) and explain between 23% to 40% of the variance in uptake velocity values. In Equation (4.1), uptake velocity is shown to be positively correlated with dispersion coefficient, fraction of median travel time along the reach due to exchange with storage, and flow depth. Higher dispersion is associated with increased uptake velocity. When compared to advection processes, where solutes are transported downstream, greater dispersion allows solutes to spread out more as they move downstream, leading to a greater likelihood of entering into transient storage areas and undergoing biogeochemical transformations (i.e., denitrification). Increases in uptake velocity are also associated with increases in F_{med}^{200} and flow depth. Increases in flow depth can lead to increased pressure head above the bed that can promote hyporheic exchange, and more time in transient storage, including the hyporheic zone, allows for greater probability of biogeochemical processes that lead to nitrate removal. Equation (4.2) also shows uptake velocity to be positively correlated with F_{med}^{200} , as well as Reynolds number. A previous component of this study also shows Reynolds number to be positively correlated with uptake velocity (Baker 2009).

In addition to associations between uptake velocity and transient storage (F_{med}^{200}), Equation (4.3) shows that increases in uptake velocity are also associated with increased median grain size. Because interstitial space among particles increases as grain size increases, there is more pore space allowing surface water to flow into the bed, resulting in greater probability of hyporheic exchange, compared to a bed composed of fine material. Increases in grain size, which can lead to increases in transient storage in the hyporheic zone where denitrification can occur, are shown to correspond with increases in uptake velocity.

Regression models describing uptake length and F_{med}^{200} are not as significant and explain less variance than the models of uptake velocity. Equation (4.4) describes a significant relationship ($p < 0.1$) in which uptake length is negatively correlated with dispersion coefficient, fraction of median travel time along the reach due to exchange with storage, and longitudinal roughness. As longitudinal roughness increases (more variation in thalweg elevation), uptake length decreases, showing greater uptake. Shorter uptake lengths also correspond with greater values of F_{med}^{200} , which can be associated with more hyporheic exchange as induced by more longitudinal roughness and bed variability. A similar relationship of uptake length with longitudinal roughness and F_{med}^{200} , as shown in Equation (4.5), does not include dispersion coefficient. This yields a weaker model of uptake length as compared to Equation (4.4), which shows the strength of the relationship between dispersion and uptake length. Similar to the association of dispersion and uptake velocity, the inverse relationship of dispersion with uptake length shows that higher dispersion leads to short uptake lengths and greater uptake.

Another significant relationship ($p < 0.1$) is shown in Equation (4.6), which describes F_{med}^{200} as being positively correlated with median grain size and relative submergence and negatively correlated with fine benthic organic matter. Increases in grain size could lead to increases in hyporheic exchange through more pore space in the bed, which allows for greater transient storage in the hyporheic zone. Conversely, increases in FBOM can clog interstitial spaces in the substrate and lead to decreases in permeability and hyporheic exchange. The relationship in Equation (4.6) implies that F_{med}^{200} is proportional to the square root of the term $d_{50}/FBOM$. By incorporating the term $d_{50}/FBOM$ into Equation (4.7), bed permeability is described as an interaction between fine and coarse bed material.

A mechanism underlying the consistent association of F_{med}^{200} with relative submergence may be reflected in the relationship between relative submergence and velocity profile and flow resistance (Julien 2002; Figure 4.12). As relative submergence drops below a value of 3, its relationship with flow resistance drastically shifts. In this study, the majority of relative submergence values range from 1 to 3 and are in the region in which flow resistance becomes highly sensitive to relative submergence. This shows that the behavior of the near bed velocity is sensitive to low relative submergence values and is potentially important in describing transient storage, as F_{med}^{200} , in these reaches. Equation (4.8) describes a similar relationship but does not include median grain size to describe F_{med}^{200} .

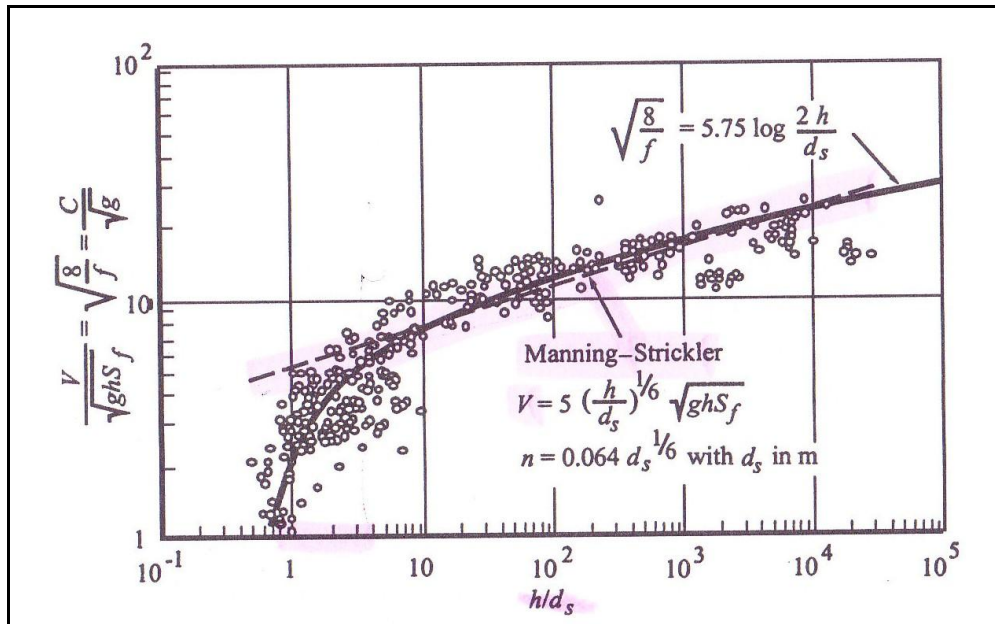


Figure 4.12: Relative submergence relationship (Julien 2002)

4.3 DISCUSSION

Quantifying nitrate uptake in natural systems is challenging due to various complex interactions among hydraulic and geomorphic characteristics and biogeochemical processes. The datasets and models developed in this study suggest that transient storage and biogeochemical processing of nitrate are mediated by hydraulic and geomorphic influences. Regression modeling indicates that nitrate uptake is significantly associated with increasing grain size, Reynolds number, flow depth, and longitudinal roughness. Similarly, hyporheic exchange is influenced by characteristics of flow (shear velocity) and substrate condition (porosity and grain size) (O'Connor and Harvey 2008). Although shear velocity was not a significant descriptor of nitrate uptake or transient storage in this study, increases in flow depth and Reynolds number are associated with increases in nitrate uptake velocity. This suggests that flow depth is more influential than slope for the reaches in this study because shear velocity scales with the square root of

flow depth and slope and Reynolds number scales with flow depth. Corresponding with previous studies (Mulholland *et al.* 2009; Hall *et al.* 2009), increases in nitrate uptake, as described by higher v_f and shorter S_w , are associated with increased time in transient storage, as described by F_{med}^{200} . A portion of F_{med}^{200} describes transient storage in the hyporheic zone. In this study, regression models show that F_{med}^{200} relates to substrate conditions with positive correlation to median grain size and negative correlation to FBOM. This shows that reaches with coarser substrate will have greater potential for hyporheic exchange, leading to greater capability for nitrate uptake, than reaches with finer substrate. Furthermore, accumulation and evacuation of FBOM could affect the potential for hyporheic transient storage. As various models of hyporheic exchange have used different grain sizes, from fine to coarse grains, to describe bed permeability (O'Connor and Harvey 2008), the term $d_{50}/FBOM$ in Equation (4.7) expresses the interaction of fine and coarse bed material as a descriptor of bed permeability. Increases in $d_{50}/FBOM$ describe increases in bed permeability, which can yield more hyporheic exchange. Other metrics of transient storage, including the exchange coefficient (α) and the ratio of storage area to main channel area (A_s/A) were investigated for negative correlations to FBOM, similar to that shown with F_{med}^{200} . Both α ($r = -0.62$; $p = 0.002$) and A_s/A ($r = -0.35$; $p = 0.09$) were negatively correlated to FBOM, further supporting that FBOM can clog porous space in the streambed and reduce potential for hyporheic exchange. Relationships between thalweg variation and hyporheic exchange have also been previously described (Anderson *et al.* 2005; Wondzell 2006; Hester and Doyle 2008), and the models developed in this study show relationships between greater thalweg variation (longitudinal roughness) and shorter uptake lengths (greater uptake)

and between shorter uptake lengths and greater residence time in transient storage (greater F_{med}^{200}), including hyporheic exchange.

Linkages among geomorphic characteristics, hydraulics, transient storage, and nutrient uptake are important for developing empirical relationships that can be applied to stream restoration design (O'Connor *et al.* 2009). Empirical relationships developed in this study show associations among v_f , median grain size, F_{med}^{200} (including hyporheic storage), FBOM, longitudinal roughness, and S_w . Prior studies have also shown links between hyporheic exchange and substrate permeability (Packman and Salehin 2003) and between hyporheic exchange and bed material size (Tonina and Buffington 2009). Additionally, the models developed in this study suggest that the behavior of near bed velocity is important in describing transient storage, as indicated by the relationship of F_{med}^{200} with low values of relative submergence.

This study demonstrates that nitrate uptake and transient storage are detectably influenced by flow variability and geomorphic characteristics, including median grain size and longitudinal roughness. The geomorphic context of streams mediates physical characteristics of substrate condition and roughness, which influence amounts of hyporheic storage versus in-channel storage. In turn, nitrate uptake is linked to transient storage, as it behaves differently in each storage zone and varies with changes in discharge. Accordingly, it is important to measure nitrate uptake over various flow rates to adequately characterize its behavior in streams. Furthermore, much of the focus on F_{med}^{200} as a parameter describing transient storage emphasizes hyporheic exchange; however, in-channel storage is also included in transient storage values of F_{med}^{200} and nitrate uptake behaves differently in the hyporheic zone as compared to in-channel

storage. Differentiating between in-channel storage and hyporheic storage, which is explored further in Chapter 5, is important in future studies to more fully understand nitrate uptake and other biogeochemical processes occurring within stream ecosystems.

5 RESTORATION INTRASITE COMPARISON

5.1 OVERVIEW

Land use and restoration activities affect a variety of stream attributes and processes, including the behavior of nutrient processing. Stream restoration techniques have the potential to promote hyporheic exchange and reduce downstream nutrient pollution through biogeochemical processing in the hyporheic zone (Hester and Gooseff 2010). Because headwater streams are crucial to nutrient processing in watersheds (Peterson *et al.* 2001), I examined the potential of two stream restoration approaches to promote nitrate uptake and reduce downstream nitrogen pollution in two headwater streams. Both streams, Sheep Creek and Nunn Creek, have been influenced by livestock grazing. Sheep Creek is located in open rangeland in northern Colorado and has been impacted by cattle grazing for several decades. Sections of Sheep Creek were fenced off and exclosed from cattle grazing in the 1950s. The riparian corridors of these sections naturally regenerated and are now dense with willows (*Salix* spp.). Other sections of Sheep Creek have been continuously grazed for more than a half century.

In contrast to the non-structural practice of removing the grazing stressor on Sheep Creek, structural interventions have occurred along Nunn Creek. In 2003, J-hook and log vane restoration structures (NRCS 2007) were constructed along portions of Nunn Creek for bank stabilization and trout habitat enhancement. I studied four reaches

along Sheep Creek and two reaches along Nunn Creek. Of the four Sheep Creek study reaches (Figure 3.6 in Chapter 3), two reaches have been exclosed from grazing, and two reaches are currently grazed. One reach in each exclosed section has similar geomorphic characteristics to match a reach in the grazed section. These reaches were chosen to compare a similar stream type between a reach that has largely recovered from grazing pressure and a reach that is currently grazed. Of the two Nunn Creek reaches (Figure 3.7 in Chapter 3), one was located within the portions of the stream with restoration structures and one was located within the portion of the stream without restoration structures. Table 5.1 displays a brief description of each study reach.

Table 5.1: Description of paired study reaches

	Within exclosures	Exposed to grazing
Relatively straighter & higher gradient	Sheep Creek A: $S_o = 0.0146$ Sinuosity = 1.11	Sheep Creek C: $S_o = 0.0115$ Sinuosity = 1.24
	Sheep Creek B: $S_o = 0.0074$ Sinuosity = 1.63	Sheep Creek D: $S_o = 0.0029$ Sinuosity = 1.49
	Restoration structures	No structures
Relatively similar gradient and sinuosity	Nunn Creek B: $S_o = 0.0134$ Sinuosity = 1.61	Nunn Creek A: $S_o = 0.0133$ Sinuosity = 1.44

To investigate how restoration techniques of natural revegetation and in-channel structures in agricultural streams can affect transient storage and nitrate uptake, several visits were made to each study reach, involving nutrient injections and physical characterizations. Comprehensive data sets were collected to characterize physical complexity along each reach, including pebble counts, longitudinal profiles, cross-section

surveys, hydraulic measurements, and benthic organic matter (fine and coarse). Field injections of bromide and nitrate were used to estimate transient storage and nitrate uptake in each reach using the methods described in Chapter 3. The measured physical data and modeled transient storage and nitrate uptake data were examined for patterns and relationships among physical measurements, transient storage values, and nitrate uptake values. Although two reaches may have similar transient storage parameter estimates, one reach may have more hyporheic exchange than the other. In transient storage modeling, it is important to distinguish between in-channel storage (backwater areas and eddies) and hyporheic exchange. Briggs *et al.* (2009) utilized the OTIS model to develop a two-zone model, separating in-stream surface transient storage from hyporheic transient storage, as biogeochemical processes operate differently in each zone. In this study, first order estimates of in-channel storage and hyporheic storage were ascertained by comparing modeled values of main channel area and storage area with actual cross-sectional area from field hydraulic measurements and survey data. The area of in-channel storage was approximated as the difference between the field-measured cross-sectional area and the modeled main channel area. The hyporheic storage was then approximated as the difference between the modeled storage area and estimated in-channel storage.

By exploring the differences in parameter estimates between paired reaches (Sheep A and C; Sheep B and D; and Nunn A and B), the implemented restoration techniques were examined as to whether or not they are associated with increased transient storage and nitrate uptake. I hypothesize that reaches with restoration techniques (natural riparian revegetation due to fenced enclosures around Sheep Creek

and in-channel structures creating physical habitat variability in Nunn Creek) would have more transient storage and greater nitrate uptake than reaches without restoration techniques. In general, I hypothesize that more transient storage would be associated with faster uptake velocities and shorter uptake lengths. Preliminary analyses of the model results appeared to show that the restoration structures in Nunn Creek increased nitrate uptake. This seemed reasonable because the structures increase longitudinal roughness, which has been shown to promote hyporheic exchange (Harvey and Bencala 1993; Wondzell 2006). Increased hyporheic exchange leads to a greater potential for denitrification; however, upon further scrutiny of the modeled parameter estimates, it was discovered that the confidence limits and coefficients of variation (standard deviation/mean) were too large for a significant difference to be inferred among the parameter estimates.

The fits of the models were subsequently refined through iterative optimization of OTIS through UCODE until the smallest confidence limits and variation in the parameter estimates were achieved for each study reach. Monte Carlo simulations were performed on these modeled parameter values, assuming a normal distribution based upon the mean value and standard deviation given for each parameter in the model output from optimization in UCODE. Ranges of values for parameters of A_s/A , F_{med}^{200} , S_w , and v_f were also obtained through calculations of the distribution of values for the modeled parameters that were acquired through the Monte Carlo simulations. These simulations yielded mean values, standard deviations, and percentiles describing the range of values for each parameter.

5.2 RESULTS

By estimating the amount of transient storage and nitrate uptake along each reach, I explored how the geomorphic complexity associated with restoration techniques in each reach may influence transient storage and nitrate uptake in various geomorphic settings. Data from Sheep Creek show that Sheep A (exclosed reach) demonstrated greater transient storage and nitrate uptake than Sheep C (grazed reach). The data also show that Sheep D (grazed reach) had greater nitrate uptake than Sheep B (exclosed reach), although Sheep B had higher transient storage in one injection. In one case, the rehabilitated reach (Sheep A) had higher estimated uptake, while in another case, the non-rehabilitated reach (Sheep D) had higher estimated uptake. Data from Nunn Creek suggest that Nunn A (unrestored reach) had more transient storage than Nunn B (restored reach), but nitrate uptake values in Nunn A and Nunn B were relatively similar and varied as flow changed within each reach.

Quantified measures of geomorphic complexity, including longitudinal roughness, width variability, cross-sectional area variability, sinuosity, and bed substrate distribution; and ecological characteristics, including FBOM, CBOM, and GPP; vary among Sheep Creek study reaches (Table 5.2) and Nunn Creek study reaches (Table 5.3). In addition to differences in physical characteristics, mean values of modeled transient storage and nitrate uptake parameters also vary among Sheep Creek reaches (Table 5.4) and Nunn Creek reaches (Table 5.5). Due to poor model fits of transient storage and nitrate uptake parameters from the third visit to Nunn Creek A on 8-29-09 and the 2008 visit to Sheep Creek A, these values were removed from this portion of the study. For the rest of the study reaches, the OTIS/UCODE models converged on BTCs that were used

to estimate transient storage parameters from bromide BTCs (Figures 4.3 and 4.5 in Chapter 4) and nitrate uptake parameters from nitrate BTCs (Figures 4.4 and 4.6 in Chapter 4). As described in Chapter 3, Monte Carlo simulations were performed on the modeled parameter estimates and yielded median values, inter-quartile ranges, and 90% confidence intervals for the distribution of possible values for transient storage and nitrate uptake parameters (Figures 5.1 through 5.7). For parameter estimates with more variance than others, the ends of the boxes or whiskers extend beyond the plot but are cut off for purposes of contrasting the parameter estimates with narrower distributions.

The analyses of physical attributes along Sheep Creek show more similarities within stream type than within rehabilitated reaches and non-rehabilitated reaches, which confirm the site selection of the paired reaches. Sheep A and C have similar values for longitudinal roughness and cross-sectional area variability when compared to the slightly higher values in Sheep B and D. Sheep A, B, and D have similar values of width variability, while Sheep C has higher width variability than the other Sheep Creek study reaches. Sheep D has a higher percentage of fine substrate (<2 mm) and smaller substrates sizes than its paired rehabilitated reach, Sheep B. The grain size distribution also shows that Sheep C has slightly finer substrate than its paired rehabilitated reach, Sheep A. As a measure of channel roughness, relative submergence values in Sheep B and D are higher than in Sheep A and C, which demonstrate another similarity within stream type, as opposed to restoration technique. Both study reaches that are currently impacted by grazing pressure, Sheep C and D, have higher amounts of FBOM than their paired rehabilitated reaches, Sheep A and B, respectively.

The analyses of physical attributes along Nunn Creek show that thalweg variability and cross-sectional area variability were higher in the restored reach, Nunn B, while width variability was higher in the unrestored reach, Nunn A. According to the grain size distributions, the restored reach has slightly larger substrate than the unrestored reach, partly due to the introduction of large boulders for the construction of the J-hook vane structures. Although the restored reach has more FBOM, the unrestored reach has more CBOM. Higher values of CBOM in the unrestored reach originate from more instream wood in this reach compared to the restored reach.

Table 5.2: Summary of Sheep Creek physical and ecological characteristics

	Sheep A July 2007	Sheep C July 2007	Sheep A September 2008	Sheep B September 2008	Sheep C September 2008	Sheep D September 2008	Sheep B September 2009	Sheep D September 2009
Reach length (m)	189	191	189	184	189	185	176	194
Flow (L/s)	104	102	72	72	34	32	52	35
Unit discharge, q (m ² /s)	0.029	0.022	0.022	0.022	0.009	0.011	0.016	0.012
Ambient [NO ₃ ⁻ -N] (mg/L)	0.00	0.13	0.10	0.10	0.10	0.10	0.10	0.10
Unit stream power, ω (W/m ²)	4.20	2.51	3.15	1.67	1.00	0.30	1.12	0.34
Reynolds number, Re	29,310	13,540	10,710	22,120	9,100	10,790	15,830	11,790
Longitudinal roughness (m)	0.07	0.08	0.07	0.11	0.09	0.14	0.11	0.14
Width variability (m)	0.65	1.23	0.58	0.56	1.06	0.60	0.63	0.69
XS area variability (m)	0.10	0.18	0.12	0.20	0.15	0.29	0.21	0.27
Percent fines (<2 mm)	13%	10%	6%	1%	9%	9%	0.2%	8%
d_{16} (mm)	4	5	10	13	7	8	12	6
d_{50} (mm)	37	34	38	39	27	21	29	18
d_{84} (mm)	142	117	105	76	74	48	56	40
Gradation coefficient	6.3	5.0	3.2	2.5	3.3	2.5	2.2	2.7
Relative submergence, R/d_{84}	0.9	1.0	1.1	1.8	1.3	4.1	2.0	3.7
Metric of complexity	1.1E-03	1.2E-03	1.1E-03	1.3E-03	1.2E-03	5.8E-04	1.3E-03	6.2E-04
FBOM AFDM (g/m ²)	8	58	10	22	16	85	21	27
CBOM AFDM (g/m ²)	16	4	1	7	7	11	3	3
GPP (gO ₂ /m ² /day)	0.64	0.07	0.01	0.04	0.01	0.04	0.03	0.05

Table 5.3: Summary of Nunn Creek physical and ecological characteristics

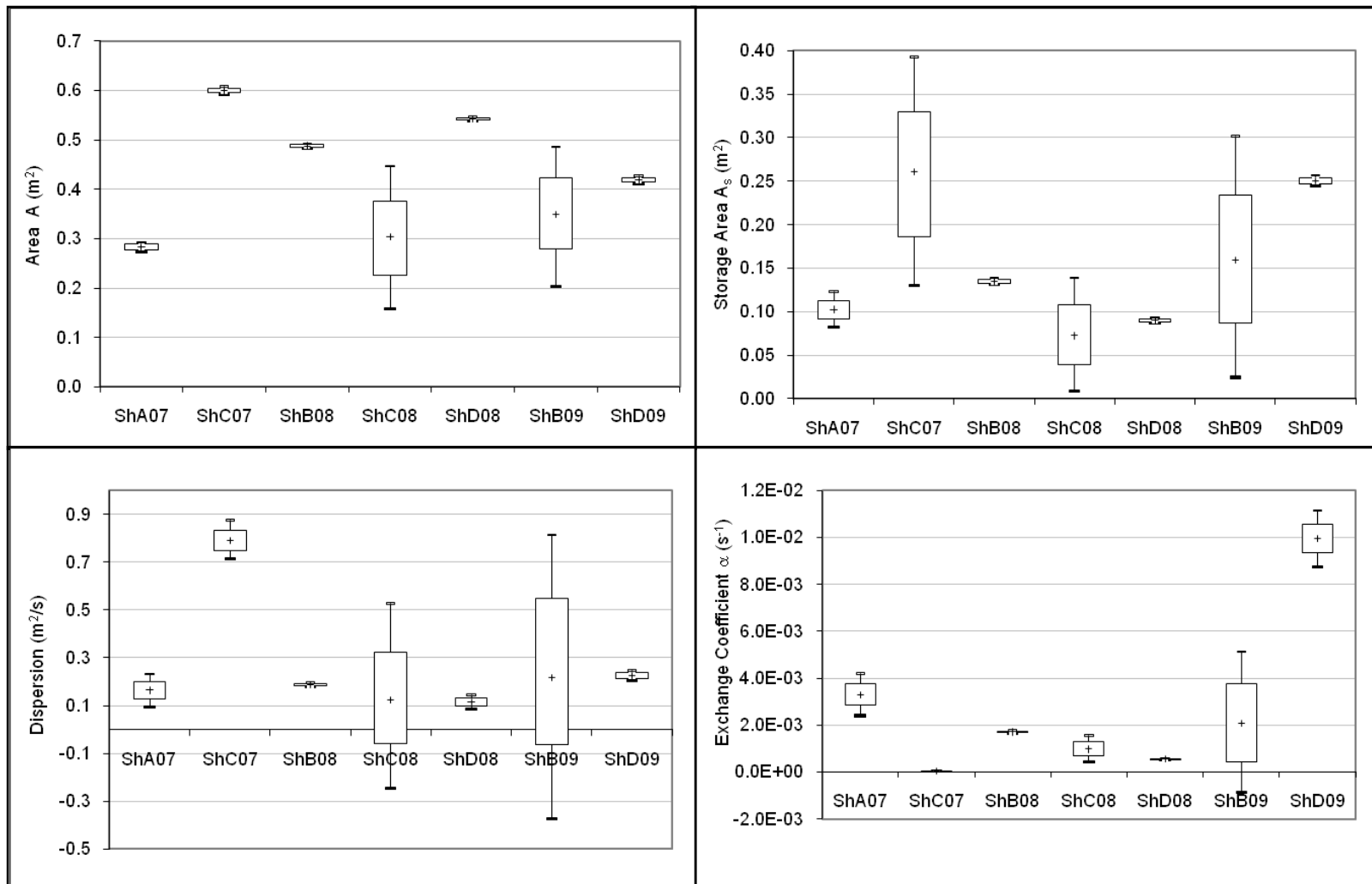
	Nunn Creek A 8-1-09	Nunn Creek A 8-12-09	Nunn Creek A 8-29-09	Nunn Creek B 8-2-09	Nunn Creek B 8-13-09	Nunn Creek B 8-30-09
Reach length (m)	174	174	174	163	163	163
Flow (L/s)	209	98	87	191	125	101
Unit discharge, q (m ² /s)	0.043	0.023	0.020	0.038	0.027	0.022
Ambient [NO ₃ ⁻ -N] (mg/L)	0.10	0.10	0.10	0.10	0.10	0.10
Unit stream power, ω (W/m ²)	5.64	2.96	2.65	4.97	3.56	2.88
Reynolds number, Re	43,250	22,690	20,330	37,800	27,070	21,880
Longitudinal roughness (m)	0.12	0.12	0.12	0.16	0.16	0.16
Width variability (m)	0.94	0.88	0.81	0.66	0.48	0.52
XS area variability (m)	0.19	0.17	0.16	0.29	0.40	0.42
Percent fines (<2 mm)	0%	0%	0%	0.4%	0.4%	0.4%
d_{16} (mm)	28	28	28	30	30	30
d_{50} (mm)	63	63	63	74	74	74
d_{84} (mm)	112	112	112	197	197	197
Gradation coefficient	2.0	2.0	2.0	2.6	2.6	2.6
Relative submergence, R/d_{84}	1.3	1.1	1.1	1.1	1.2	1.1
Metric of complexity	2.3E-03	2.3E-03	2.3E-03	3.5E-03	3.5E-03	3.5E-03
FBOM AFDM (g/m ²)	16	21	11	33	27	33
CBOM AFDM (g/m ²)	72	8	24	10	4	5
GPP (gO ₂ /m ² /day)	0.07	0.04	0.04	0.07	0.04	0.03

Table 5.4: Summary of Sheep Creek transient storage and nitrate uptake parameter estimates

	Sheep A July 2007	Sheep C July 2007	Sheep B September 2008	Sheep C September 2008	Sheep D September 2008	Sheep B September 2009	Sheep D September 2009
A (m ²)	0.28	0.60	0.49	0.30	0.54	0.35	0.42
A_s (m ²)	0.10	0.26	0.13	0.07	0.09	0.16	0.25
D (m ² /s)	0.16	0.79	0.19	0.14	0.11	0.24	0.23
α (s ⁻¹)	3.3E-03	3.4E-05	1.7E-03	1.0E-03	5.5E-04	2.1E-03	9.9E-03
λ (s ⁻¹)	2.1E-04	2.6E-05	1.2E-05	2.8E-05	4.8E-05	4.9E-05	8.3E-05
λ_s (s ⁻¹)	4.2E-10	3.4E-04	4.0E-04	4.8E-04	9.6E-06	7.9E-05	8.6E-08
A_s/A	0.36	0.43	0.28	0.24	0.17	0.46	0.60
F_{med}^{200}	0.25	0.01	0.19	0.17	0.12	0.30	0.37
S_w (m)	1,090	7,380	13,770	3,350	1,130	2,850	960
v_f (m/s)	3.3E-05	3.6E-06	2.0E-06	3.4E-06	1.1E-05	6.6E-06	1.4E-05

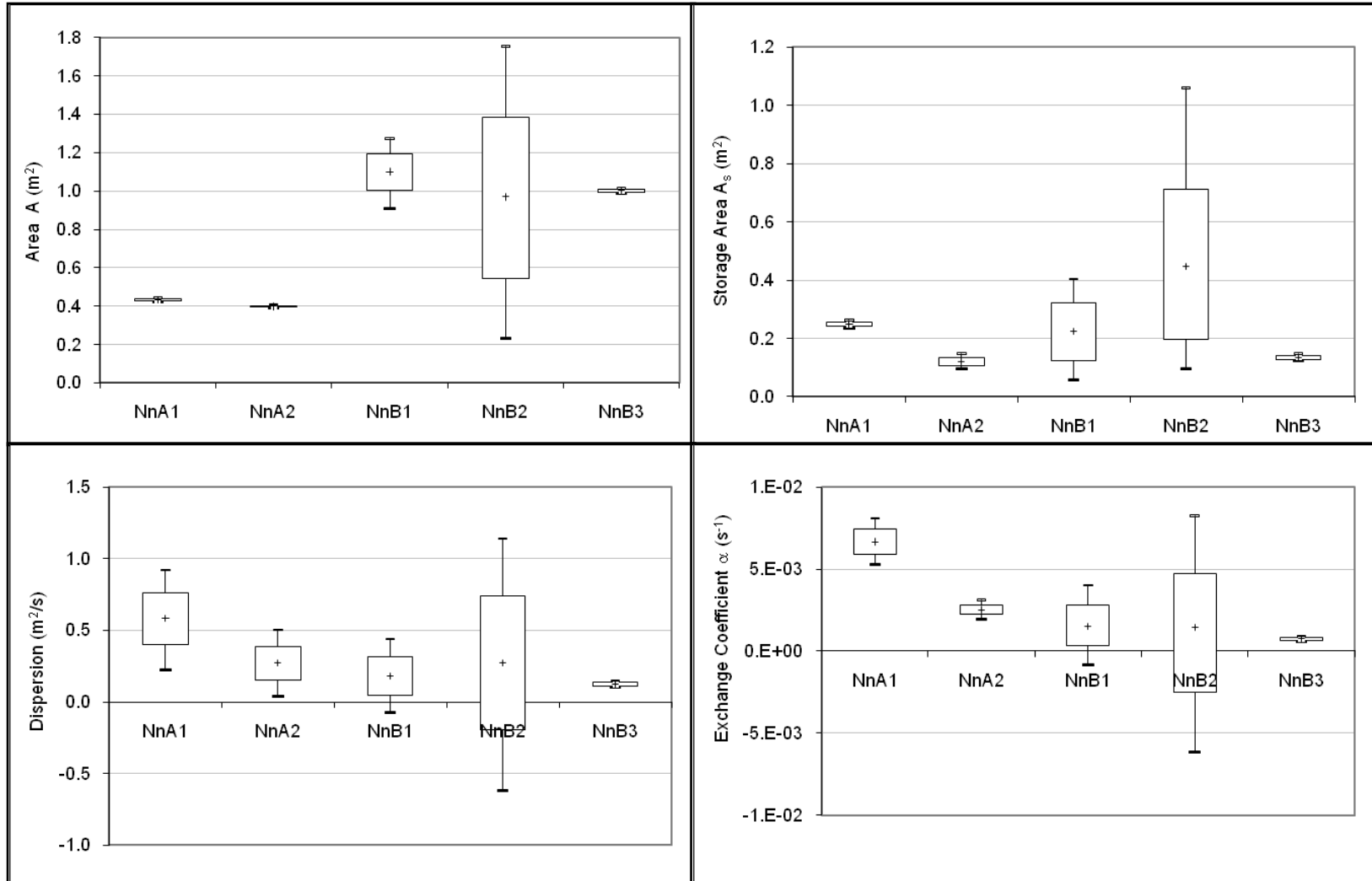
Table 5.5: Summary of Nunn Creek transient storage and nitrate uptake parameter estimates

	Nunn Creek A 8-1-09	Nunn Creek A 8-12-09	Nunn Creek B 8-2-09	Nunn Creek B 8-13-09	Nunn Creek B 8-30-09
A (m ²)	0.43	0.40	1.09	0.98	1.00
A_s (m ²)	0.25	0.12	0.22	0.21	0.13
D (m ² /s)	0.56	0.27	0.19	0.27	0.13
α (s ⁻¹)	6.7E-03	2.5E-03	1.5E-03	1.1E-03	7.5E-04
λ (s ⁻¹)	3.0E-04	3.4E-04	1.4E-04	2.3E-04	5.8E-05
λ_s (s ⁻¹)	2.1E-04	5.2E-05	7.6E-05	5.5E-10	1.8E-03
A_s/A	0.57	0.30	0.20	0.21	0.13
F_{med}^{200}	0.36	0.22	0.14	0.15	0.09
S_w (m)	1,000	560	1,250	510	1,690
v_f (m/s)	5.8E-05	4.7E-05	3.9E-05	6.2E-05	1.4E-05



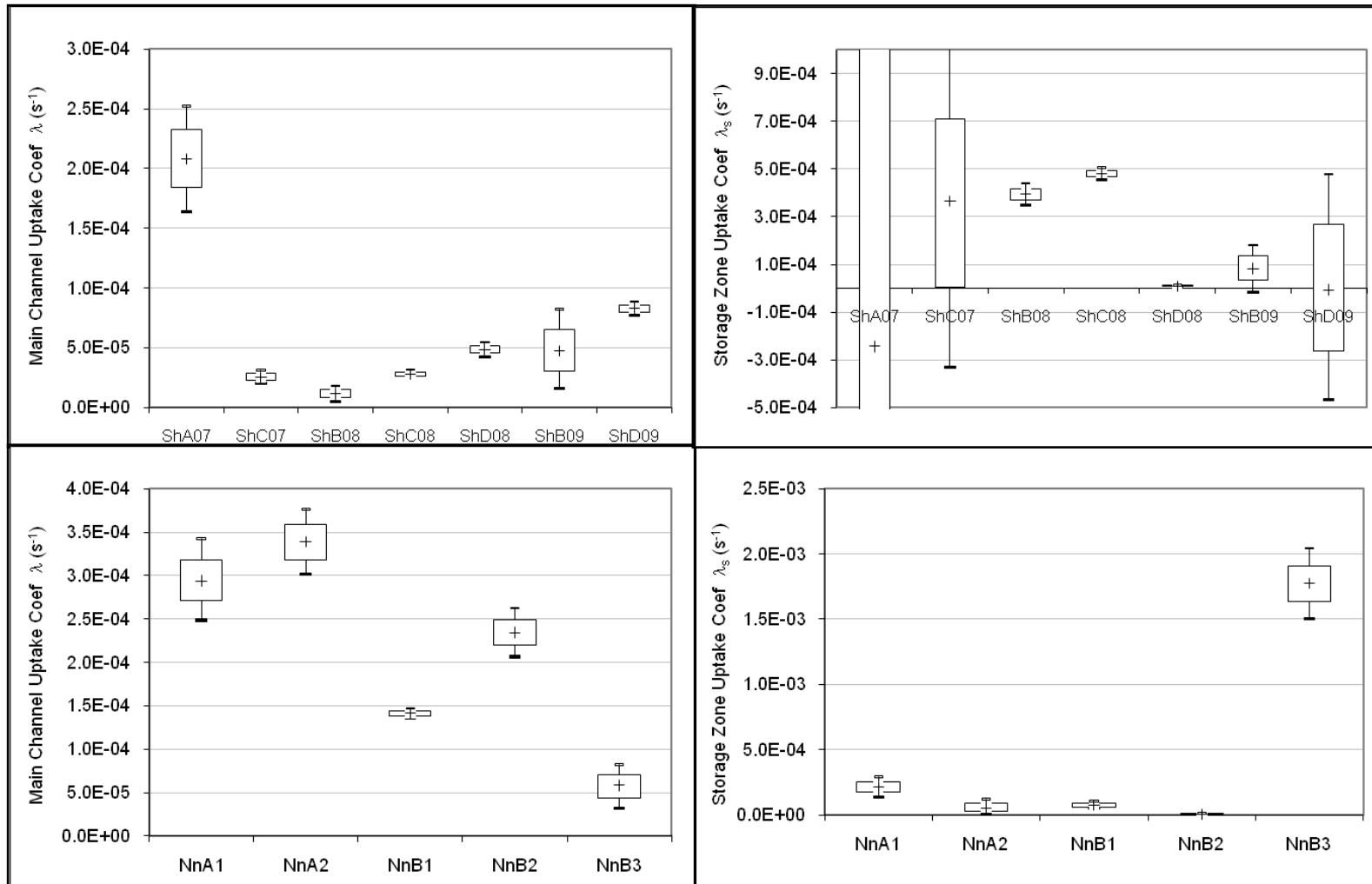
Note: Sheep A July 2007 is represented as ShA07; whiskers = 10th and 90th percentiles, box = 25th and 75th percentiles, crossbar = median

Figure 5.1: Results of Monte Carlo simulations of transient storage parameters for Sheep Creek study reaches



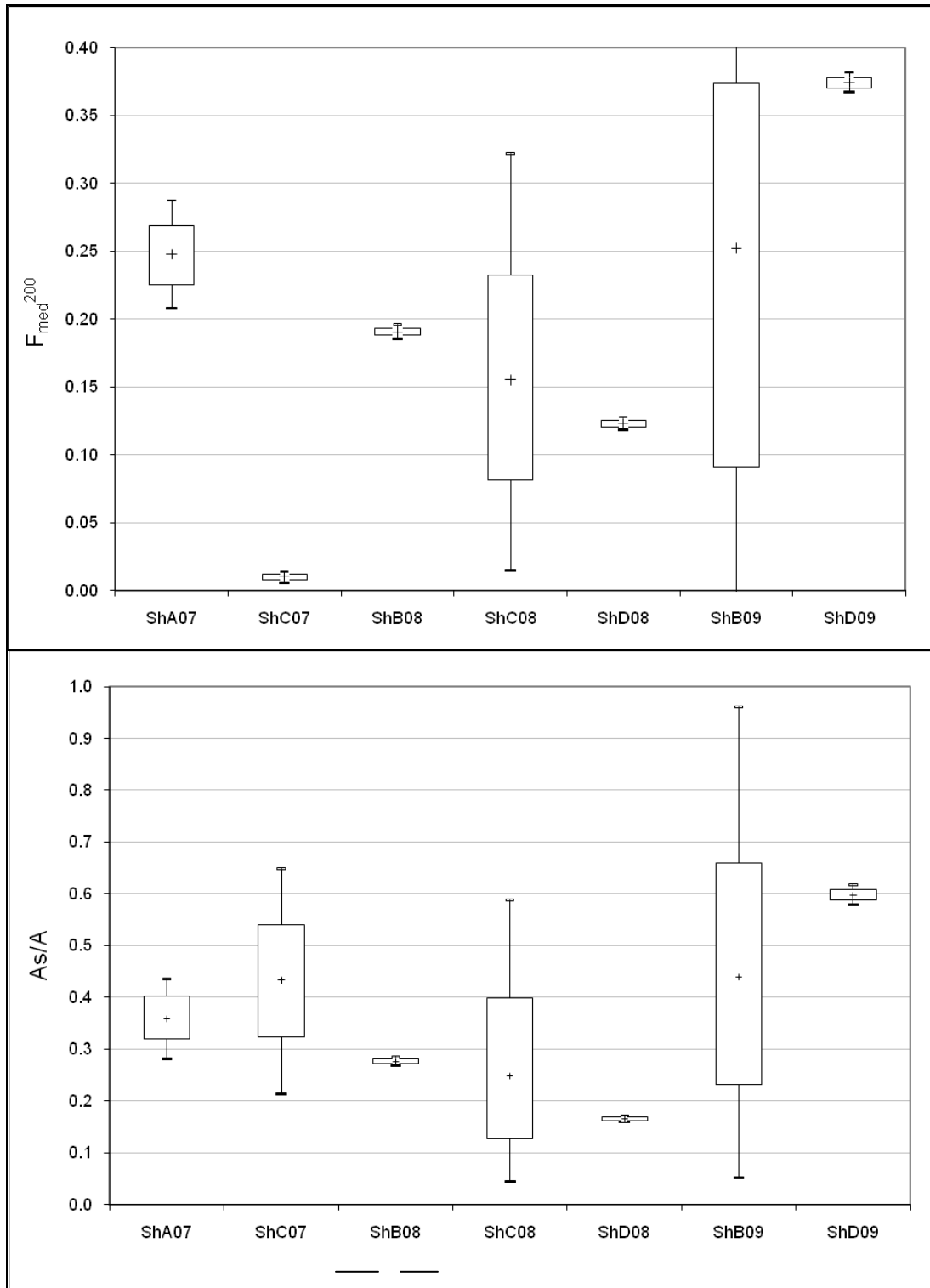
Note: Nunn A 8-1-09 is represented as NnA1; whiskers = 10th and 90th percentiles, box = 25th and 75th percentiles, crossbar = median

Figure 5.2: Results of Monte Carlo simulations of transient storage parameters for Nunn Creek study reaches



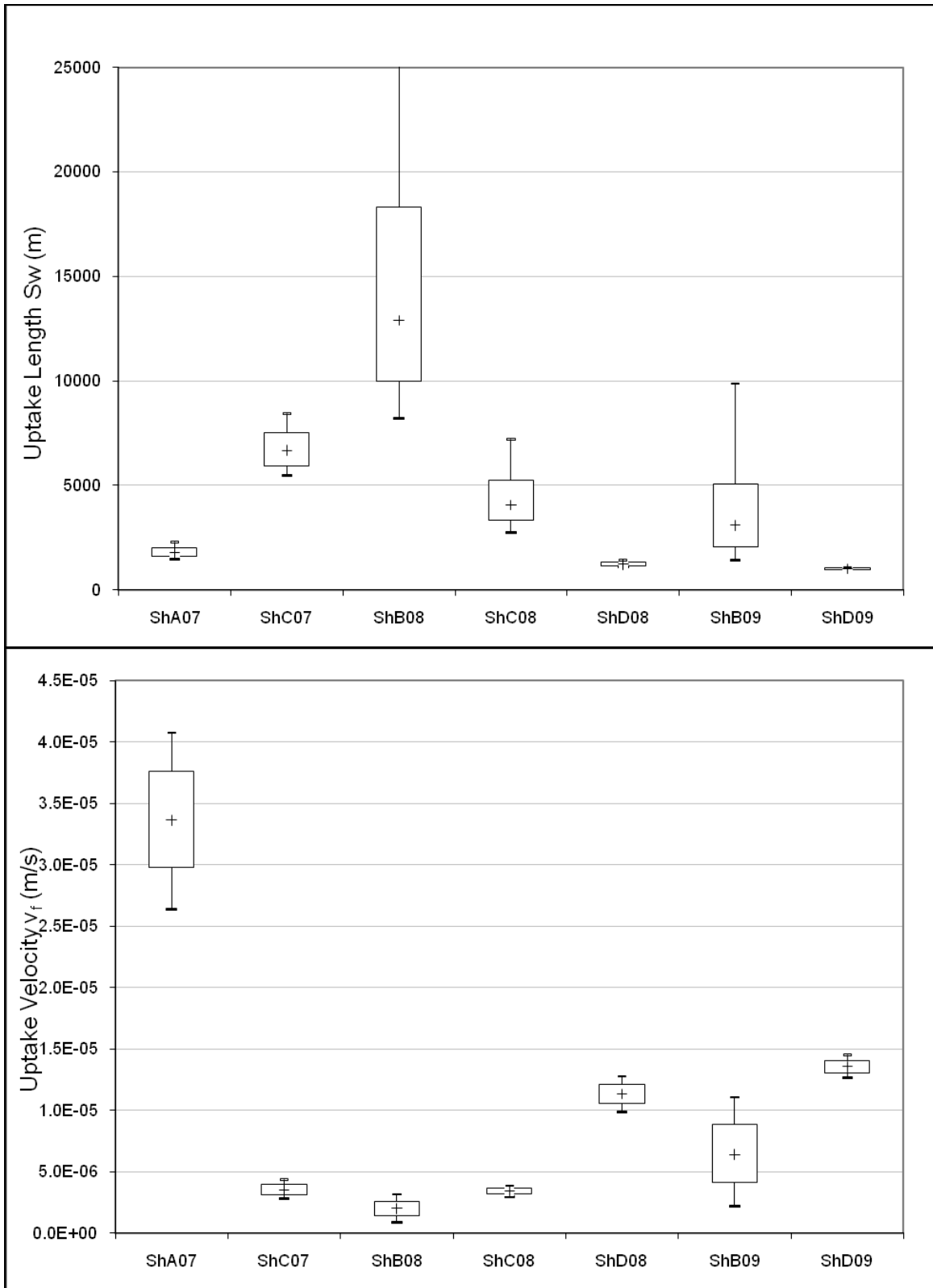
Note: whiskers = 10th and 90th percentiles, box = 25th and 75th percentiles, crossbar = median

Figure 5.3: Results of Monte Carlo simulations of nitrate uptake parameters for Sheep Creek and Nunn Creek study reaches



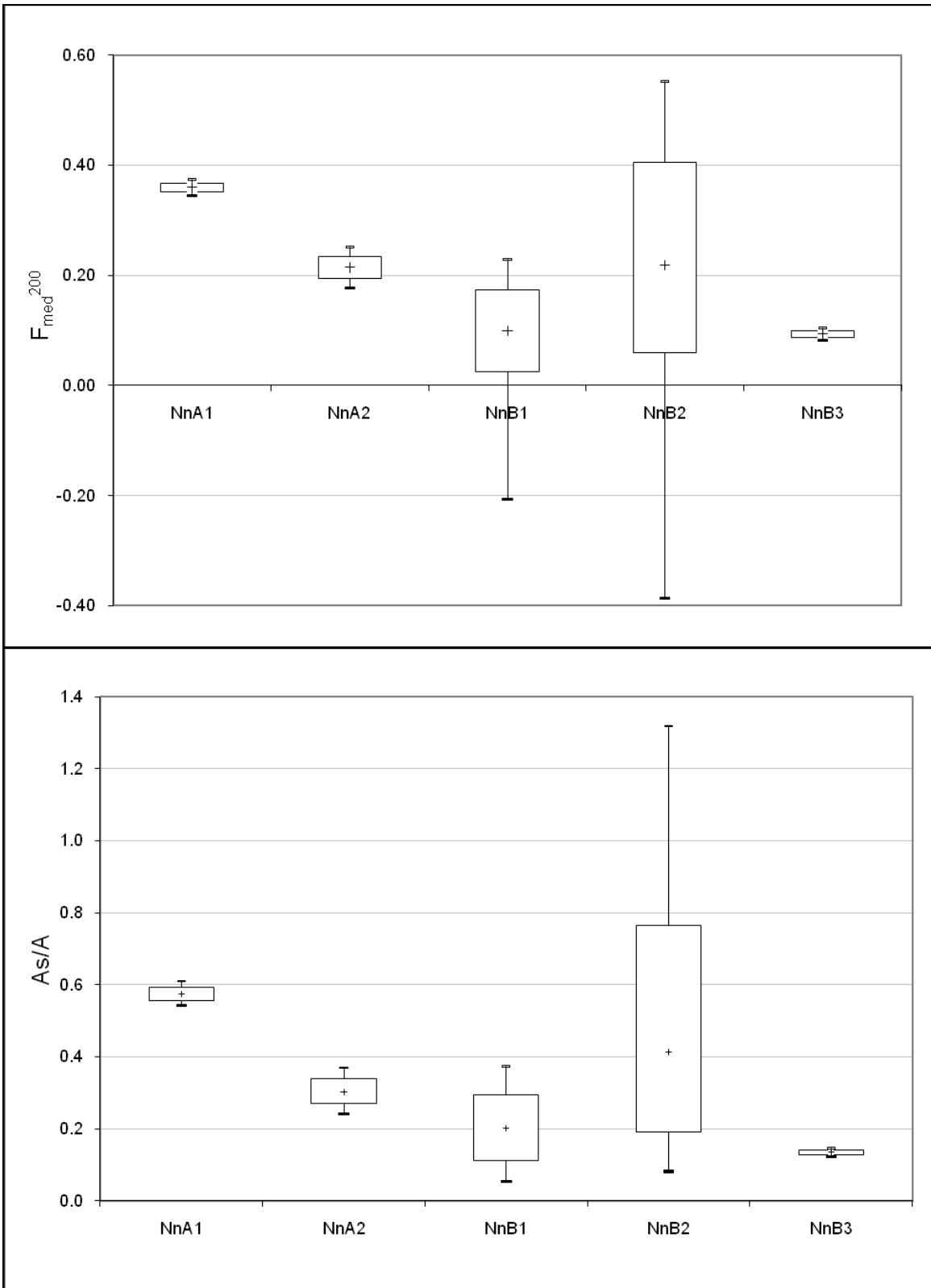
Note: Sheep A July 2007 is represented as ShA07; whiskers = 10th and 90th percentiles, box = 25th and 75th percentiles, crossbar = median

Figure 5.4: Results of Monte Carlo simulations of F_{med}^{200} and A_s/A for Sheep Creek



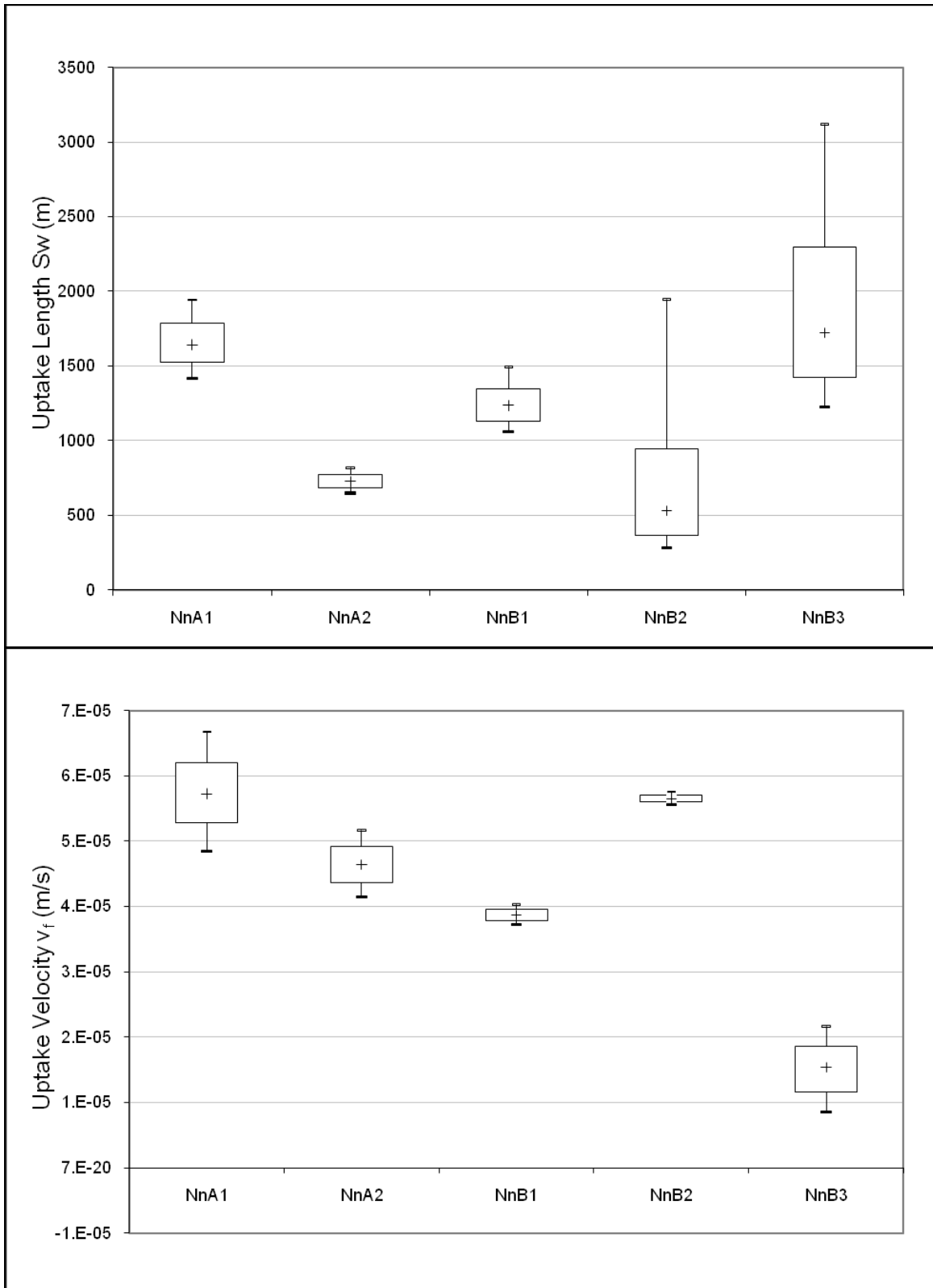
Note: Sheep A July 2007 is represented as ShA07; whiskers = 10th and 90th percentiles, box = 25th and 75th percentiles, crossbar = median

Figure 5.5: Results of Monte Carlo simulations of S_w and v_f for Sheep Creek



Note: Nunn A 8-1-09 is represented as NnA1; whiskers = 10th and 90th percentiles, box = 25th and 75th percentiles, crossbar = median

Figure 5.6: Results of Monte Carlo simulations of F_{med}^{200} and A_s/A for Nunn Creek



Note: Nunn A 8-1-09 is represented as NnA1; whiskers = 10th and 90th percentiles, box = 25th and 75th percentiles, crossbar = median

Figure 5.7: Results of Monte Carlo simulations of S_w and v_f for Nunn Creek

Differences among parameter estimates describing restored reaches and unrestored reaches were compared to investigate the influence of restoration techniques on transient storage and nitrate uptake. The ranges of estimates based on the output parameter distributions from the OTIS/UCODE modeling approach were compared between paired reaches on Sheep Creek and Nunn Creek (Figures 5.1 through 5.3). For Sheep Creek, Sheep A (exclosed from grazing) is compared to Sheep C (currently grazed), and Sheep B (exclosed from grazing) is compared to Sheep D (currently grazed). These reaches are paired together based upon similar stream type. For Nunn Creek, Nunn A (unrestored) is compared to Nunn B (restored).

The parameters A_s/A , F_{med}^{200} , S_w , and v_f yield more complete descriptions of transient storage and nitrate uptake and are examined in greater detail. Sheep C has a smaller F_{med}^{200} value than Sheep A in the July 2007 injections, but A_s/A shows no significant difference between Sheep A and C for the same set of injections (Figure 5.4). Based on F_{med}^{200} , Sheep A appears to have more transient storage than Sheep C at the observed flows, but the ratio of storage area to main channel area is not significantly different between Sheep A and C in the July 2007 injections. For Sheep B and D in the September 2008 injections, Sheep B has a higher F_{med}^{200} value and a higher A_s/A value than Sheep D. In this case, the rehabilitated reach, Sheep B, has greater amounts of transient storage at the observed flows than the grazed reach, Sheep D. According to the September 2009 injections, the ranges of both F_{med}^{200} and A_s/A for Sheep B are too large to show a significant difference between amounts of transient storage in Sheep B and D, but the higher mean and median values of F_{med}^{200} and A_s/A for Sheep D suggest that Sheep D has more transient storage at the observed flows than Sheep B.

Corresponding with higher F_{med}^{200} values (greater transient storage) in Sheep A than Sheep C in the July 2007 injections, Sheep A also has a significant difference in nitrate uptake with lower S_w and higher v_f than Sheep C in the July 2007 injections. In both September 2008 and 2009 injections, Sheep D shows greater nitrate uptake than Sheep B, which coincides with mean values of transient storage in the September 2009 injection. Sheep D shows shorter S_w and higher v_f than Sheep B in both injections. Overall, Sheep A (exclosed reach) demonstrated greater transient storage and nitrate uptake than Sheep C (grazed reach). The data also show that Sheep D (grazed reach) had greater nitrate uptake than Sheep B (exclosed reach), although Sheep B had higher transient storage in one injection. In one case, the rehabilitated reach (Sheep A) seemed to have greater uptake, while in another case, the non-rehabilitated reach (Sheep D) seemed to have greater uptake.

For the Nunn Creek reaches, comparisons are made between Nunn A1 (8-1-09) and Nunn B1 (8-2-09), and between Nunn A2 (8-12-09) and Nunn B2 (8-13-09), corresponding with the different site visits. Within each pair, the injections were performed in consecutive days, so flows and ambient conditions are more similar than between site visits. The only significant difference noted in transient storage parameters is shown in the first injection, when Nunn A1 has higher F_{med}^{200} and A_s/A values than Nunn B1. In general, the median and mean values for F_{med}^{200} and A_s/A appear higher in Nunn A than in Nunn B, suggesting more transient storage in Nunn A than in Nunn B at the observed flows, but there is no significant difference in the transient storage parameters for the second injection. Overall, Nunn A had higher mean values of F_{med}^{200} than Nunn B, but results of nitrate uptake values in Nunn A and Nunn B were

inconclusive. The difference in v_f values are significant, with Nunn A showing faster uptake velocities in the first injection and Nunn B showing faster uptake velocities in the second injection, but the differences are small. Although Nunn B showed less transient storage, it seems to have shorter uptake lengths (greater nitrate uptake) than Nunn A for the first two injections. According to v_f values in the first injection, the unrestored reach with higher transient storage values, Nunn A, shows greater nitrate uptake. This supports the hypothesis that greater transient storage is associated with higher nitrate uptake. However, according to S_w values, the restored reach, Nunn B, appears to have shorter uptake lengths and greater nitrate uptake, although the S_w comparisons do not show significant differences. These patterns are shown within Nunn B for the first two injections, but the third injection at Nunn B has the greatest uptake length and lowest uptake velocity (least nitrate uptake). This could be due to the date of the injection being at the very end of August when the temperatures become colder at high elevations. As the season was beginning to change, the colder water temperatures could have led to less microbial and biotic activity and less biogeochemical processing.

5.3 DISCUSSION

Responses of transient storage and nitrate uptake to restoration techniques depend upon the type and extent of restoration implemented, as well the context and physical setting of each study reach. Based upon Sheep Creek data, there is no clear evidence to support the hypothesis that the restoration technique of removing grazing pressure to allow natural rehabilitation of riparian vegetation enhances nitrate uptake relative to the grazed reach. This technique involves a more passive rehabilitation approach of allowing

willows to colonize along the streambanks to create a wider riparian corridor than reaches with minimal riparian vegetation due to livestock grazing. In one case, the rehabilitated reach (Sheep A) seemed to have greater uptake, while in another case, the non-rehabilitated reach (Sheep D) seemed to have greater uptake. Perhaps other factors, including stream type, flow rate, and transient storage in the channel versus in the hyporheic zone, have a greater influence on nitrate uptake than this restoration technique. Seasonality could also be a confounding factor influencing nitrate uptake in studies on Sheep Creek, as the first set of injections were performed in July 2007, while the following injections were performed in September 2008 and 2009.

In Nunn Creek, greater amounts of transient storage in Nunn A appear to be linked to areas of instream wood that obstructed flow and slowed local velocities, creating backwater areas. The nitrate uptake results for Nunn Creek, as described by v_f and S_w , do not yield distinct patterns (Figure 5.7). Furthermore, flow also decreased with subsequent injections at Nunn Creek. As nitrate uptake values varied with changes in flow along each reach, the discrepancy in v_f and S_w trends could be due to flow variation. In calculating nitrate uptake values, v_f is positively correlated with flow depth, and S_w is positively correlated with flow velocity. Accordingly, differences between reaches in how velocity and depth respond to changes in discharge influence patterns in v_f and S_w estimates across injections. To investigate how variations in flow rate may influence v_f and S_w , I performed at-a-station hydraulic geometry calculations for each reach to explore if the flow depth or velocity was more greatly affected by changes in flow. For both reaches, velocity increased more with flow than did depth. Based on this hydraulic geometry analysis, S_w is more sensitive to changes in flow than v_f in these study reaches.

I used the Nunn Creek experiments to further investigate flow variability and implications for transient storage and nitrate uptake. As opposed to Sheep Creek reaches, where there was about a 1-yr time lapse between repeat injections, all nutrient injections on Nunn Creek were performed within one month. Few studies have performed multiple nutrient injections along the same stream reach. In this study, repeat injections were performed in this study with two injections on each of the Sheep Creek reaches and three injections on each of the Nunn Creek reaches. By performing repeat injections on the same study reach, it is possible to capture flow variability with different discharges over time, which may affect uptake more than geomorphological characteristics.

Initially, I hypothesized that more transient storage would be associated with greater nitrate uptake, but as the study progressed, the importance of in-channel versus hyporheic transient storage became apparent. Overall, transient storage parameters (A_s/A and F_{med}^{200}) decreased as flow decreased. This is likely due to decreases in flow area and less in-channel storage, as well as decreases in flow depth and less pressure head driving flow into the hyporheic zone. Because transient storage consists of both in-channel storage and hyporheic zone storage, first order estimates of in-channel storage and hyporheic storage were calculated by comparing physical measurements of total cross-sectional area with modeled parameters of main channel and storage areas. For each reach, the average cross-sectional area was calculated from hydraulic measurements for each injection. The difference between the total measured cross-sectional area and the modeled main channel area, A , was assumed to be the amount of in-channel storage along each reach. This estimate of in-channel storage was subtracted from the modeled storage

area, A_s , to yield an estimate of hyporheic storage, assuming that any storage not located in the channel was hyporheic storage.

The differentiation of storage area between in-channel storage and hyporheic storage (Figure 5.8) suggests that Nunn B (restored reach) storage area consisted of predominantly hyporheic storage, while Nunn A (unrestored reach) consisted of predominantly in-channel storage. This illustrates that two reaches with different amounts of total transient storage, may nevertheless have similar potential for nutrient uptake owing to varying extents of in-channel versus hyporheic storage. Due to greater thalweg variability in Nunn B than in Nunn A, more flow could be driven into the hyporheic zone, thereby enhancing nitrate uptake. This is supported by shorter S_w mean values in Nunn B for the first two injections and greater percentages of hyporheic storage in total storage area, as compared to Nunn A. Additionally, as flow decreased with subsequent injections, hyporheic zone storage seemed to decrease more rapidly than in-channel storage within both study reaches on Nunn Creek. As flow decreased, there was less of a driving force of flow over structures, less pressure head at lower flow depths, and possibly more periphyton settling out and clogging porous space in the streambed, all leading to less hyporheic exchange.

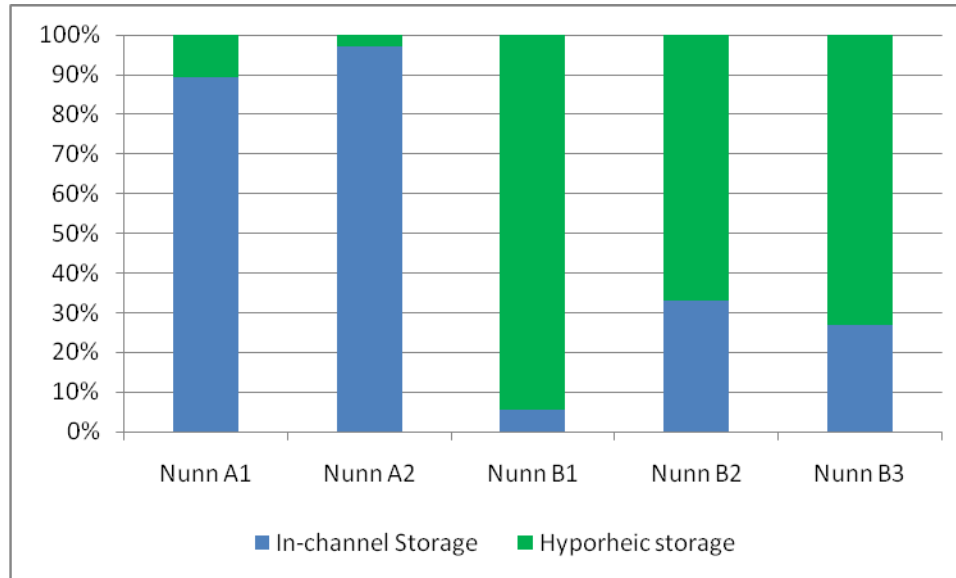


Figure 5.8: Percentage of storage zone area composed of instream and hyporheic storage

Because the two Nunn Creek reaches had different degrees of in-channel versus hyporheic storage, the ratios of surface area to volume (SA:V) were also examined for each reach. Overall, Nunn A had higher SA:V than Nunn B. As flow decreased across injections, the SA:V for Nunn A increased from 6.8 m^{-1} to 8.4 m^{-1} . In Nunn A, surface area decreased faster than volume did as flow decreased, showing that wetted perimeter is more greatly affected by changes in flow than depth. In contrast, the SA:V slightly decreased from 4.7 m^{-1} to 4.4 m^{-1} as flow decreased in Nunn B. In Nunn B, volume decreased faster than surface area did as flow decreased, showing that depth is more greatly affected by flow changes than wetted perimeter. Because the banks are stabilized in Nunn B, the flow cannot spread onto the banks during higher flows as much as in Nunn A. In Nunn A, flow can spread out more and yield higher SA:V and more in-channel storage than Nunn B. In Nunn B, flow is confined by bank stabilization and can influence flow depths with pressure head above the bed that can promote hyporheic

exchange. According to uptake velocity values, both reaches showed similar nitrate uptake. Due to the differences in SA:V and in partitioning of storage area into hyporheic and in-channel storage between the restored and unrestored reaches of Nunn Creek, it is plausible that each reach processes nitrate differently through hyporheic exchange in Nunn B and in-channel storage in Nunn A. As biogeochemical processing occurs differently in hyporheic and in-channel storage, it is important to strive toward separating these storage zones when estimating nutrient uptake. Although Nunn A may show greater transient storage and higher nitrate uptake velocity during one injection, this does not necessarily mean that it has more denitrification occurring than in Nunn B. Furthermore, it is more likely that nitrate will be denitrified in the hyporheic zone where anoxic conditions exist, while in-channel storage may lead to greater short term retention of nitrate. The ratio of in-channel to hyporheic storage is sensitive to both geomorphic characteristics and discharge, which strongly influence nitrate removal via denitrification in small streams. This study shows that the association among changes in flow and processes driving transient storage and nitrate uptake is not a monotonic relationship as described by Doyle (2005), but it involves complex interactions of geomorphic characteristics and in-channel versus hyporheic storage, as well as flow variability.

Preliminary analyses of the model results appeared to show that the restoration structures in Nunn Creek increased nitrate uptake. Further scrutiny of the modeled parameter estimates revealed that the confidence limits and coefficients of variation (standard deviation/mean) were too large for significant differences to be inferred among the parameter estimates. Although many studies have been performed to estimate transient storage and nutrient uptake, few have closely examined the uncertainty involved

in the values of the parameter estimates. When examining the range of parameter estimate values, the outcome of the analysis can be different from what is initially observed. In a notable exception, Gooseff *et al.* (2005) performed a sensitivity analysis of reactive solute transport models, including simulations sensitivities and coefficients of variation, and found that reactive solute simulations were sensitive to reaction (uptake) parameters, as well as modeled transport parameters. As shown in Figures 5.1 through 5.7, the resulting parameter estimates have ranges of values and uncertainty involved in the mean value of the estimate. Although the data in this study were modeled until standard deviations were at a minimum for each parameter estimate, there were still a few parameter estimates that yielded ranges too large to determine a significant difference with other parameters. Overall, after rigorous assessment of the uncertainty among parameters, I was able to determine significant differences that allowed a more robust analysis and more accurate interpretation of the modeled parameters that showed significant differences.

Although there is growing interest in how nitrate dynamics are affected by geomorphic restoration techniques, few studies have documented effects of restoration implementation on nitrate uptake. In a notable exception, transient storage and nitrate uptake were investigated in a channelized reach prior to restoration and again after restoration of constructed meanders and pool-riffle sequences (Bukaveckas 2007). Restoration techniques increased transient storage and nutrient uptake by decreasing water velocities, compared to the previously channelized reach (Bukaveckas 2007). In addition to the two restoration techniques studied here (natural revegetation and in-channel structures), Craig *et al.* (2008) discussed the creation of “hotspots” of structures

containing a carbon source to act as flow obstructions in streams, leading to slower velocities and greater contact time with biogeochemically active substrate. This is similar to backwater areas from instream wood in Nunn A and likely describes the process of nitrate uptake in Nunn A reaches that have higher SA:V than Nunn B reaches. By enhancing hydrologic connectivity with the hyporheic zone to increase residence times of stream solutes within the hyporheic zone, stream restoration could promote reach-scale denitrification (Klockner *et al.* 2009). As nitrate uptake velocities are similar among Nunn Creek reaches, it seems that hydrologic connectivity is achieved through backwater areas in Nunn A and structures driving hyporheic exchange in Nunn B. Similar to Nunn B, constructed steps and riffles have been found to induce hyporheic exchange and enhance hydrologic connectivity between surface water and groundwater (Kasahara and Hill 2006). Channel features that lead to more complexity by creating backwater areas (i.e., Nunn A) and local variations in bedslope (i.e., Nunn B structures) help restore a range of ecosystem functions (Hester and Gooseff 2010). Because restoration projects are often implemented without verification in the field, it is important to evaluate methods and outcomes of restoration projects, including ecological responses (Palmer 2009).

Furthermore, when studying nutrient uptake and stream restoration techniques, it is important to remember that restoring form does not always restore function. As shown in the data of Sheep Creek and Nunn Creek study reaches, there is not a distinguishable trend between rehabilitated and non-rehabilitated reaches in terms of nitrate uptake. This is the case for this study of looking at just two styles of restoration and should not be generalized to all restoration techniques. Although Sheep Creek was rehabilitated by

removing the grazing pressure and the riparian corridor has naturally revegetated, this did not necessarily improve nutrient processing in the form of nitrate uptake. Based upon findings in this study and relationships shown in Chapter 4, geomorphic attributes that are associated with transient storage and nitrate uptake include substrate size and longitudinal roughness. This restoration technique did not directly influence these particular in-channel geomorphic attributes, and so stream type seemed to affect transient storage and nitrate uptake more than natural revegetation of the riparian zone. The restoration structures in Nunn Creek promote in-stream habitat and bank stabilization to restore the form on the stream, but there was no distinct pattern connecting this restoration technique to the function of nitrate uptake when looking at uptake velocities. Both reaches of Nunn Creek (restored and unrestored) had similar values of uptake velocity, and the unrestored reach exhibited more transient storage. I suggest that instream wood could be used as a cost-effective restoration technique to promote backwater areas, similar to that in Nunn A, as an alternative to building rock structures. Additionally, both reaches were influenced by flow variation, possibly more than the restoration structures. Although nutrient processing is just one goal of stream restoration projects, it is important to consider stream function and processes of river systems and not just form and local results of stream restoration. In order to restore and maintain processes of transient storage and nitrate uptake, it is necessary to sustain geomorphic attributes of longitudinal roughness (Chapter 4) and substrate permeability (O'Connor and Harvey 2008), as well as accounting for variations in discharge. Taking uncertainty into consideration and performing repeat injections on reaches are important to fully describe nitrate uptake as it varies with flow and geomorphic characteristics.

6 FLASH FLOOD EFFECTS ON SPRING CREEK

6.1 OVERVIEW

Changes in the physical template of urban streams can occur rapidly due to flashy high flows events. These high flow conditions can influence the characteristics and behavior of streams, including transient storage and nitrate uptake. I selected three reaches of varying geomorphic and hydraulic characteristics in Spring Creek (Figure 3.3 in Chapter 3), an urban stream in Fort Collins, Colorado, to investigate changes in physical characteristics, transient storage, and nitrate uptake due to a high flow event. The study reaches are characterized based upon their geomorphic setting as a pool-riffle reach (Edora Park), a stabilized reach (Stuart), and a channelized reach (Railroad). Edora Park, the most naturalized reach, is located in a city park and has areas of sparse riparian vegetation due to lawn maintenance and mowing close to the stream banks. Edora Park is the most sinuous of the three reaches and has the median gradient and grain size of the three chosen reaches. Stuart is highly modified with grouted bank stabilization and a grade-control structure. Stuart has the highest gradient and grain size and has the median sinuosity of the three reaches. Railroad has grassy banks and has also been modified through channelization. Railroad is the straightest reach and has the lowest gradient and smallest grain size of the three reaches on Spring Creek.

On August 2, 2007, a flash flood occurred in Fort Collins, CO, resulting in sudden changes in discharge of Spring Creek. Table 6.1 summarizes the storm characteristics and flood conditions (Anderson Consulting Engineers, Inc. 2008). The August 2, 2007 storm led to a peak discharge in Spring Creek of 30 m³/s, which is about a 10-year discharge (Table 11). This discharge was measured at a gaging station on Centre Avenue, which is located about 300m upstream from Railroad, which is the most upstream reach of the three study reaches. Just prior to the flash flood, physical characterizations and nutrient injections were completed on the three study reaches of Spring Creek. Following the storm event, obvious physical changes were visually observed in the reaches, including coarser substrates and bank failures. Another set of physical characterizations and nutrient injections was performed on each study reach within 4 to 6 days of the flash flood to explore the extent of physical changes caused by the sudden high flows and how these may influence transient storage and nitrate uptake. A third set of physical characterizations and nutrient injections was performed on each study reach one year after the flash flood to examine whether stream characteristics and behavior returned to pre-flood conditions or remained similar to post-flood conditions. During the one-year period between the flash flood and the third set of data collection, no other flow event of magnitude similar to the August 2, 2007 storm occurred along Spring Creek.

Table 6.1: Characteristics of August 2, 2007 storm in Fort Collins, Colorado

Characteristic	Measurement ^a
Spring Creek basin area	9 mi ²
Fort Collins annual rainfall	15.1 in.
Fort Collins average August rainfall	1.4 in.
Previous maximum rainfall depth on August 2	1.93 in. (in 1933)
Previous largest single day of rainfall in August	3.06 in. (August 3, 1951)
Total 24-hr rainfall depth from storm	5-6 in. ^b
Highest intensity of storm	2 in./hr, lasting for 2 hrs
Peak discharge of Spring Creek during storm	1,050 cfs (30 m ³ /s) ^c
Spring Creek 2-yr discharge	390 cfs (11 m ³ /s) ^c
Spring Creek 10-yr discharge	1,110 cfs (31 m ³ /s) ^c
Spring Creek 100-yr discharge	3,420 cfs (97 m ³ /s) ^c

^a Data courtesy of Anderson Consulting Engineers, Inc.

^b Fort Collins Utilities Flood Warning System = 5.12 in.; Community Collaborative Rain and Hail Study Network = 5.47 in.; Local residents = 6 in.

^c Peak discharge and return interval discharges as measured at Centre Avenue

Although previous studies have explored nitrate uptake in urban streams (Meyer *et al.* 2005; Walsh *et al.* 2005), little work has been done that involves looking specifically at effects of high flow events on nitrate uptake in streams. One such study in a field-scale flume showed that hyporheic exchange is a prominent cause of nutrient uptake shortly after high flow events because high flows can reconfigure substrate material and flush streambeds of algal biomass (Orr *et al.* 2009). In this study, I explore temporal variation in an urban stream by comparing data collected from physical measurements and nutrient injections performed immediately before and after the flash flood. A detailed description of methods used is provided in Chapter 3. I compare changes in physical stream characteristics among the three study reaches resulting from the flash flood and examine these physical changes in relation to differences in pre-versus post-flood transient storage and nitrate uptake. Prior to this study, little work has captured responses of transient storage and nitrate uptake due to a high flow event such

as this. In this way, this study takes an initial glimpse into flashy hydrology by collecting data before and after a flash flood that induced physical changes that varied among three different geomorphic settings along the study reaches. I hypothesize that increases in substrate size and removal of fine sediment due to the flashy high flow event will increase porosity and permeability, leading to greater potential for hyporheic exchange and increases transient storage and nitrate uptake. Furthermore, the potential responses to the flash flood will likely differ among the three study reaches due to variations in the geomorphic setting of the most “natural” reach (Edora Park), the structurally stabilized reach (Stuart), and the channelized reach (Railroad).

6.2 RESULTS

Post-flood responses in channel characteristics, transient storage, and nutrient uptake were mediated by geomorphic setting and varied appreciably among reaches. Shortly after the storm, visual observations of changes in physical stream attributes were noted, including coarser substrate among all three reaches. Deposition was prominent on the downstream side of the grade-control structure along Stuart, and bank failure was evident near the downstream ends of Stuart and Edora Park (Figure 6.1). Due to the various geomorphic settings of the three study reaches, they exhibited differing responses to the flash flood. These differences were quantified in measures of geomorphic complexity (longitudinal roughness, width variability, cross-sectional area variability, sinuosity, bed substrate distribution) and variables describing ecological processes (FBOM, CBOM, and GPP) from pre- and post-flood conditions, as well as stream conditions one year after the flash flood (Table 6.2). Bromide and nitrate BTCs were

used to estimate transient storage and nitrate uptake parameters, respectively (Figures 4.1 and 4.2 in Chapter 4). The mean values of modeled transient storage parameter estimates (A , A_s , D , and α) and of nitrate uptake parameters (λ and λ_s) were used to calculate mean values for A_s/A , F_{med}^{200} , S_w , and v_f (Table 6.3). Monte Carlo simulations, as described in Chapter 3, were performed on the modeled parameter estimates, yielding median values, inter-quartile ranges, and 90% confidence intervals for the distribution of possible values for transient storage and nitrate uptake parameters (Figures 6.2 through 6.5). For parameter estimates with more variance than others, the ends of the boxes or whiskers extend beyond the plot but are cut off for purposes of contrasting the parameter estimates with narrower distributions.



(a) Edora Park



(b) Stuart

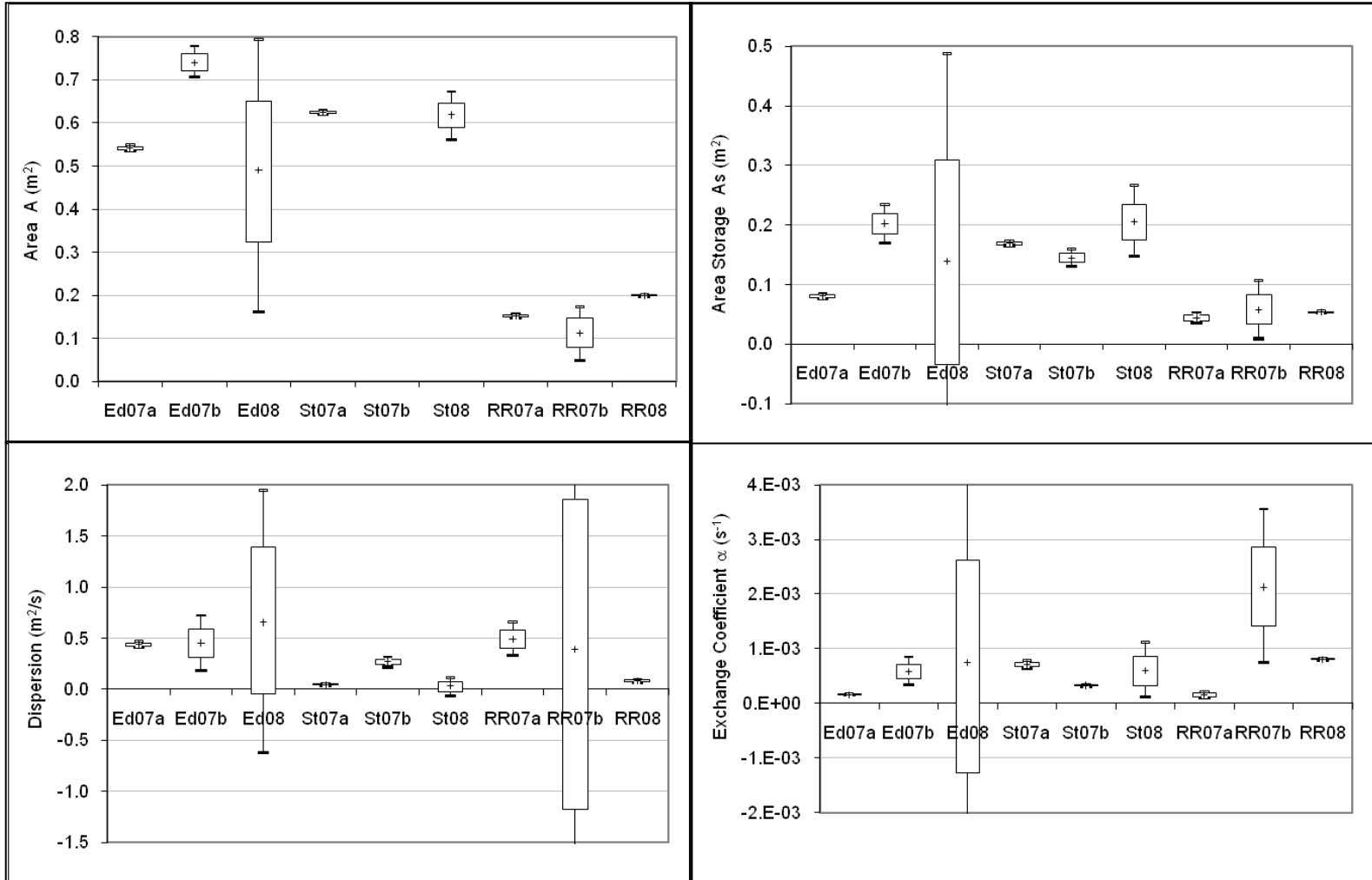
Figure 6.1: Post-flood conditions include bank failure at Edora Park and deposition below grade-control structure at Stuart

Table 6.2: Summary of Spring Creek physical and ecological parameters

	Pre-flood: Edora Park 7-30-07	Post-flood: Edora Park 8-8-07	After 1 year: Edora Park 7-21-08	Pre-flood: Stuart 7-31-07	Post-flood: Stuart 8-9-07	After 1 year: Stuart 7-22-08	Pre-flood: Railroad 8-1-07	Post-flood: Railroad 8-8-07	After 1 year: Railroad 7-24-08
Reach length (m)	178	180	176	180	181	181	181	181	186
Flow (L/s)	72	152	66	46	107	57	17	21	21
Unit discharge, q (m ² /s)	0.017	0.037	0.015	0.011	0.026	0.014	0.007	0.010	0.008
Ambient [NO ₃ ⁻ -N] (mg/L)	0.74	0.71	0.64	0.72	0.66	0.64	1.07	1.60	0.93
Sinuosity	1.16	1.18	1.15	1.05	1.05	1.05	1.01	1.02	1.04
Bed slope, S_o	0.0046	0.0044	0.0050	0.0108	0.0108	0.0109	0.0025	0.0024	0.0024
Unit stream power, ω (W/m ²)	0.78	1.58	0.73	1.18	2.75	1.47	0.18	0.23	0.19
Reynolds number, Re	16,500	45,090	26,800	12,530	34,520	24,920	6,100	7,930	12,710
Longitudinal roughness (m)	0.13	0.13	0.14	0.11	0.10	0.12	0.05	0.04	0.05
Width variability (m)	1.0	1.13	1.20	0.96	0.83	0.86	0.45	0.48	0.62
XS area variability (m)	0.22	0.40	0.37	0.24	0.49	0.46	0.04	0.05	0.10
Percent fines (< 2 mm)	34%	1%	9%	25%	0.4%	7%	75%	33%	75%
d_{16} (mm)	4	13	8	9	17	13	< 2	< 2	< 2
d_{50} (mm)	14	28	21	26	41	28	< 2	5	< 2
d_{84} (mm)	40	65	63	84	129	72	4	14	7
Gradation coefficient	3.1	2.3	2.8	3.1	2.8	2.4	1.7	2.9	2.6
Relative submergence, R/d_{84}	3.1	2.8	2.7	1.7	1.6	3.2	22.9	6.2	22.2
Metric of complexity	7.1E-04	6.8E-04	8.1E-04	1.3E-03	1.2E-03	1.4E-03	1.1E-04	8.9E-05	1.3E-04
FBOM AFDM (g/m ²)	320	98	207	389	79	316	120	101	209
CBOM AFDM (g/m ²)	26	10	63	107	7	171	48	24	97
GPP (gO ₂ /m ² /day)	0.35	0.19	0.32	0.13	0.22	0.12	0.14	0.27	0.11

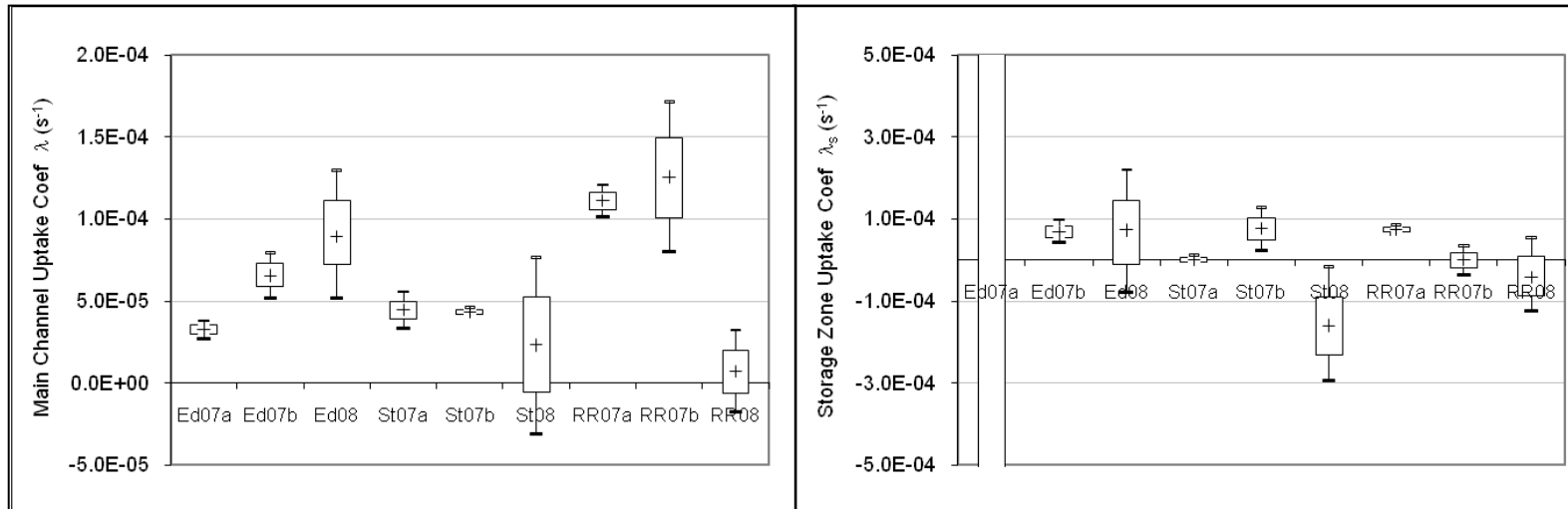
Table 6.3: Summary of Spring Creek transient storage and nitrate uptake parameters

	Pre-flood: Edora Park 7-30-07	Post-flood: Edora Park 8-8-07	After 1 year: Edora Park 7-21-08	Pre-flood: Stuart 7-31-07	Post-flood: Stuart 8-9-07	After 1 year: Stuart 7-22-08	Pre-flood: Railroad 8-1-07	Post-flood: Railroad 8-8-07	After 1 year: Railroad 7-24-08
A (m ²)	0.54	0.74	0.49	0.62	0.91	0.62	0.15	0.11	0.20
A_s (m ²)	0.08	0.20	0.12	0.17	0.14	0.21	0.04	0.06	0.05
D (m ² /s)	0.44	0.45	0.67	0.05	0.27	0.03	0.49	0.30	0.08
α (s ⁻¹)	1.6E-04	5.9E-04	8.3E-04	7.1 E-04	3.3E-04	6.1E-04	1.6E-04	2.1E-03	8.1E-04
λ (s ⁻¹)	3.2E-05	6.5E-05	9.1E-05	4.4E-05	4.3E-05	2.6E-05	1.1E-04	1.3E-04	6.3E-06
λ_s (s ⁻¹)	2.3E-10	7.0E-05	6.8E-05	6.0E-09	7.7E-05	-1.6E-04	7.4E-05	2.6E-09	-3.8E-05
A_s/A	0.15	0.27	0.25	0.27	0.16	0.33	0.29	0.52	0.27
F_{med}^{200}	0.03	0.09	0.17	0.18	0.06	0.22	0.07	0.33	0.20
S_w (m)	4,350	3,120	980	1,740	2,950	2,300	700	920	8,190
v_f (m/s)	4.7E-06	1.4E-05	1.7E-05	7.9E-06	1.1E-05	7.1E-06	1.3E-05	1.3E-05	1.2E-06



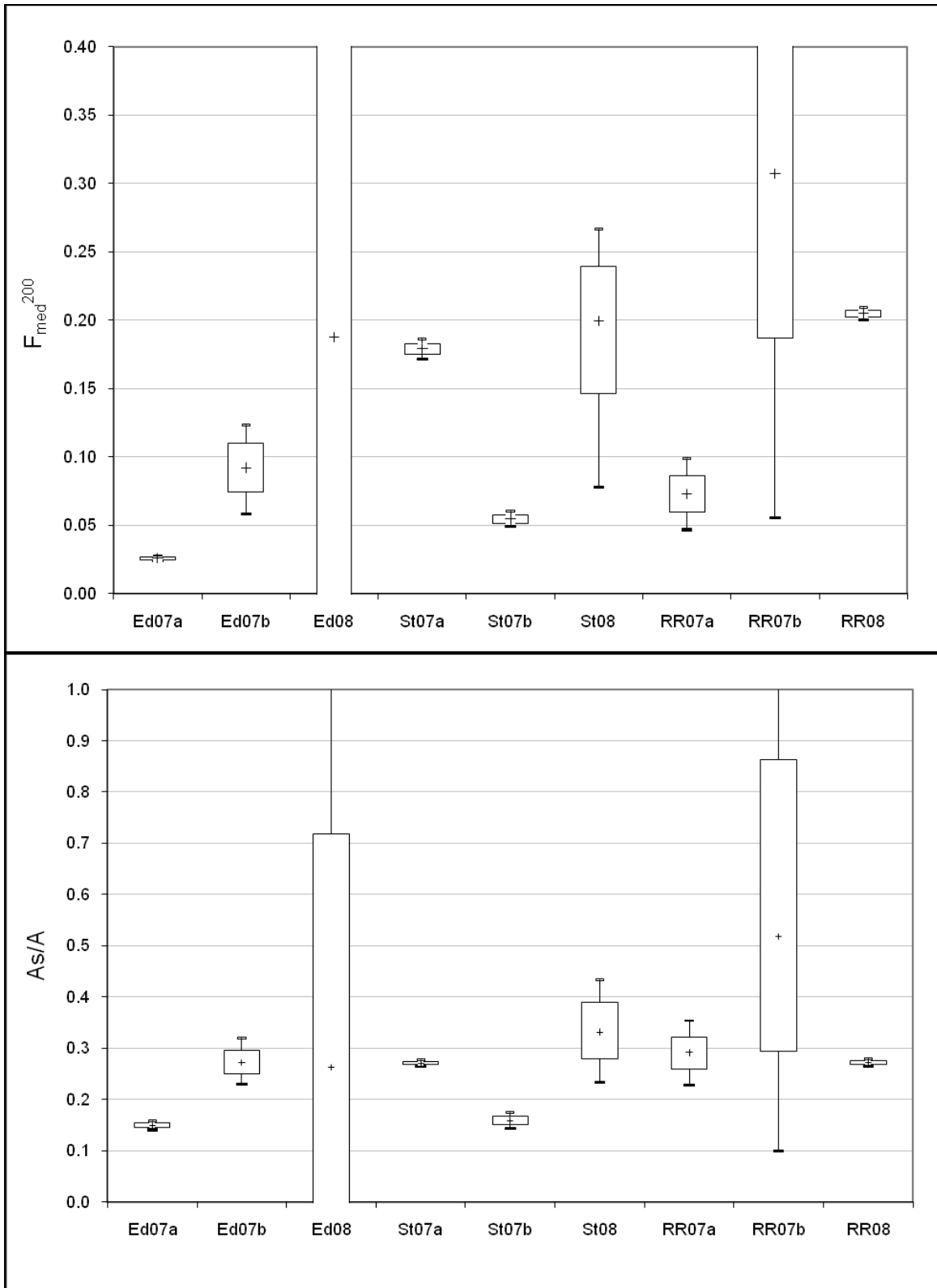
Note: Edora 2007a is represented as Ed07a; whiskers = 10th and 90th percentiles, box = 25th and 75th percentiles, crossbar = median

Figure 6.2: Results of Monte Carlo simulations of transient storage parameters for Spring Creek study reaches



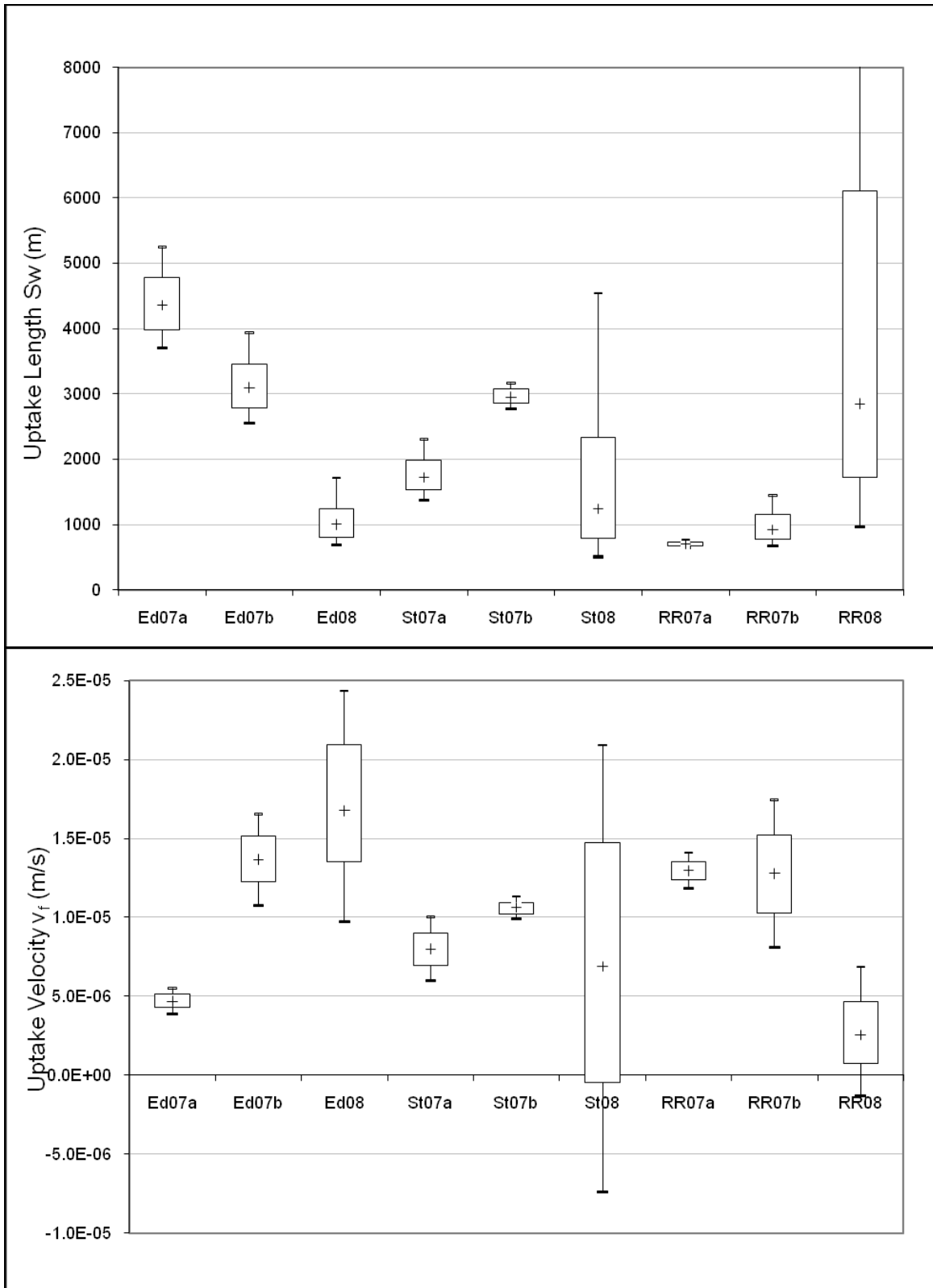
Note: Edora 2007a is represented as Ed07a; whiskers = 10th and 90th percentiles, box = 25th and 75th percentiles, crossbar = median

Figure 6.3: Results of Monte Carlo simulations of nitrate uptake parameters for Spring Creek study reaches



Note: Edora 2007a is represented as Ed07a; whiskers = 10th and 90th percentiles, box = 25th and 75th percentiles, crossbar = median

Figure 6.4: Results of Monte Carlo simulations of F_{med}^{200} and A_s/A for Spring Creek



Note: Edora 2007a is represented as Ed07a; whiskers = 10th and 90th percentiles, box = 25th and 75th percentiles, crossbar = median

Figure 6.5: Results of Monte Carlo simulations of S_w and v_f for Spring Creek

Analyses of the physical attributes showed that longitudinal roughness, bed slope, and sinuosity were not substantially altered by the high flow event. Overall, substrate size and variability in cross-sectional area increased, as percentage of fine sediment, relative submergence (based upon the flow on the date of injection), and benthic organic matter decreased when comparing post-flood physical characteristics to pre-flood characteristics. There were no consistent patterns found in comparing changes in width variability, substrate gradation coefficient, and GPP resulting from the flash flood conditions among the three study reaches. It should be noted that increases in cross-sectional area variability are likely due to higher flows when data were collected for post-flood conditions compared to pre-flood conditions. Higher flows measured in post-flood conditions led to greater flow areas, and in turn, greater potential for cross-sectional area variability than in lower flows measured in pre-flood conditions. This pattern is not as clearly shown in width variability, which can also be affected by flow level, because the bank slopes of the study reaches are not steep enough to cause much change in width with increases in flow area.

For Edora Park and Railroad, the amount of transient storage was higher in the post-flood conditions compared to pre-flood conditions, based on values of both A_s/A and F_{med}^{200} . At Edora Park, the increased amount of transient storage after the storm event coincides with increased nitrate uptake, as shown in shorter S_w and faster v_f . Conversely, Railroad did not exhibit the same pattern as Edora Park. Increased values of transient storage in post-flood conditions were not followed by increases in nitrate uptake. At Railroad, the high flows caused bank vegetation, mainly tall grasses, to lie flat and eventually drift into the channel. This enhanced the effect of vegetation on in-channel

storage in stagnant areas where the grass lay flat along the ground and streambed. Furthermore, Stuart demonstrated the opposite pattern of transient storage decreasing in post-flood conditions from pre-flood conditions, which is likely due to substantial aggradation below the grade-control structure that filled in pools and reduced in-channel storage. Nitrate uptake values at Stuart seem inconclusive and appear to be counter-intuitive as both v_f and S_w increased in post-flood conditions compared to pre-flood conditions. The uptake coefficients (λ) of post-flood and pre-flood conditions remained nearly constant, while the flow more than doubled in post-flood conditions compared to pre-flood conditions. In calculating nitrate uptake values, v_f is positively correlated with flow depth, and S_w is positively correlated with flow velocity. As velocity and depth both increased with flow in post-flood conditions, with no change in λ , both S_w and v_f showed increases.

The largest percent change of post-flood characteristics compared to pre-flood characteristics was in the F_{med}^{200} parameter, which greatly increased at Edora Park and Railroad (Figure 6.6). Edora Park also showed a large increase in v_f and a decrease in S_w , showing greater uptake, while Railroad did not. It is plausible that the primary mechanisms responsible for these changes are entirely different; i.e., increased uptake in Edora Park corresponds with an increase in hyporheic exchange (more potential for nitrate processing, including denitrification) as a major portion in the transient storage increase, whereas increased transient storage at Railroad is likely due to increased amounts of stagnant water from flattened grasses on the bank that drifted into the channel. It is not likely that hyporheic exchange increased much at Railroad because the bed was still composed of fine sediment, with more than 30% of the bed material being

fines (<2mm). Consistent increases occurred in cross-sectional area variability and median grain size, while consistent decreases occurred in benthic organic matter and percentage of fines in the substrate. This confirms the visual observation of coarser substrate after the flood, as high flows flushed fines and benthic organic matter from the streambed. Bed slope and longitudinal roughness only showed very slight decreases from pre- to post-flood conditions.

When examining characteristics of the study reaches one year after the flood, the degree to which parameter values returned to pre-flood conditions was also variable among sites (Figure 6.7). A large percent change occurs again in the F_{med}^{200} parameter at Edora Park. This implies that there was a large increase in transient storage one year after the flood compared to pre-flood conditions at Edora Park. Again, this is followed by a large increase in v_f and a decrease in S_w at Edora Park. At Edora Park and Stuart, the substrate remained coarser one year after the flood when compared to pre-flood conditions, as shown in decreases of the percentage of fines and increases of d_{50} and d_{84} . Conversely, the substrate of Railroad returned to the finer grain sizes that were characteristic of the reach before the flash flood, and so no changes in the percentage of fines and median grain size were observed when comparing conditions one year after the flood to pre-flood conditions.

Values of the F_{med}^{200} and A_s/A ratio parameters at Stuart showed slight increases one year after the flood when compared to pre-flood conditions, implying that transient storage throughout the reach increased from post-flood conditions and returned close to pre-flood conditions. Increases in transient storage one year after the flood compared to post-flood parameters are likely due to greater in-channel storage from partial flushing of

particles that had been deposited below the grade-control structure. Conditions one year after the flood compared to pre-flood conditions at Stuart showed that v_f slightly decreased and S_w slightly increased, showing a slight decrease in nitrate uptake along the reach (Figure 6.7). At Stuart, uptake via hyporheic exchange may be constrained by a shallow concrete apron extending approximately 20 m downstream of the grade-control structure, and so a large portion of transient storage is likely due to in-channel storage. Edora Park showed increases in F_{med}^{200} and nitrate uptake (higher v_f and shorter S_w), while Railroad showed decreases in F_{med}^{200} and nitrate uptake (lower v_f and longer S_w), when comparing conditions one year after the flood to post-flood conditions. Decreased transient storage and uptake velocity at Railroad one year after the flood are likely due to less vegetation encroachment into the channel, which had been a major source of increased in-channel storage immediately after the high flow event.

When comparing conditions one year after the flood with post-flood conditions (Figure 6.8), the percent changes are much more evident than in comparisons with pre-flood conditions. In the cases of benthic organic matter and percent fines, all three study reaches showed large increases one year following the flood. Although the absolute values of these characteristics are not as markedly different from pre-flood conditions, these were the predominant changes of the streambed as a result of the sudden high flows during the storm. Because the values of benthic organic matter and percent fines were low after the flood, the increases in these values were larger percentages of the small values immediately after the flood.

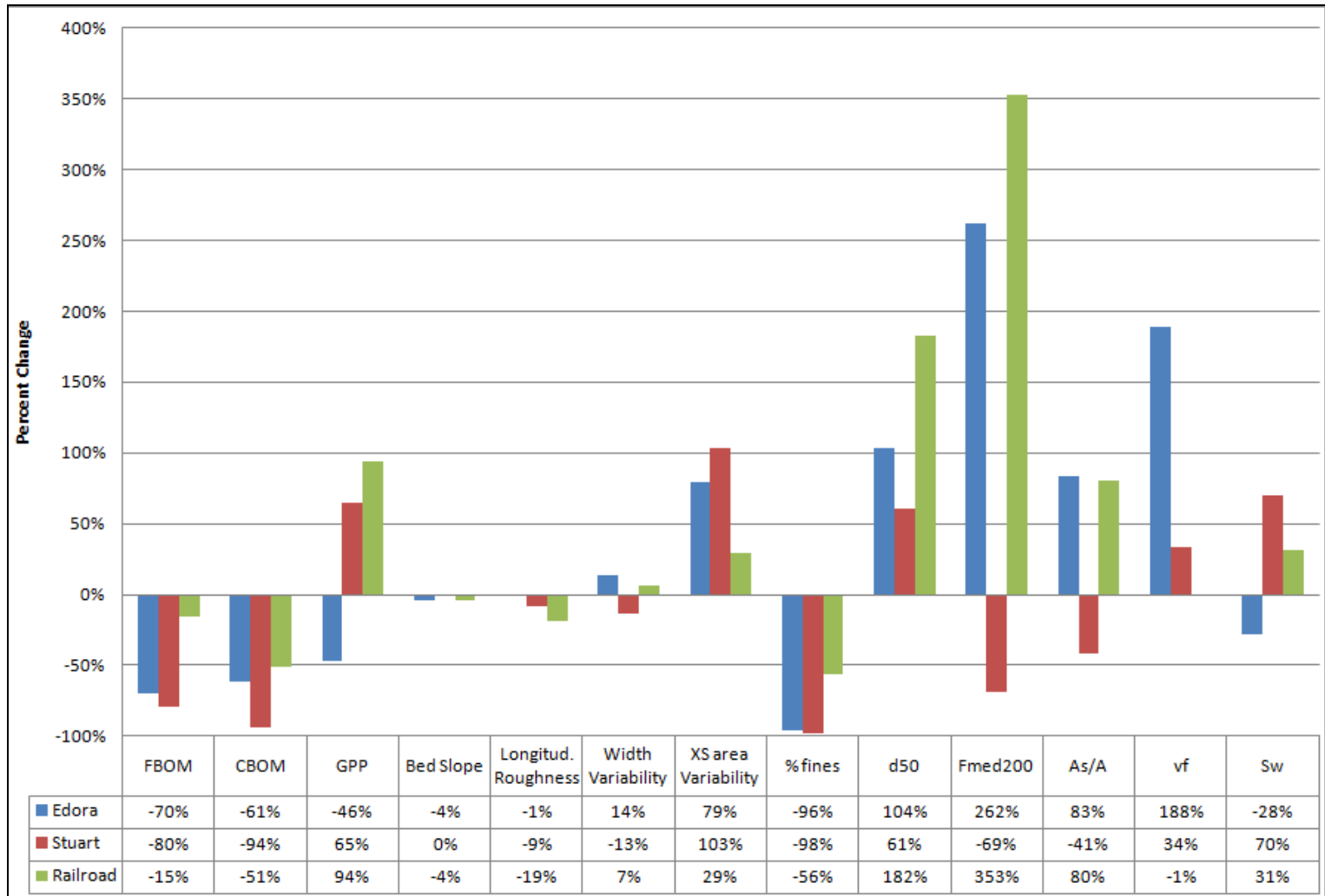


Figure 6.6: Percent change of post-flood parameters from pre-flood parameters

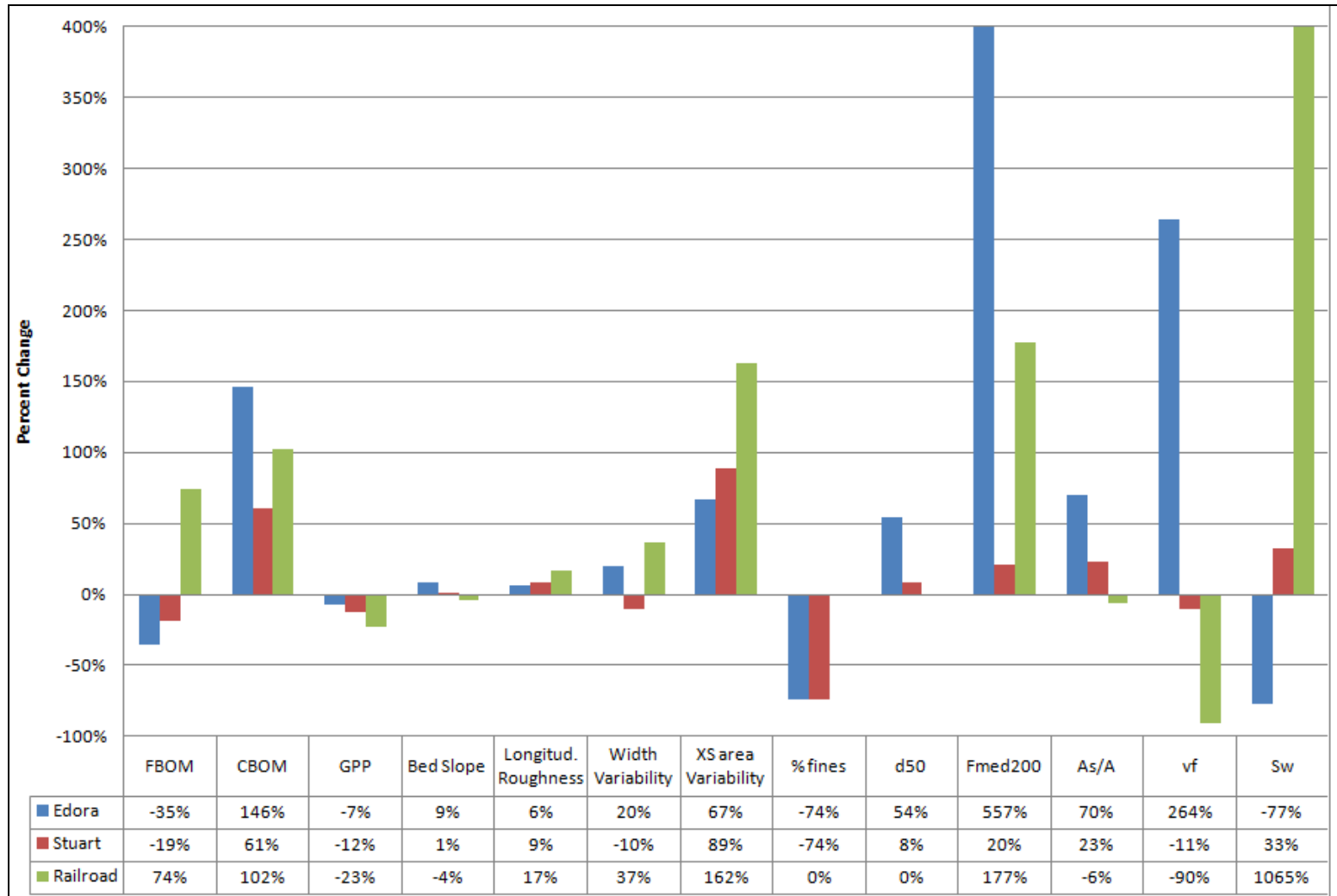


Figure 6.7: Percent change of 1-yr parameters from pre-flood parameters

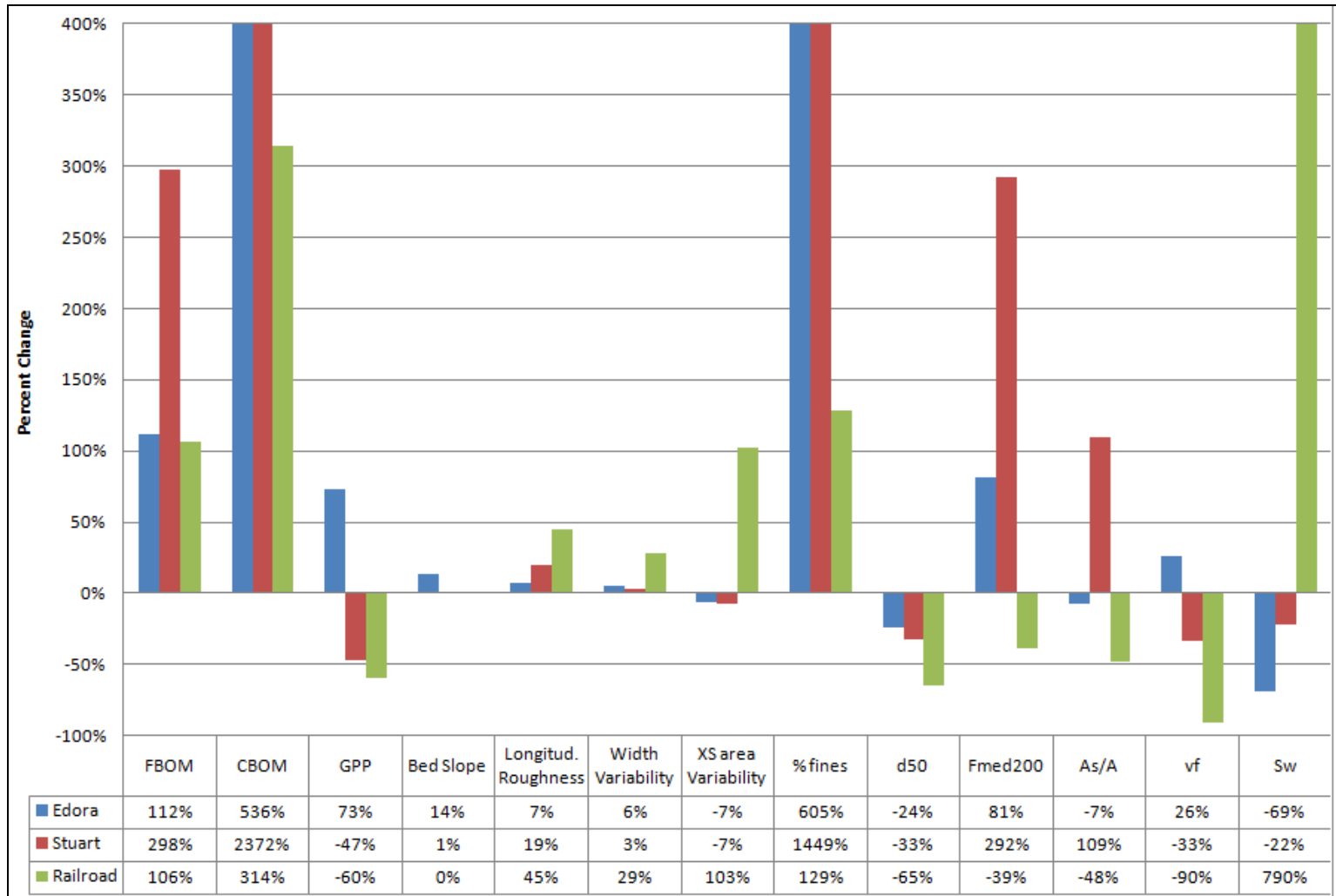
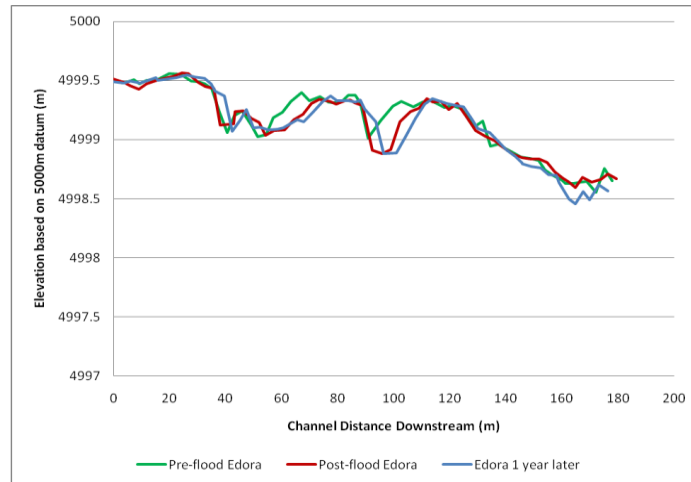
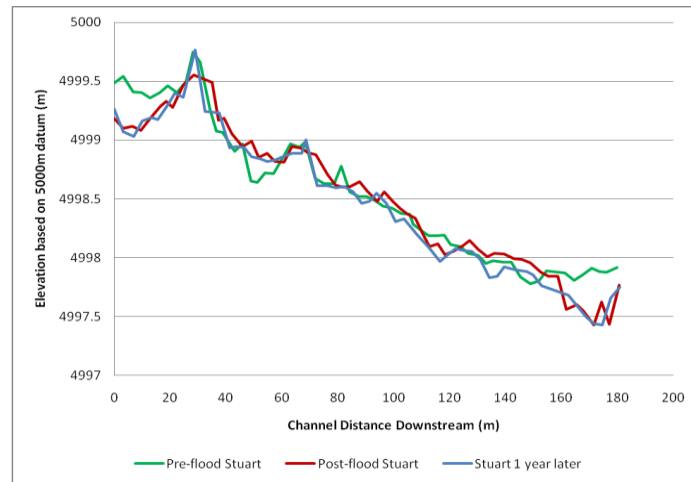


Figure 6.8: Percent change of 1-yr parameters from post-flood parameters

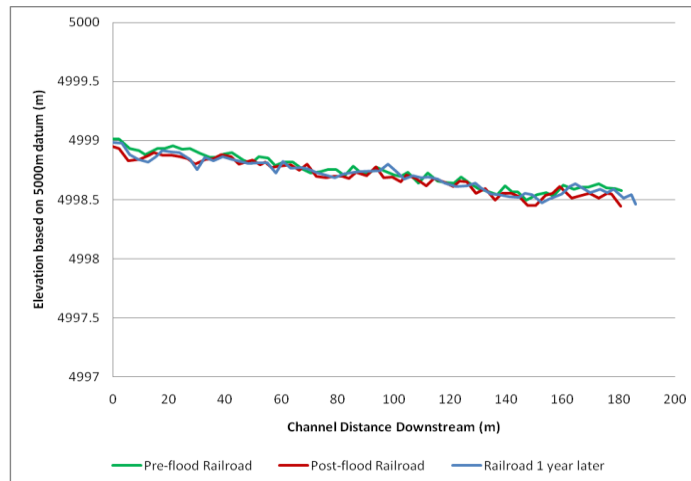
Another physical aspect investigated after the sudden high flow in Spring Creek was the bed topography in the form of changes in the longitudinal profiles of thalweg elevations (Figure 6.9). In these plots, the green line represents pre-flood conditions, the red line represents post-flood conditions, and the blue line represents conditions of the bed elevation one year after the flash flood. The bed elevation was based upon an arbitrary datum of 5000 m. At Edora Park, post-flood conditions exhibited local scour in pools near 60 m and 100 m along the channel length. These local scour areas in pools along the streambed remained one year after the flood when compared to pre-flood conditions, which could contribute to the in-channel storage portion of the increases seen in transient storage due to larger pool size. At Stuart, post-flood elevations and elevations measured one year after the flood showed local scour at the start and end of the study reach, as well as deposition around 50 m along the channel length, when compared to pre-flood conditions. The deposition corresponds with the location just downstream of the grade-control structure (Figure 6.1), as well as decreases in transient storage from less in-channel storage due to pools being filled with sand and gravel. The thalweg elevation of Railroad showed relatively little adjustment, but it exhibited slight scour around 25 m along the channel length in post-flood and conditions one year after the flood when compared to pre-flood conditions.



(a) Edora Park



(b) Stuart



(c) Railroad

Figure 6.9: Thalweg elevation along the study reaches at pre-flood, post-flood, and conditions 1 yr after flash flood

Due to visual observations of bank failure at Edora Park, I explored the centerline of the channel for evidence of channel planform rerouting due to the flash flood. Although the sinuosity did change slightly at Edora Park and Railroad, the position of the channel centerline of these reaches did not show substantial adjustments in the survey planform data of post-flood and conditions one year after the flood compared to pre-flood conditions.

6.3 DISCUSSION

By comparing variations in stream characteristics before and after flash flood conditions, this study explores how high flow spates can modify physical attributes of a small urban stream in three geomorphic settings. The observed changes in transient storage and nitrate uptake in response to the high flow spate, as well as responses one year after the event, were not consistent among sites and appear to be mediated by the unique geomorphic setting of each study reach. Prior to this research, few studies have captured rapid changes in geomorphic, transient storage, and nitrate uptake characteristics of streams due to high flow events. In a study investigating the effects of a flood on channel morphology and hyporheic zones in mountain streams, the extent of hyporheic zones both increased and decreased, depending upon the location along the stream, and locations of upwelling and downwelling zones were adjusted by flood-induced channel change (Wondzell and Swanson 1999). In this study, I investigated an urban stream and show that temporal changes from sudden increases in flow, as often experienced in urban streams, can lead to physical changes in stream attributes. Urban streams are also highly spatially variable, as shown by distinct responses to the flood and differences in physical

characteristics among the three reaches, which are in close proximity to each other along the stream.

As described in previous studies (Meyer *et al.* 2005; Orr *et al.* 2009), high flows flush streambeds of benthic organic matter and fine sediment. The most prominent change that resulted from sudden high-flow conditions along Spring Creek was the flushing of fines and benthic organic matter. Similarly, Konrad and Booth (2005) showed that the movement of organic matter in flashy flow regimes mainly occurs in quick high-flow periods with limited retention. In all three study reaches, the streambed was predominantly affected with outcomes of coarser substrate and less benthic organic matter. This suggests that controls on uptake vary with time as substrate conditions and biotic influences change after a disturbance such as high flows (Orr *et al.* 2009). The results of this study extend this conceptual framework by underscoring the site-specific nature of bed material dynamics and biomass flushing and their dependence upon the particular geomorphic setting of a stream reach. After a disturbance, such as a high flow event, the sediments may reattain full capacity for hyporheic exchange as all biomass may not have been completely flushed from the streambed, with fine materials continuing to reduce porosity and permeability of the bed. In this way, the starting point of biomass growth and decline of hyporheic exchange is a function of the antecedent interaction between discharge and substrate characteristics in a particular stream context.

The flash flood did modify characteristics of the study reaches, which could have led to the variation shown in transient storage and uptake parameters. In addition to prominent changes in streambed characteristics of benthic organic matter and substrate size along the study reaches, slight changes in other physical characteristics were also

observed, including cross-sectional area variability, width variability, and thalweg elevation. However, the nutrient injections were performed at various discharges, which may also influence transient storage and nitrate uptake. At this point we might ask “are the differences in transient storage and nitrate uptake parameters likely due to morphological changes in the study reaches as a result of the flash flood, or are they due to nutrient injections being performed at various discharges?”

In an effort to resolve this uncertainty, a correlation matrix was developed, including all parameters of physical, transient storage, and nitrate uptake, to determine whether storage and uptake parameters are more closely related to discharge measurements or physical stream characteristics. Metrics describing flow, including unit discharge and unit stream power, were compared with transient storage parameters (F_{med}^{200} and A_s/A) and nitrate uptake parameters (v_f and S_w) for significant Pearson correlation coefficients ($p < 0.10$). In the same way, metrics describing physical stream morphology, including grain size, longitudinal roughness, and cross-sectional area variability, were compared with transient storage and nitrate uptake parameters. The only significant correlation to note was an inverse relationship between FBOM and the storage nitrate uptake coefficient ($r = -0.59$, $p = 0.09$). This relationship is likely due to FBOM clogging pore space in the streambed, reducing hyporheic exchange and nitrate uptake. This inverse relationship between benthic organic matter and nutrient uptake is not consistent with findings of Meyer *et al.* (2005), in which FBOM was directly related to uptake velocity. However, statistical inferences are limited by a small sample size ($n = 9$) in this study.

Among the three study reaches, it is important to note the reach-specific nature of stream response to the flash flood. Variations in response could be due to inherently different geomorphic characteristics among the three study reaches. For example, Stuart has bed and bank stabilization structures throughout. Edora Park and Railroad have more natural and changeable channel structure, as well as stagnant areas near the vegetated banks, which allow for greater changes in storage. The physical characterizations of the reaches indicated differences in geomorphic complexity. Edora Park and Stuart each consisted of seven different physical habitat units, while Railroad consisted of one continuous habitat unit. Although the number of physical habitat units along each reach did not change as a result of the sudden high flows in Spring Creek, reaches with greater variability in the distribution of habitat units (increased patchiness) could potentially have greater hyporheic exchange and more transient storage and nitrate uptake than reaches with fewer habitat units. Edora Park and Stuart have more longitudinal reach scale variability, with varying substrate size and physical habitat units. Conversely, Railroad had lateral cross-sectional scale variability with ineffective flow regions due to vegetation encroachment into the flow field near the banks.

Physical habitat complexity in Edora Park and Stuart are associated with both hydraulic and geomorphic heterogeneity. In contrast, Railroad is channelized and geomorphically homogeneous but hydraulically complex due to bank vegetation encroachment that results in substantial ineffective flow areas. Increases in nitrate uptake parameters of Edora Park followed increases in transient storage parameters (Figures 6.2 through 6.4). This implies that transient storage in the hyporheic zone may be associated with nitrate uptake. I hypothesize that a large portion of transient storage increase was

due to increased hyporheic exchange from flushing of fines and coarsening of bed material in Edora Park, which would lead to more potential for nitrate processing and uptake to occur. On the other hand, increases of transient storage parameters at Railroad and Stuart were not consistently followed with increased nitrate uptake. Hyporheic exchange may be limited at Railroad due to a streambed of predominantly fine substrate, which does not allow for as much hyporheic exchange as a streambed consisting of coarser or more heterogeneous substrate.

Whether the variation among transient storage and uptake parameters is linked to physical changes resulting from a flash flood, general flow variability, or inherent differences in characteristics among the study reaches remains uncertain. Additionally, the amount of nutrient enrichment could have led to nonlinear uptake responses. Although nitrate was added to achieve a consistent 4-fold increase of instream concentrations, the ambient nitrate concentrations varied among reaches and injection dates. Nutrient uptake has been found to not always follow a linear relationship with concentration, where nutrient enrichment could lead to saturation (Dodd *et al.* 2002). Depending upon the absolute amount of nitrate added to the stream during each injection, this could be an additional source of variability among sites. Further research in partitioning hyporheic exchange and in-channel storage is important to fully describe the transient storage and nutrient uptake behavior. As Doyle (2005) included hydrologic variability in nutrient uptake modeling to determine an effective discharge that accounts for the largest quantity of nutrient retention, I suggest that the relationship between nitrate uptake and discharge is not monotonic and is highly variable in both space and time. Instead, this work suggests that transient storage and uptake are highly heterogeneous

along streams traversing varied geomorphic settings and sensitive to the temporal sequence of flow events that alter substrate, vegetative, and longitudinal characteristics. Stream reaches exhibit distinct responses to various flows depending on their distinct geomorphic characteristics and antecedent conditions, among other factors. Processes of transient storage and nitrate uptake are sensitive to conditions that describe the physical setting of the reach, which can be altered by a single geomorphically effective flow. Characteristics and behavior of urban streams are spatially variable, as demonstrated by the Spring Creek study reaches and their distinct responses to the high flow event, as well as temporally variable due to flashy urban hydrology.

7 CONCLUSION

Describing nitrate uptake in natural systems involves understanding complex interactions among hydraulic and geomorphic characteristics and biogeochemical processes. In this study, I found associations among nitrate uptake parameters (v_f and S_w) and transient storage parameters (F_{med}^{200}), which are influenced by key factors of geomorphic complexity (LR), flow (Re), and substrate condition (d_{50} and FBOM). Repeat injections at individual sites suggested that nitrate uptake and transient storage were mediated by complex interactions of geomorphic attributes and flow variability. Few studies have performed multiple nutrient injections along the same stream reach. By performing repeat injections on the same study reach, it is possible to capture flow variability with different discharges over time, which may affect uptake more than geomorphological characteristics. Responses of nitrate uptake due to flow variability were not consistent among reaches of different geomorphic context, as shown in the unique responses of each Spring Creek reach to a single high flow event. This study suggests that transient storage and nitrate uptake are highly dynamic and spatially heterogeneous along streams traversing varied geomorphic settings as temporal sequences of flow events alter substrate, vegetative, and longitudinal characteristics.

A single geomorphically effective flow appears to have the capacity to considerably alter the magnitudes and relative proportions of hyporheic versus in-channel

storage, which are both components of transient storage. As nitrate uptake behaves differently in the hyporheic zone compared to in-channel storage, it is recommended that future research be focused on differentiating between in-channel storage and hyporheic storage, as in Briggs *et al.* (2009; 2010), to more fully understand nitrate uptake and other biogeochemical processes occurring within stream ecosystems. Because temporal sequences of flow events effectively reset both the physical template and biological processes controlling nitrate uptake, it behaves as a stochastic process in both space and time that does not lend itself to simple monotonic relationships with discharge. This presents ongoing challenges for upscaling these processes using magnitude-frequency analysis and other techniques.

In the streams I examined, no discernable differences in nitrate uptake were observed between rehabilitated and non-rehabilitated reaches; however, this study only examined certain styles of restoration and cannot be extrapolated to all restoration techniques. In Nunn Creek, the reach without structures showed similar nitrate uptake velocities as the reach with constructed features. Backwater areas created by instream wood in the unrestored reach seemed to have a similar effect on nitrate uptake levels as the restoration structures in the restored reach, although the specific mechanisms remain unclear. Creating backwater zones with instream wood could be a cost-effective alternative to building rock structures, as the unrestored reach with natural backwater areas exhibited higher surface area-to-volume ratios and more transient storage than the restored reach. Although nitrate uptake is just one goal of stream restoration projects, it is important to consider how stream processes can sustain the geomorphic attributes that enhance nutrient uptake, as opposed to simply building static channel features. Explicitly

quantifying uncertainty and performing repeat injections are also important for describing nitrate uptake as it varies with flow and geomorphic characteristics.

8 REFERENCES

- Alexander, R., J. Böhlke, E. Boyer, M. David, J. Harvey, P. Mulholland, S. Seitzinger, C. Tobias, C. Tonitto, and W. Wollheim (2009). "Dynamic modeling of nitrogen losses in river networks unravels the coupled effects of hydrological and biogeochemical processes." *Biogeochemistry* **93**(1): 91-116.
- Allan, J. D. (2004). "Landscapes and riverscapes: the influence of land use on stream ecosystems." *Annual Review of Ecology Evolution and Systematics* **35**: 257-284.
- American Public Health Association (APHA) (1998). "Standard Methods for the Examination of Water and Wastewater." American Public Health Association. Washington, DC.
- Anderson, J. K., S. M. Wondzell, M. N. Gooseff, and R. Haggerty (2005). "Patterns in stream longitudinal profiles and implications for hyporheic exchange flow at the H. J. Andrews Experimental Forest, Oregon, USA." *Hydrological Processes* **19**(15): 2931-2949.
- Anderson Consulting Engineers, Inc. (2008). "Flood Documentation Report." Chapter 8, City of Fort Collins, CO, Flood of August 2, 2007, March.
- Baker, D. W. (2009). "Land Use Effects on Physical Habitat and Nitrate Uptake in Small Streams of the Central Rocky Mountain Region." PhD

Dissertation, Civil and Environmental Engineering Department, Colorado State University, Fort Collins, CO.

- Bales, J. D. and M. R. Nardi (2007). "Automated Routines for Calculating Whole-stream Metabolism: Theoretical Background and User's Guide." U. S. Geological Survey Techniques and Methods 4-C2, 33 p.
- Bencala, K. E. (2005). Hyporheic exchange flows. In: M. G. Anderson (Ed.), Encyclopedia of Hydrological Sciences, John Wiley & Sons, Ltd., Vol. 3, Part 10, pp. 1733-1740.
- Boulton, A. J., S. Findlay, P. Marmonier, E. H. Stanley, and H. M. Valett (1998). "The functional significance of the hyporheic zone in streams and rivers." *Annual Review of Ecology and Systematics* **29**: 59-81.
- Briggs, M. A., M. N. Gooseff, C. D. Arp, and M. A. Baker (2009). "A method for estimating surface transient storage parameters for streams with concurrent hyporheic storage." *Water Resources Research* **45**: W00D27.
- Briggs, M. A., M. N. Gooseff, B. J. Peterson, K. Morkeski, W. M. Wollheim, and C. S. Hopkinson (2010). "Surface and hyporheic transient storage dynamics throughout a coastal stream network." *Water Resources Research* **46**: W06516.
- Brooks, K. N., P. F. Ffolliott, H. M. Gregersen, and L. F. DeBano (2003). Hydrology and the Management of Watersheds. Iowa State Press, Ames, IA.
- Buffington, J. M. and D. Tonina (2009). "Hyporheic exchange in mountain rivers, II: effects of channel morphology on mechanics, scales, and rates of exchange." *Geography Compass* **3**(3): 1038-1062.

- Bukaveckas, P. A. (2007). "Effects of channel restoration on water velocity, transient storage, and nutrient uptake in a channelized stream." *Environmental Science & Technology* **41**(5): 1570-1576.
- Bunte, K. and S. R. Abt (2001a). "Sampling frame for improving pebble count accuracy in coarse gravel-bed streams." *Journal of the American Water Research Association* **37**(4): 1001-1014.
- Bunte, K. and S. R. Abt (2001b). "Sampling Surface and Subsurface Particle-size Distributions in Wadable Gravel- and Cobble-bed Streams for Analyses in Sediment Transport, Hydraulics, and Streambed Monitoring." General Technical Report RMRS-GTR-74, U. S. Department of Agriculture, Forest Service, Rocky Mountain Research Station, 428 p.
- Camargo, J. A. and Á. Alonso (2006). "Ecological and toxicological effects of inorganic nitrogen pollution in aquatic ecosystems: a global assessment." *Environment International* **32**(6): 831-849.
- Cooper, S. D., L. Barmuta, Sarnelle, O., K. Kratz, and S. Diehl (1997). "Quantifying spatial heterogeneity in streams." *Journal of the North American Benthological Society* **16**(1): 174-188.
- Craig, L. S., M. A. Palmer, D. C. Richardson, S. Filoso, E. S. Bernhardt, B. P. Bledsoe, M. W. Doyle, P. M. Groffman, B. Hassett, S. S. Kaushal, P. M. Mayer, S. M. Smith, and P. R. Wilcock (2008). "Stream restoration strategies for reducing river nitrogen loads." *Frontiers in Ecology and the Environment* **6**(10): 529-538.
- D'Angelo, D. J., J. R. Webster, S. V. Gregory, and J. L. Meyer (1993). "Transient storage in Appalachian and Cascade Mountain streams as related to hydraulic

- characteristics." *Journal of the North American Benthological Society* **12**(3): 223-235.
- Dodds, W. K., A. J. Lopez, W. B. Bowden, S. Gregory, N. B. Grimm, S. K. Hamilton, A. E. Hershey, E. Marti, W. H. McDowell, J. L. Meyer, D. Morrall, P. J. Mulholland, B. J. Peterson, J. L. Tank, H. M. Valett, J. R. Webster, and W. Wollheim. (2002). "N uptake as a function of concentration in streams." *Journal of the North American Benthological Society* **21**(2): 206-220.
- Doyle, M. W. (2005). "Incorporating hydrologic variability into nutrient spiraling." *Journal of Geophysical Research* **110**(G1): G01003.
- Ensign, S. H. and M. W. Doyle (2005). "In-channel transient storage and associated nutrient retention: evidence from experimental manipulations." *Limnology and Oceanography* **50**(6): 1740-1751.
- Ensign, S. H. and M. W. Doyle (2006). "Nutrient spiraling in streams and river networks." *Journal of Geophysical Research-Biogeosciences* **111**(G4): 13.
- Findlay, S. (1995). "Importance of surface-subsurface exchange in stream ecosystems - the hyporheic zone." *Limnology and Oceanography* **40**(1): 159-164.
- Fisher, D. E. and M. J. Fisher (2001). "The nitrogen bomb." *Discover* (April): 52-57.
- Gijzen, H. J. and A. Mulder (2001). "The nitrogen cycle out of balance." *Water* **21**(August): 38-40.
- Golladay, S. W., J. R. Webster, and E. F. Benfield (1989). "Changes in stream benthic organic matter following watershed disturbance." *Holarctic Ecology* **12**(2): 96-105.

- Gooseff, M. N., K. E. Bencala, D. T. Scott, R. L. Runkel, and D. M. McKnight (2005). "Sensitivity analysis of conservative and reactive stream transient storage models applied to field data from multiple-reach experiments." *Advances in Water Resources* 28(5): 479-492.
- Gooseff, M. N., R. O. Hall Jr., and Tank, J. L. (2007). "Relating transient storage to channel complexity in streams of varying land use in Jackson Hole, Wyoming." *Water Resources Research* 43(W01417), doi:10.1029/2005WR004626.
- Hall, R. O., E. S. Bernhardt, and G. E. Likens (2002). "Relating nutrient uptake with transient storage in forested mountain streams." *Limnology and Oceanography* 47(1): 255-265.
- Hall, R. O., J. L. Tank, D. J. Sobota, P. J. Mulholland, J. M. O'Brien, W. K. Dodds, J. R. Webster, H. M. Valett, G. C. Poole, B. J. Peterson, J. L. Meyer, W. H. McDowell, S. L. Johnson, S. K. Hamilton, N. B. Grimm, S. V. Gregory, C. N. Dahm, L. W. Cooper, L. R. Ashkenas, S. M. Thomas, R. W. Sheibley, J. D. Potter, B. R. Niederlehner, L. T. Johnson, A. M. Helton, C. M. Crenshaw, A. J. Burgin, M. J. Bernot, J. J. Beaulieu, and C. P. Arango (2009). "Nitrate removal in stream ecosystems measured by 15N addition experiments: total uptake." *Limnology and Oceanography* 54(3): 653-665.
- Harrelson, C. C., C. L. Rawlins, and J. P. Potyondy (1994). "Stream Channel Reference Sites: An Illustrated Guide to Field Technique." General Technical Report RM-245, U. S. Department of Agriculture, Forest Service, Rocky Mountain Forest and Range Experiment Station, Fort Collins, CO, 61 p.

- Harvey, J. W. and K. E. Bencala (1993). "The effect of streambed topography on surface-subsurface water exchange in mountain catchments." *Water Resources Research* **29**(1): 89-98.
- Hawkins, C. P., J. L. Kershner, P. A. Bisson, M. D. Bryant, L. M. Decker, S. V. Gregory, D. A. McCullough, C. K. Overton, G. H. Reeves, R. J. Steedman, and M. K. Young (1993). "A hierarchical approach to classifying stream habitat features." *Fisheries* **18**(6): 3-11.
- Hester, E. T. and M. W. Doyle (2008). "In-stream geomorphic structures as drivers of hyporheic exchange." *Water Resources Research* **44**(3): W03417.
- Hester, E. T. and M. N. Gooseff (2010). "Moving beyond the banks: hyporheic restoration is fundamental to restoring ecological services and functions of streams." *Environmental Science & Technology* **44**(5): 1521-1525.
- Hey, R. D. and C. R. Thorne (1986). "Stable channels with mobile gravel beds." *Journal of Hydraulic Engineering* **112**(8): 671-689.
- Jacobson, R. B., S. R. Femmer, and R. A. McKenney (2001). "Land-use Changes and the Physical Habitat of Streams: A Review with Emphasis on Studies within the U.S. Geological Survey Federal-State Cooperative Program." U. S. Geological Survey Circular 1175, Reston, VA.
- Julien, P. Y. (1998). Erosion and Sedimentation. Cambridge University Press.
- Julien, P.Y. (2002). River Mechanics. Cambridge University Press.
- Kasahara, T. and A. R. Hill (2006). "Effects of riffle-step restoration on hyporheic zone chemistry in N-rich lowland streams." *Canadian Journal of Fisheries and Aquatic Sciences* **63**(1): 120-133.

- Kasahara, T. and S. M. Wondzell (2003). "Geomorphic controls on hyporheic exchange flow in mountain streams." *Water Resources Research* **39**(1): 14.
- Klocker, C., S. Kaushal, P. Groffman, P. Mayer, and R. Morgan (2009). "Nitrogen uptake and denitrification in restored and unrestored streams in urban Maryland, USA." *Aquatic Sciences - Research Across Boundaries* **71**(4): 411-424.
- Konrad, C. B. and D. B. Booth (2005). "Hydrologic changes in urban streams and their ecological significance." *American Fisheries Society Symposium* **47**: 157-177.
- Marion, A., M. Zaramella, and A. Bottacin-Busolin (2008). "Solute transport in rivers with multiple storage zones: the STIR model." *Water Resources Research* **44**(W10406).
- Marzolf, E. R., P. J. Mulholland, and A. D. Steinman (1994). "Improvements to the diurnal upstream-downstream dissolved-oxygen change technique for determining whole-stream metabolism in small streams." *Canadian Journal of Fisheries and Aquatic Sciences* **51**(7): 1591-1599.
- Meyer, J. L., M. J. Paul, and W. K. Taulbee (2005). "Stream ecosystem function in urbanizing landscapes." *Journal of the North American Benthological Society* **24**(3): 602-612.
- Montgomery, D. R. and J. M. Buffington (1997). "Channel-reach morphology in mountain drainage basins." *Geological Society of America Bulletin* **109**(5): 596-611.
- Morrice, J. A., H. M. Valett, C. N. Dahm, and M. E. Campana (1997). "Alluvial characteristics, groundwater-surface water exchange and hydrological retention in headwater streams." *Hydrological Processes* **11**(3): 253-267.

- Mulholland, P. J. (2004). "The importance of in-stream uptake for regulating stream concentrations and outputs of N and P from a forested watershed: evidence from long-term chemistry records for Walker Branch Watershed." *Biogeochemistry* **70**(3): 403-426.
- Mulholland, P. J., R. Hall, D. Sobota, W. Dodds, S. Findlay, N. Grimm, S. Hamilton, W. McDowell, J. O'Brien, J. Tank, L. Ashkenas, L. W. Cooper, C. Dahm, S. Gregory, S. Johnson, J. Meyer, B. Peterson, G. Poole, H. M. Valett, J. Webster, C. Arango, J. Beaulieu, M. Bernot, A. Burgin, C. Crenshaw, A. Helton, L. Johnson, B. Niederlehner, J. Potter, R. Sheibley, and S. Thomas (2009). "Nitrate removal in stream ecosystems measured by ¹⁵N addition experiments: 2. denitrification." *Limnology and Oceanography* **54**(3): 666-680.
- Mulholland, P. J., A. M. Helton, G. C. Poole, R. O. Hall, S. K. Hamilton, B. J. Peterson, J. L. Tank, L. R. Ashkenas, L. W. Cooper, C. N. Dahm, W. K. Dodds, S. E. G. Findlay, S. V. Gregory, N. B. Grimm, S. L. Johnson, W. H. McDowell, J. L. Meyer, H. M. Valett, J. R. Webster, C. P. Arango, J. J. Beaulieu, M. J. Bernot, A. J. Burgin, C. L. Crenshaw, L. T. Johnson, B. R. Niederlehner, J. M. O'Brien, J. D. Potter, R. W. Sheibley, D. J. Sobota, and S. M. Thomas (2008). "Stream denitrification across biomes and its response to anthropogenic nitrate loading." *Nature* **452**(7184): 202-205.
- Mulholland, P. J., E. R. Marzolf, R. W. Jackson, D. R. Hart, and S. P. Hendricks (1997). "Evidence that hyporheic zones increase heterotrophic metabolism and phosphorus uptake in forest streams." *Limnology and Oceanography* **42**(3): 443-451.

- Mulholland, P. J., B. J. Peterson, S. Hamilton, J. L. Tank, R. O. Hall, J. L. Meyer, G. Poole, S. Findlay, W. K. Dodds, J. R. Webster, H. M. Valett, N. Grimm, C. N. Dahm, S. Johnson, S. Gregory, and W. H. McDowell (2004). Nitrate uptake and retention in streams: mechanism and effects of human disturbance from stream reaches to landscapes.
- Mulholland, P. J., J. L. Tank, J. R. Webster, W. B. Bowden, W. K. Dodds, S. V. Gregory, N. B. Grimm, S. K. Hamilton, S. L. Johnson, E. Martí, W. H. McDowell, J. L. Merriam, J. L. Meyer, B. J. Peterson, H. M. Valett, and W. M. Wollheim (2002). "Can uptake length in streams be determined by nutrient addition experiments? Results from an interbiome comparison study." *Journal of the North American Benthological Society* **21**(4): 544-560.
- Natural Resources Conservation Service (NRCS) (2007). "Part 654 Stream Restoration Design National Engineering Handbook, Chapter 11 Rosgen Geomorphic Channel Design." 210-VI-NEH, U. S. Department of Agriculture, August.
- Newbold, J., J. W. Elwood, R. V. O'Neill, and W. Van Winkle (1981). "Measuring nutrient spiralling in streams." *Canadian Journal of Fisheries and Aquatic Sciences* **38**(7): 860-863.
- O'Connor, B. L. and J. W. Harvey (2008). "Scaling hyporheic exchange and its influence on biogeochemical reactions in aquatic ecosystems." *Water Resources Research* **44**(12): W12423.
- O'Connor, B. L., M. Hondzo, and J. W. Harvey (2009). "Predictive modeling of transient storage and nutrient uptake: implications for stream restoration." *Journal of*

Hydraulic Engineering Permalink: [http://dx.doi.org/10.1061/\(ASCE\)HY.1943-7900.0000180](http://dx.doi.org/10.1061/(ASCE)HY.1943-7900.0000180).

- Orr, C. H., J. J. Clark, P. R. Wilcock, J. C. Finlay, and M. W. Doyle (2009). "Comparison of morphological and biological control of exchange with transient storage zones in a field-scale flume." *Journal of Geophysical Research* **114**(G2): G02019.
- Packman, A. I. and M. Salehin (2003). "Relative roles of stream flow and sedimentary conditions in controlling hyporheic exchange." *Hydrobiologia* **494**(1): 291-297.
- Palmer, M. (2009). "Reforming watershed restoration: science in need of application and applications in need of science." *Estuaries and Coasts* **32**(1): 1-17.
- Payn, R. A., J. R. Webster, P. J. Mulholland, H. M. Valett, and W. K. Dodds (2005). "Estimation of stream nutrient uptake from nutrient addition experiments." *Limnology and Oceanography: Methods* **3**: 174-182.
- Peterson, B. J., W. M. Wollheim, P. J. Mulholland, J. R. Webster, J. L. Meyer, J. L. Tank, E. Martí, W. B. Bowden, H. M. Valett, A. E. Hershey, W. H. McDowell, W. K. Dodds, S. K. Hamilton, S. Gregory, and D. D. Morrall (2001). "Control of nitrogen export from watersheds by headwater streams." *Science* **292**(5514): 86-90.
- Poeter, E. P. and M. C. Hill (1999). "UCODE, a computer code for universal inverse modeling." *Computers & Geosciences* **25**(4): 457-462.
- Poeter, E. P., M. C. Hill, E. R. Banta, S. Mehl, and S. Christensen (2005). UCODE 2005 and six other computer codes for universal sensitivity analysis, inverse modeling, and uncertainty evaluation. US Geological Survey Techniques and Methods Report TM 6-A11.

- Poff, N. L., J. D. Allan, M. B. Bain, J. R. Karr, K. L. Prestegard, B. D. Richter, R. E. Sparks, and J. C. Stromberg (1997). "The natural flow regime." *BioScience* 47(11): 769-784.
- Poff, N. L., B. P. Bledsoe, and C. O. Cuhaciyan (2006). "Hydrologic variation with land use across the contiguous United States: geomorphic and ecological consequences for stream ecosystems." *Geomorphology* 79(3-4): 264-285.
- Poor, C. J. and J. J. McDonnell (2007). "The effects of land use on stream nitrate dynamics." *Journal of Hydrology* 332(1-2): 54-68.
- Powell, K. L. and V. Bouchard (2010). "Is denitrification enhanced by the development of natural fluvial morphology in agricultural headwater ditches?" *Journal of the North American Benthological Society* 29(2): 761-772.
- Pringle, C. M., R. J. Naiman, G. Bretschko, J. R. Karr, M. W. Oswood, J. R. Webster, R. L. Welcomme, and M. J. Winterbourn (1988). "Patch dynamics in lotic systems - the stream as a mosaic." *Journal of the North American Benthological Society* 7(4): 503-524.
- Runkel, R. L. (1998). One-dimensional Transport with Inflow and Storage (OTIS): A Solute Transport Model for Streams and Rivers. U.S. Geological Survey Water-Resources Investigations Report 98 – 4018, Denver, CO, 73 p.
- Runkel, R. L. (2002). "A new metric for determining the importance of transient storage." *Journal of the North American Benthological Society* 21(4): 529-543.
- Runkel, R. L. (2007). "Toward a transport-based analysis of nutrient spiraling and uptake in streams." *Limnology and Oceanography: Methods* 5: 50-62.

- Scott, D. T., M. N. Gooseff, K. E. Bencala, and R. L. Runkel (2003). "Automated calibration of a stream solute transport model: implications for interpretation of biogeochemical parameters." *Journal of the North American Benthological Society* **22**(4): 492-510.
- SAS Institute, Inc. (2008). "SAS 9.2 companion for windows." SAS Institute, Cary, NC.
- Stream Solute Workshop (1990). "Concepts and methods for assessing solute dynamics in stream ecosystems." *Journal of the North American Benthological Society* **9**(2): 95-119.
- Tank, J. L., E. J. Rosi-Marshall, M. A. Baker, and R. O. Hall (2008). "Are rivers just big streams? A pulse method to quantify nitrogen demand in a large river." *Ecology* **89**(10): 2935-2945.
- Tonina, D. B. and J. M. Buffington (2009). "Hyporheic exchange in mountain rivers I: mechanics and environmental effects." *Geography Compass* **3**(3): 1063-1086.
- Tukey, J. W. (1977). Exploratory Data Analysis. Addison-Wesley, Reading, MA.
- Valett, H. M., J. A. Morrice, C. N. Dahm, and M. E. Campana (1996). "Parent Lithology, Surface-Groundwater Exchange, and Nitrate Retention in Headwater Streams." *Limnology and Oceanography* **41**(2): 333-345.
- Valett, H. M., C. N. Dahm, M. E. Campana, J. A. Morrice, M. A. Baker, and C. S. Fellows (1997). "Hydrologic influences on groundwater surface water ecotones: Heterogeneity in nutrient composition and retention." *Journal of the North American Benthological Society* **16**(1): 239-247.

- Wagner, B. J. and J. W. Harvey (1997). "Experimental design for estimating parameters of rate-limited mass transfer: Analysis of stream tracer studies." *Water Resources Research* **33**(7): 1731-1741.
- Walsh, C. J., A. H. Roy, J. W. Feminella, P. D. Cottingham, P. M. Groffman, and R. P. Morgan (2005). "The urban stream syndrome: current knowledge and the search for a cure." *Journal of the North American Benthological Society* **24**(3): 706-723.
- Waters, T. F. (1995). "Sediment in Streams: Sources, Biological Effects and Control." American Fisheries Society, Bethesda, MD.
- Webster, J. R. and H. M. Valett (2007). "Solute dynamics." In: F. R. Hauer and G. A. Lamberti (Eds.), Methods in Stream Ecology, Elsevier, London, pp. 169-185.
- Wondzell, S. M. and F. J. Swanson (1999). "Floods, channel change, and the hyporheic zone." *Water Resources Research* **35**(2): 555-567.
- Wondzell, S. M. (2006). "Effect of morphology and discharge on hyporheic exchange flows in two small streams in the Cascade Mountains of Oregon, USA." *Hydrological Processes* **20**(2): 267-287.

APPENDIX A:
SUMMARY OF UNCERTAINTY AND SENSITIVITY IN
PARAMETER ESTIMATES FROM OTIS/UCODE
MODELING

Table A.1: Uncertainty and sensitivity summary of parameter estimates from OTIS/UCODE modeling on Spring Creek

Reach	Variable	Estimate (μ)	Standard Deviation (σ)	Coefficient of Variance ($CV=\sigma/\mu$)	Composite Scaled Sensitivities (CSS)	Ratio to Maximum CSS
Edora Park 2007a	<i>A</i>	0.54	5.1E-03	0.01	11.32	1.00
	<i>A_s</i>	0.08	3.6E-03	0.04	0.78	0.07
	<i>D</i>	0.44	2.2E-02	0.05	0.62	0.06
	α	1.6E-04	8.4E-06	0.05	0.64	0.06
	λ	3.3E-05	4.1E-06	0.13	0.34	1.00
	λ_s	2.3E-10	4.7E-02	203,000,000	0.00	0.00
	<i>Dal</i>	1.5	NE	NE	NE	NE
Edora Park 2007b	<i>A</i>	0.74	2.9E-02	0.04	9.00	1.00
	<i>A_s</i>	0.20	2.6E-02	0.13	1.62	0.18
	<i>D</i>	0.45	2.1E-01	0.46	0.38	0.04
	α	5.9E-04	2.1E-04	0.35	0.87	0.10
	λ	6.5E-05	1.1E-05	0.17	0.27	1.00
	λ_s	7.0E-05	2.2E-05	0.31	0.07	0.24
	<i>Dal</i>	2.4	NE	NE	NE	NE
Edora Park 2008	<i>A</i>	0.49	2.3E-01	0.48	17.80	1.00
	<i>A_s</i>	0.12	2.8E-01	2.25	3.29	0.18
	<i>D</i>	0.67	1.0E+00	1.52	1.16	0.06
	α	8.3E-04	2.8E-03	3.42	1.06	0.06
	λ	9.1E-05	3.0E-05	0.32	0.94	1.00
	λ_s	6.8E-05	1.2E-04	1.81	0.17	0.18
	<i>Dal</i>	8.1	NE	NE	NE	NE
Stuart 2007a	<i>A</i>	0.62	4.2E-03	0.01	16.92	1.00
	<i>A_s</i>	0.17	2.8E-03	0.02	3.56	0.21
	<i>D</i>	0.05	7.7E-03	0.17	0.24	0.01
	α	7.1E-04	6.0E-05	0.08	1.33	0.08
	λ	4.4E-05	8.8E-06	0.20	22.49	1.00
	λ_s	6.0E-09	9.2E-06	1,550	21.59	0.96
	<i>Dal</i>	7.8	NE	NE	NE	NE
Stuart 2007b	<i>A</i>	0.91	7.1E-03	0.01	10.76	1.00
	<i>A_s</i>	0.14	1.2E-02	0.08	1.10	0.10
	<i>D</i>	0.27	4.0E-02	0.15	0.40	0.04
	α	3.3E-04	1.8E-05	0.06	0.62	0.06
	λ	4.3E-05	2.2E-06	0.05	11.49	1.00
	λ_s	7.7E-05	4.3E-05	0.56	1.60	0.14
	<i>Dal</i>	3.4	NE	NE	NE	NE

Reach	Variable	Estimate (μ)	Standard Deviation (σ)	Coefficient of Variance ($CV=\sigma/\mu$)	Composite Scaled Sensitivities (CSS)	Ratio to Maximum CSS
Stuart 2008	<i>A</i>	0.62	4.4E-02	0.07	18.40	1.00
	<i>A_s</i>	0.21	4.6E-02	0.23	4.61	0.25
	<i>D</i>	0.03	7.3E-02	2.29	0.20	0.01
	α	6.1E-04	3.8E-04	0.63	1.79	0.10
	λ	2.6E-05	4.3E-05	1.65	0.41	0.41
	λ_s	-1.6E-04	1.1E-04	0.67	0.99	1.00
	<i>Dal</i>	7.3	NE	NE	NE	NE
Railroad 2007a	<i>A</i>	0.15	4.5E-03	0.03	9.51	1.00
	<i>A_s</i>	0.04	7.3E-03	0.16	0.75	0.08
	<i>D</i>	0.49	1.3E-01	0.26	0.62	0.07
	α	1.6E-04	4.6E-05	0.29	0.93	0.10
	λ	1.1E-04	7.8E-06	0.07	10.74	1.00
	λ_s	7.4E-05	8.7E-06	0.12	1.71	0.16
	<i>Dal</i>	1.6	NE	NE	NE	NE
Railroad 2007b	<i>A</i>	0.11	4.8E-02	0.42	5.97	1.00
	<i>A_s</i>	0.06	3.7E-02	0.62	2.59	0.43
	<i>D</i>	0.30	2.1E+00	7.00	0.17	0.03
	α	2.1E-03	1.1E-03	0.51	0.83	0.14
	λ	1.3E-04	3.7E-05	0.29	5.46	0.77
	λ_s	2.6E-09	2.8E-05	10,900	7.13	1.00
	<i>Dal</i>	9.7	NE	NE	NE	NE
Railroad 2008	<i>A</i>	0.20	2.0E-03	0.01	24.64	1.00
	<i>A_s</i>	0.05	1.1E-03	0.02	5.12	0.21
	<i>D</i>	0.08	1.5E-02	0.18	0.45	0.02
	α	8.1E-04	1.2E-05	0.02	2.08	0.08
	λ	6.3E-06	2.0E-05	3.10	0.18	0.94
	λ_s	-3.8E-05	7.0E-05	1.83	0.19	1.00
	<i>Dal</i>	13.7	NE	NE	NE	NE

NE = not estimated

Note: Parameter estimates have the least uncertainty when *Dal* is on the order of 1.0 (Wagner and Harvey 1997)

Table A.2: Uncertainty and sensitivity summary of parameter estimates from OTIS/UCODE modeling on Sheep Creek

Reach	Variable	Estimate (μ)	Standard Deviation (σ)	Coefficient of Variance ($CV=\sigma/\mu$)	Composite Scaled Sensitivities (CSS)	Ratio to Maximum CSS
Sheep A 2007	<i>A</i>	0.28	7.8E-03	0.03	6.08	1.00
	<i>A_s</i>	0.10	1.6E-02	0.16	1.58	0.26
	<i>D</i>	0.16	5.4E-02	0.33	0.04	0.01
	α	3.3E-03	6.4E-04	0.20	0.67	0.11
	λ	2.1E-04	3.5E-05	0.17	3.79	1.00
	λ_s	4.2E-10	4.7E-01	1,120,000,000	0.00	0.00
	<i>Dal</i>	10.4	NE	NE	NE	NE
Sheep C 2007	<i>A</i>	0.60	6.3E-03	0.01	6.70	1.00
	<i>A_s</i>	0.26	1.0E-01	0.39	0.15	0.02
	<i>D</i>	0.79	6.1E-02	0.08	0.92	0.14
	α	3.4E-05	1.3E-06	0.04	1.49	0.22
	λ	2.6E-05	4.3E-06	0.17	8.50	1.00
	λ_s	3.4E-04	5.5E-04	1.64	0.07	0.01
	<i>Dal</i>	0.1	NE	NE	NE	NE
Sheep A 2008	<i>A</i>	0.33	4.3E-01	1.31	10.28	1.00
	<i>A_s</i>	0.11	4.3E-01	3.84	3.49	0.34
	<i>D</i>	0.15	1.9E+00	12.5	0.21	0.02
	α	4.2E-03	2.8E-02	6.57	0.95	0.09
	λ	3.2E-05	2.1E-05	0.66	0.19	0.22
	λ_s	4.2E-04	5.9E-05	0.14	0.88	1.00
	<i>Dal</i>	15.9	NE	NE	NE	NE
Sheep B 2008	<i>A</i>	0.49	3.5E-03	0.01	14.97	1.00
	<i>A_s</i>	0.14	3.3E-03	0.02	3.60	0.24
	<i>D</i>	0.19	6.4E-03	0.03	0.43	0.03
	α	1.7E-03	5.6E-05	0.03	1.10	0.07
	λ	1.2E-05	6.3E-06	0.54	0.10	0.12
	λ_s	4.0E-04	4.1E-05	0.10	0.84	1.00
	<i>Dal</i>	9.0	NE	NE	NE	NE
Sheep C 2008	<i>A</i>	0.30	1.1E-01	0.36	24.72	1.00
	<i>A_s</i>	0.07	4.9E-02	0.68	5.29	0.21
	<i>D</i>	0.14	3.1E-01	2.14	0.69	0.03
	α	1.0E-03	4.3E-04	0.43	1.84	0.07
	λ	2.8E-05	2.8E-06	0.10	0.41	0.30
	λ_s	4.8E-04	2.0E-05	0.04	1.39	1.00
	<i>Dal</i>	10.3	NE	NE	NE	NE

Reach	Variable	Estimate (μ)	Standard Deviation (σ)	Coefficient of Variance ($CV=\sigma/\mu$)	Composite Scaled Sensitivities (CSS)	Ratio to Maximum CSS
Sheep D 2008	<i>A</i>	0.54	3.8E-03	0.01	38.29	1.00
	<i>A_s</i>	0.09	2.6E-03	0.03	5.67	0.15
	<i>D</i>	0.11	2.4E-02	0.21	1.64	0.04
	α	5.5E-04	2.4E-05	0.04	1.61	0.04
	λ	4.8E-05	5.0E-06	0.10	1.38	1.00
	λ_s	9.6E-06	2.2E-06	0.23	0.05	0.03
	<i>Dal</i>	13.1	NE	NE	NE	NE
Sheep B 2009	<i>A</i>	0.35	1.1E-01	0.31	3.70	1.00
	<i>A_s</i>	0.16	1.1E-01	0.66	1.24	0.33
	<i>D</i>	0.24	4.4E-01	1.83	0.16	0.04
	α	2.1E-03	2.5E-03	1.19	0.35	0.10
	λ	4.9E-05	2.7E-05	0.55	0.17	1.00
	λ_s	7.9E-05	7.4E-05	0.94	0.10	0.58
	<i>Dal</i>	8.4	NE	NE	NE	NE
Sheep D 2009	<i>A</i>	0.42	6.7E-03	0.02	6.71	1.00
	<i>A_s</i>	0.25	4.7E-03	0.02	4.03	0.60
	<i>D</i>	0.23	1.7E-02	0.08	0.56	0.08
	α	1.0E-02	9.4E-04	0.09	0.25	0.04
	λ	8.3E-05	4.3E-06	0.05	0.55	1.00
	λ_s	8.6E-08	4.0E-04	4,710	0.04	0.08
	<i>Dal</i>	65.5	NE	NE	NE	NE

NE = not estimated

Note: Parameter estimates have the least uncertainty when *Dal* is on the order of 1.0 (Wagner and Harvey 1997)

Table A.3: Uncertainty and sensitivity summary of parameter estimates from OTIS/UCODE modeling on Nunn Creek

Reach	Variable	Estimate (μ)	Standard Deviation (σ)	Coefficient of Variance ($CV=\sigma/\mu$)	Composite Scaled Sensitivities (CSS)	Ratio to Maximum CSS
Nunn A 1	<i>A</i>	0.43	7.9E-03	0.02	3.87	1.00
	<i>A_s</i>	0.25	1.0E-02	0.04	1.80	0.46
	<i>D</i>	0.56	2.7E-01	0.48	0.09	0.02
	α	6.7E-03	1.1E-03	0.16	0.59	0.15
	λ	3.0E-04	3.6E-05	0.12	0.37	1.00
	λ_s	2.1E-04	6.3E-05	0.30	0.19	0.53
	<i>Dal</i>	10.9	NE	NE	NE	NE
Nunn A 2	<i>A</i>	0.40	7.2E-03	0.02	24.06	1.00
	<i>A_s</i>	0.12	2.1E-02	0.17	5.99	0.25
	<i>D</i>	0.27	1.7E-01	0.62	0.64	0.03
	α	2.5E-03	4.6E-04	0.18	2.13	0.09
	λ	3.4E-04	2.9E-05	0.08	0.44	1.00
	λ_s	5.2E-05	5.9E-05	1.14	0.02	0.05
	<i>Dal</i>	10.0	NE	NE	NE	NE
Nunn A 3	<i>A</i>	0.37	4.7E-01	1.29	2.07	1.00
	<i>A_s</i>	0.22	4.7E-01	2.12	1.25	0.60
	<i>D</i>	0.81	1.2E+01	14.20	0.18	0.09
	α	2.0E-02	4.4E-01	22.60	0.11	0.05
	λ	3.4E-04	5.8E-05	0.17	0.36	1.00
	λ_s	1.3E-04	8.7E-05	0.65	0.08	0.23
	<i>Dal</i>	52.5	NE	NE	NE	NE
Nunn B 1	<i>A</i>	1.09	1.4E-01	0.13	6.82	1.00
	<i>A_s</i>	0.22	1.4E-01	0.64	1.15	0.17
	<i>D</i>	0.19	1.9E-01	0.99	0.21	0.03
	α	1.5E-03	1.8E-03	1.18	0.42	0.06
	λ	1.4E-04	4.5E-06	0.03	0.41	1.00
	λ_s	7.6E-05	2.2E-05	0.29	0.04	0.10
	<i>Dal</i>	8.4	NE	NE	NE	NE
Nunn B 2	<i>A</i>	0.98	6.3E-01	0.64	2.94	1.00
	<i>A_s</i>	0.21	6.3E-01	3.02	0.28	0.09
	<i>D</i>	0.27	6.9E-01	2.52	0.20	0.07
	α	1.2E-03	5.9E-03	5.11	0.09	0.03
	λ	2.3E-04	2.2E-05	0.09	0.41	1.00
	λ_s	5.5E-10	2.9E-01	535,000,000	0.02	0.06
	<i>Dal</i>	9.0	NE	NE	NE	NE

Reach	Variable	Estimate (μ)	Standard Deviation (σ)	Coefficient of Variance ($CV=\sigma/\mu$)	Composite Scaled Sensitivities (CSS)	Ratio to Maximum CSS
Nunn B 3	<i>A</i>	1.00	1.1E-02	0.01	4.16	1.00
	<i>A_s</i>	0.13	9.8E-03	0.07	0.73	0.17
	<i>D</i>	0.13	1.8E-02	0.15	0.11	0.03
	α	7.5E-04	1.2E-04	0.17	0.51	0.12
	λ	5.8E-05	2.0E-05	0.34	0.13	0.31
	λ_s	1.8E-03	2.1E-04	0.12	0.43	1.00
	<i>DaI</i>	10.7	NE	NE	NE	NE

NE = not estimated

Note: Parameter estimates have the least uncertainty when *DaI* is on the order of 1.0 (Wagner and Harvey 1997)